Leveraging paleo, historical, and modern records to understand the effects
of management and fire on forest carbon biomass

by

Clarke A. Knight

A dissertation submitted in partial satisfaction of the

requirements for the degree of

Doctor of Philosophy

in

Environmental Science, Policy, and Management

in the

Graduate Division

of the

University of California, Berkeley

Committee in charge:

Professor John J. Battles, Co-Chair
Professor Matthew D. Potts, Co-Chair
Professor Wayne Sousa
Professor David Wahl

Summer 2021

Leveraging paleo, historical, and modern records to understand the effects
of management and fire on forest carbon biomass

© 2021

by

Clarke A. Knight

Abstract

Leveraging paleo, historical, and modern records to understand the effects
of management and fire on forest carbon biomass

by

Clarke A. Knight

Doctor of Philosophy in Environmental Science, Policy, and Management

University of California, Berkeley

Professor John J. Battles, Co-Chair

Professor Matthew D. Potts, Co-Chair

My dissertation weaves together paleo-ecological data, archival records, historical evidence, and modern inventories to understand the long-term impacts of fire disturbance on forest carbon dynamics in Six Rivers National Forest, California. Over three chapters, I use my results to evaluate the consequences of management activities, namely anthropogenic manipulation of fire, on aboveground live forest biomass. In the first chapter, I present a reconstruction of forest structure and composition during the 1880s and compare it to modern forests conditions. I found that modern forests are considerably denser and increasingly favor shade-tolerant taxa, likely due to twentieth century fire suppression. In the second chapter, I focus on developing an emerging fossil pollen analysis technique as the first step in quantitative reconstruction of past vegetation biomass. By modeling the relationship between modern pollen influx and modern biomass, I demonstrated that calibrated pollen influx-biomass relationships provide a robust means to infer changes in past plant biomass. My third chapter concludes with the application of the models I developed in the previous chapter to 3000 years of pollen influx data. These models allowed me to estimate aboveground biomass in a mixed conifer forest over the late Holocene. Taking a trans-disciplinary approach in this chapter, I integrate empirical datasets about biomass and fire with Native oral history to illustrate the significant and important role that Indigenous peoples played pre-contact in shaping the forest ecosystems of northwestern California. With this dissertation, I document forest dynamics at different spatial scales over three millennia and provide a practical benchmark for land managers by indicating the scale of intervention needed to move California forests closer to their long-term historical conditions.

TABLE OF CONTENTS

INTRODUCTION

Historical ecology – which entails the reconstruction of past ecological patterns and dynamics (Rhemtulla and Mladenoff 2007) – has large potential value for ecosystem management (Swetnam et al. 1999). The field of historical ecology is broad and includes land use history from archival or documentary sources, long-term monitoring and field experiments, and paleo-ecology records derived from proxies such as lake sediments, ice cores, and tree rings (Higgs et al. 2014). Such records have clear applications to restoration ecology and modern ecosystem management because many ecological processes take place over decades or centuries (Morecroft et al. 2009). Moreover, the consequences of system change on long-lived species like trees might not be evident until considerable time has passed (e.g., Lindbladh et al. 2008). As such, quantifying the patterns and processes of past ecosystems informs the stewardship of contemporary ecosystems (Beller et al. 2020).

Forest resiliency to disturbance is one area of historical ecology that could be more robustly understood over longer time periods and requires long-term data to investigate. For long-lived organisms such as trees, the relevant time frame for historical ecology is centuries to millennia (Swetnam et al. 1999). Long-term records that incorporate the fate of multiple generations of tree populations under different climatic stressors or land managers provide more relevant context than shorter records. Such records are derived from fossil pollen or other paleo-ecological data. Paleo-ecological records can assist in quantifying long-term variability as well as identifying alternate steady states, such as fossil records that document transitions from steppes to forests. However, paleo-ecology remains an underused resource in land management and restoration ecology (Davies and Bunting 2010), in part because paleo records typically provide qualitative information, i.e., narratives of ecological change, rather than actionable quantitative data.

In the U.S., forest management for restoration goals often relies on the determination of historical baselines, but they are seldom based on paleoecological information. Instead, baselines are typically informed by forest inventories from the period of Euro-American colonization (Hanberry and Dey 2019), which in the western United States began in 1848 (Busam 2006). A common baseline for the fire-prone forests of California is the state of forests before fire suppression (USDA Forest Service 2013). The underlying assumption of this baseline is that forests maintained their form and function despite reoccurring disturbances before 1850 (Landres et al. 1999). For example, in the Sierra Nevada, the US Forest Service defines the "natural range of variation" in terms of the variation in ecosystem processes and structure during the 16th to mid-19th centuries (1500-1850 AD, Safford and Stevens 2017). However, limiting characterizations of forests to the past few centuries has drawbacks; for example, it discounts millennia of land management and cultural burning by Indigenous people (Kimmerer and Lake 2001, Stephens et al. 2007).

A key aim of my dissertation, therefore, was to understand historic land use patterns in northern California over longer time periods than current baseline reference periods to understand the role of anthropogenic and biophysical controls on forest biomass. In California and other North American landscapes, some have argued that the impact of Native burning at the landscape scale was negligible, and that the effects of climatically-driven fires exceeded anthropogenic fires (Vale 2002, Vachula et al. 2019, Oswald et al. 2020). Yet, methodology that combines

paleoecology, local ethnographies, and archaeological information have successfully distinguished human-caused vegetation change from climatically-driven vegetation changes in California (Ejarque et al. 2015, Klimaszewski-Patterson and Mensing 2016). For example, anthropogenic impacts were indirectly detected during the cool and wet Little Ice Age in the Sierra Nevada (Klimaszewski-Patterson and Mensing 2016) and Klamath Mountains (Crawford et al. 2015), as well as modeled in the Sierra Nevada paleo-landscape (Klimaszewski-Patterson et al. 2018).

The overarching aim of my dissertation was to quantitatively understand the impacts of anthropogenic and natural fire disturbance on tree biomass and to develop a long-term record of forest conditions in Six Rivers National Forest (hereafter 'Six Rivers') in northwestern California. I chose Six Rivers as a study location for several reasons. First, it overlaps the Klamath Mountains bioregion, an area of exceptional floristic diversity (Whittaker 1960) that also contains numerous small lakes harboring sedimentary records. The Klamath Mountains bioregion contains the most diverse conifer forests in North America (Cheng 2004) as well as exceptionally diverse hardwood forests with oak dominant woodlands (Skinner et al. 2006). Presently, the forests of Six Rivers contain some of the densest forest carbon stocks in California (Gonzalez et al. 2015). Given the area's carbon density and recent history of large wildfire events (>100 000 acres), the landscape has become a 'high priority' zone according to Cal-Fire's Priority Landscapes map (Fire Resources Assessment Program 2018). However, this area of the state has received less research attention than other forested lands, such as the Sierra Nevada.

My three chapters all concern, in some form, quantitative reconstruction techniques, and my dissertation is organized as follows. Each chapter contributes to my overarching goal of understanding the historical ecology of Six Rivers in northwestern California. In chapter 1, I used robust plotless density estimation to provide a regional quantification of Six Rivers' forest composition and structure. I addressed the following questions to compare contemporary forest conditions to those from the 1880s:

> 1) Have tree density, basal area, and biomass of the contemporary forest increased in comparison to forest conditions from the 1880s?
> 2) Were oak and pine dominated forests more common during the 1880s?
> 3) Do documented changes in the disturbance regime since Euro-American colonization explain the differences in forest structure and composition?

In chapter 2, I developed an emerging paleo methodology to model the relationship between pollen influx and tree biomass using precise chronologies of the pollen system, with the goal of applying these models to longer term pollen influx datasets in chapter 3. I used modern pollen influx data and vegetation abundance data to answer the following:

> 1) What is the spatial relationship between pollen flux in small lakes and surrounding vegetation cover, through modeling of the aRSAP and tRSAP?
> 2) Can a PAR-biomass model be calibrated using distance-weighted biomass for major tree taxa?
> 3) What is the potential of this model to reconstruct past changes in assemblage-wide biomass from the region?

In chapter 3, I applied the models from chapter 2 to a 3,000-year record of pollen influx data. The fundamental question I answered was:

      1) What is the extent to which climate and/or human activity influenced major trends in reconstructed forest biomass over the past 3000 years?

The 3000-year record of biomass fluctuation is, to my knowledge, one of only three records of Holocene-era tree biomass compiled thus far. Unlike the other two quantitative biomass records (Seppä et al. 2009, Morris et al. 2015), I quantified the uncertainty in my reconstruction and took a multidisciplinary approach that included cross-referencing with independent datasets. The results from chapter 3 contribute to an ongoing debate about the influence of Native management on forest conditions pre-contact. My final chapter thus allows me to contribute not only to basic tenets of disturbance ecology, but also to contribute to ideas in land management and restoration ecology.

ACKNOWLEDGEMENTS

I am in awe of the amount of professional support I have received over the last five years at UC Berkeley. I have been privileged to know so many thoughtful, kind people who have helped me flourish at this institution.

To my advisors, John Battles and Matthew Potts: No one has shaped my development as a scientist and scholar more than you two. Thank you for helping me strive for excellence and rigor in my research, and for your confidence in my ability to undertake a dissertation outside of your primary expertise. As intellectual guides, you have been superb. Thank you for providing so much constructive feedback, which has advanced my critical thinking skills and pushed me to ask cutting-edge questions. For the past five years, I knew I could count on you for help facilitating my research plans at all stages, and that was a huge gift. Through your sponsorship, I have had unparalleled professional opportunities as well as received funding from several fellowships, all of which have boosted my career. Thank you, also, for being alert to the pressures that affect graduate students and participating in departmental endeavors to improve graduate working conditions. Above all, thank you for being available, kind, and good-humored advisors who always had my back.

I was lucky enough to meet one of my committee members, Dave Wahl, early on in my time at Berkeley, which altered the course of my dissertation research. Through your rigorous paleo-ecological lens, I was able to not only develop an ambitious research agenda, but also carry out my plans in the Quaternary paleo-ecology lab that you manage. You have an ability to weave empirical and anthropological data to tell compelling stories, and your scientific vision inspires my work. I am grateful to continue working with you as a post-doctoral researcher.

Thank you, also, to my committee member Wayne Sousa. I was pleased and intimidated that one of the giants in the field of ecology agreed to be on my committee. I soon learned that your scientific brilliance is equally matched by your helpful and supportive nature. Thank you, Wayne.

A cold email request to talk about the Klamath led me to meet one of the most important collaborators on my dissertation research: Jim Wanket. Jim, I learned so much from your 20+ years of scholarship in the Klamath area. I truly could not have embarked on this project without your expert's command of the Klamath's physical geography, as well as your guidance on key methodological techniques like lake coring and pollen identification. Thank you for generously sharing knowledge and your time. Collaborating with you has made my dissertation much more scientifically sophisticated as well as grounded in natural history.

I have been fortunate enough to collaborate with other exceptional Quaternary paleo-ecologists, namely Marie Champagne and Lysanna Anderson. Marie, I am inspired by your meticulous laboratory habits and flair for excellence. Lysanna, I aspire to your unwavering determination to produce careful datasets and to open every "black box" and understand its contents. Thank you both for bouncing ideas around and asking thoughtful questions.

CHAPTER ONE

Forest structure and composition in the Klamath Mountains in the 1880s:
Reconstructing a historical baseline[*,**]

Abstract

Historical baselines of forest conditions provide reference states to assess how forests have changed through time. In California, the Public Land Survey System (PLS) provides tree inventory data between 1872-1884 at 93.2 km^2 (36mi^2) resolution. Although these data provide a spatially extensive record of forest conditions in the 1880s, reconstructions using PLS data have been limited and controversial in western landscapes. Recent improvements in the application of plotless density estimators (PDE) have made reconstructions more accurate and robust. The purpose of this study was to use PDE to reconstruct the forest conditions during the Euro-American colonization era in Six Rivers National Forest– a floristically diverse temperate forest in the Klamath Mountains of northwestern California – to quantify differences with modern conditions. Records of fires and harvests were used in conjunction with the PLS data to understand the influence of forest management during the previous century. The contemporary forest in Six Rivers contains three times more trees than in the 1880s with a comparable increase in tree basal area. Forest composition during the late nineteenth century was predominantly Douglas-fir (34.4%), pine (24.2%) and oak (21.9%) by basal area. Contemporary forests support more Douglas-fir (45.2%) and a similar amount of pine (26.1%), while oaks have decreased by more than half (9.3%). These increases in tree abundance occurred despite extensive, mid-century timber harvesting in Six Rivers. Although large fires have burned in Six Rivers between 2000 and 2019, far fewer fires occurred during the twentieth century. Our results suggest that effective fire suppression contributed to the densification of the contemporary forests in Six Rivers.

1. Introduction

In an era of rapid climate and land-use change, quantifying the patterns and processes of past ecosystems vitally informs the stewardship of contemporary ecosystems (Beller et al. 2020). For example, global and national land management projects use 'natural' baselines (before human modification) and 'historical' baselines (data gathered in the recorded past) as starting points to detect the magnitude of landscape changes and to establish targets for restoration (Swetnam et al. 1999, Alagona et al. 2012, IPBES 2018). However, evidence for pre-modern natural baselines is constrained by poor spatial or temporal resolution, limited taxonomic resolution, and physical degradation (Egan and Howell 2005). Data for historical baselines, though obtainable, often represent only a single snapshot of a community and can underestimate or overestimate the extent of change (Barak et al. 2016). The need for robust baselines is particularly acute for ecosystems with altered disturbance regimes (Higgs et al. 2014).

For many forests in the U.S., management decisions implicitly rely on an understanding of ecosystem change relative to the recent past. For fire-prone, semi-arid forests in California, a common baseline is the state of the forest prior to the imposition of active fire suppression (Egan and Howell 2005, USDA Forest Service 2013). A century of suppression has significantly modified the structure and composition for many of California's conifer-dominated forests (Steel et al. 2015). Most efforts to date aimed at determining baselines have focused on the yellow pine and mixed-conifer forests of the Sierra Nevada and Southern Cascade Range (e.g., Taylor et al. 2000, Collins et al. 2011, Taylor et al. 2014, Hagmann et al. 2018). Results have largely converged on similar findings: Prior to fire suppression, these forests were open and dominated by large, drought and fire-tolerant trees. Presumably, this structure was maintained by frequent low and moderate severity fires. In the absence of fire, contemporary forests have increased in density and shifted species composition toward more fire-sensitive species. However, some research has argued that pre-suppression forests in the Sierra Nevada were dense, closed-canopy forests maintained by fire regimes that included historically extensive, high severity fires (Baker 2014, Baker and Hanson 2017, Baker and Williams 2018).

The structure and composition of forests from the Euro-American colonization era in northwestern California, in contrast, are dissimilar enough to warrant their own exploration. Unlike the montane forests of the Sierra Nevada and Cascade Range, the Klamath Mountains bioregion harbors the most diverse conifer forests in North America (Cheng 2004) and exceptionally diverse hardwood forests with oak dominant woodlands (Skinner et al. 2006). Prior to fire suppression, the Klamath area supported a mixed-severity fire regime characterized by mostly small, low-intensity, frequent fires, and infrequent large, burns of mixed-severity (Taylor and Skinner 2003). The region's diverse patterns of topography, climate, and soils have created heterogeneous vegetation patterns (Fig. 1) more complex than those found in the Sierra Nevada or Southern Cascade Range (Sawyer and Thornburgh 1977, Skinner et al. 2018). Taylor and Skinner's (2003) reconstruction of the historical forest in the Hayfork study area of Shasta-Trinity National Forest suggests a similar impact of fire suppression, namely an increase in tree density and a shift toward more fire-sensitive species. However, this detailed effort was limited in spatial extent (25 km^2). Given the heterogeneity of the Klamath region, the characteristics of the pre-colonial forests and the extent of its divergence from the contemporary forests remain unclear.

Northern California forests are high priority-landscapes for federal and state restoration projects (USDA Forest Service 2013), particularly the Klamath Mountains bioregion. These forests are expected to undergo rapid decline in conifer dominance (Tepley et al. 2017, Serra-Diaz et al. 2018) as climate change disrupts the mechanisms that promote forest stability, namely regeneration, growth, and fire tolerance. As forests transform, they become more at risk of increasingly large and severe fires because of dangerously high fuel loading coupled with a projected warmer climate (Westerling 2018).

The determination of historical baselines in U.S. forest management planning most often relies on forest inventories from the Euro-American colonization era (Hanberry and Dey 2019), which is defined in the western United States as the period beginning in 1848 when substantial numbers of miners settled in the region and displaced Native populations (Bright 1978, Busam 2006). Although the period between 1850-1900 is sometimes referred to as the 'settlement' era in the literature (Galatowitsch 1990, Friedman and Reich 2005, Hessburg et al. 2005), this historic period is more accurately described as the era of Euro-American colonization because Indigenous peoples had already settled the landscape. In conjunction with western migration across much of the U.S., the General Land Office (GLO) through the Public Land Survey (PLS) conducted systematic land surveys designed to demark territory, categorize resources, and aid colonization (Schulte and Mladenoff 2001). Central to the PLS data were witness trees (or bearing trees) – i.e., trees for which the bearing and distance from post markers were known (Whitney and DeCant 2001) – that today provide the best record of forest composition from this time period.

PLS records thus provide a quantitative path to understanding historic forest ecosystems in western federal landscapes, but they have not been fully leveraged (Galatowitsch 1990, Bjorkman and Vellend 2010). In southwestern Oregon, PLS data have been used to reconstruct vegetation cover (Duren et al. 2012), while other research concerning western land surveys has focused on specific phenomenon in discrete forest types (e.g., fire regime reconstruction in dry forests, Hessburg et al. 2005, Baker 2012, Odion et al. 2014, Baker 2015b, Baker and Williams 2018). Summaries of PLS data exist for some areas (e.g., the Eldorado National Forest, Fites-Kaufman 1997; Lake Tahoe Basin, Manley et al. 2000; Stanislaus, Sierra, and Sequoia National Forests, Hyde 2002). In contrast, eastern North American public land survey records have been used extensively to reconstruct forest density, biomass, and changing composition (e.g., Radeloff et al. 1999, Whitney and DeCant 2001, Rhemtulla et al. 2009, Hanberry et al. 2012b) and to guide land management (Friedman and Reich 2005, Goring et al. 2016, Kujawa et al. 2016).

This study uses robust methods for plotless density estimation (PDE, see below) to analyze the PLS data (~1880s) and characterize forest conditions in the California portion of the Klamath Mountains bioregion. Specifically, we determined historical baseline conditions for the forest, which we then compared to modern vegetation survey data to determine how fire suppression and timber harvests have changed this forest. We also used reconstructed basal area to estimate aboveground live biomass from the 1880s. Estimating this era's biomass in California is particularly important because California is one of the few jurisdictions in the world to enact greenhouse gas emissions reductions and has a legal obligation to understand, measure, and manage its forest carbon (AB-23 2006). We asked:

1) Have tree density, basal area, and biomass of the contemporary forest increased in comparison to forest conditions from the 1880s?
2) Were oak and pine dominated forests more common during the 1880s?
3) Do documented changes in the disturbance regime since Euro-American colonization explain the differences in forest structure and composition?

1.1 Study Site
Established in 1947 and named for the Smith, Klamath, Trinity, Mad, Eel, and Van Duzen rivers (USDA Forest Service 2013), the Six Rivers National Forest (hereafter, Six Rivers) encompasses 387,523 ha (957,590 acres) across northwestern California. The predominant forest type across Six Rivers is Douglas Fir at 46% (Fig. 2). As part of the Klamath Mountains, this management area is characterized by exceptional floristic and geologic diversity (Whittaker 1960). Forest assemblages of the Klamath Mountains bioregion were well established 2,000 years BP, according to Holocene-length pollen records (Mohr et al. 2000, Wanket 2002, Briles et al. 2008, Skinner et al. 2018). Over the past century, however, woodlands have become closed forest systems with more fire sensitive species (Crawford 2012). Currently, low-elevation forests are dominated by *Pseudotsuga menziesii* (Douglas-fir) and multiple *Pinus* (pine) species, with a broadleaf component of *Quercus kelloggii* (California black oak), *Notholithocarpus densiflorus* (tanoak), and *Arbutus menziesii* (Pacific madrone). Higher-elevation montane forests (above ~1200 m) are dominated by *Abies concolor* (white fir) and *Abies magnifica* (red fir; Sawyer and Thornburg, 1977), whereas sub-alpine (above ~1700 m) zones include *Tsuga mertensiana* (mountain hemlock) and *Picea breweriana* (Brewer spruce) (Sawyer and Thornburg 1977; Briles et al. 2011). On areas of ultramafic soils derived from serpentinite and peridotite bedrock, *Pinus jeffreyi* (Jeffrey pine), *Pinus monticola* (western white pine) and *Calocedrus decurrens* (incense cedar) are the dominant forest taxa (Whittaker 1960; nomenclature follows Greenhouse et al. 2012).

Fire history Prior to twentieth century fire suppression, the landscape had a mixed-severity fire regime characterized by mostly small, low-intensity, frequent fires, and infrequent large, burns of mixed-severity (Taylor and Skinner 2003; Crawford et al. 2015). On average, fire rotations were short (~15-30 years). Due to mountainous regional topography, fires burned with great spatial complexity creating openings of variable size (Taylor and Skinner 1998). At the local scale, Native burning and selective encouragement of species had significant effects on vegetation structure (Crawford et al. 2015). Native people used fire in various ways: to increase food (acorns, berries, roots) and materials (fiber for baskets), to improve hunting conditions, and to facilitate religious ceremonies (Lewis 1993). Although Native ignitions appear to have been widespread, the extent of their influence on fire regimes and regional vegetation scales remains unknown (Skinner et al. 2006). The arrival of Europeans drastically disrupted and reduced Native burning practices (Busam 2006). Fire scar records and sedimentary charcoal data indicate an abrupt fire-free period across the bioregion starting in the early 1900s (Agee 1991; Wills and Stuart 1994; Taylor and Skinner 1998, 2003; Stuart and Salazar 2000; Skinner 2003a, 2003b). Fire suppression officially began in 1905 (Shrader 1965). These efforts were effective in accessible areas by the 1920s (Agee 1991; Stuart and Salazar 2000; Skinner 2003a, 2003b; Taylor and Skinner 2003; Fry and Stephens 2006) and in remote areas after 1945 (Wills and Stuart 1994, Taylor and Skinner 1998, Stuart and Salazar 2000). The last pre-suppression fires recorded in the fire scar records for two lakes in Six Rivers occurred in 1903 and 1898

(Crawford 2012). Fire rotations increased markedly between 1900 and 1995: in the Hayfork study area, the rotation was 196 years (Taylor and Skinner 2003) and regional fire rotations reached a high of 974 years between 1959 and 1984 (Miller et al. 2012).

Land management Logging was widespread and intense throughout the Six Rivers management area. Starting in the 1930s, the Forest Service promoted new logging developments and helped the lumber industry expand (Conners 1998). Commercial forest area was largely old-growth stands estimated at 250 years old or older. For the first 15 to 20 years after the 1947 establishment of Six Rivers, the federal government projected an annual timber harvest of approximately 300,000 m^3 and their plan encouraged selective cutting of large, high-value trees that had ceased growing (USDA 1947). As a timber-producing forest, Six Rivers had enormous standing stock: an estimated 16,753 million board feet of which 80 percent was Douglas-fir (Conners 1998). (Note that this estimate is presented in board feet to match original reports (Conners 1998) and to avoid confounding harvest estimates by any changes in the scaling system over time (Spelter 2002)). An extensive road network for handling log loads was built and contained some 800 km of roads and 2,250 km of trails (Forest Situation Report 1947). The replacement of multi-aged old-growth forests with even-aged stands, coupled with fire suppression, greatly reduced the regional forest heterogeneity. These conditions allowed large wildfires, when they do occur, to become increasingly stand-replacing from the 1970s onward (Skinner et al. 2006, Miller et al. 2012).

2. Methodology
2.1 Background on PLS and PDEs
Across much of the U.S., the General Land Office (GLO) through the Public Land Survey (PLS) conducted systematic and widespread sampling of species composition. Although PLS was designed to demarcate territory and catalyze Euro-American settlement (Schulte and Mladenoff 2001), witness tree surveys provide a widespread and systematic record of species composition from this time period. PLS data consists of 6 x 6-mile townships with 36 embedded 1 x 1-mile sections (Foreman 1882). Permanent monuments mark section corners at the end of the 1-mile section lines and so-called 'quarter corners' lay halfway between two section corners (Bourdo 1956, Schulte and Mladenoff 2001). Surveyors selected nearby witness trees (bearing trees) as reference points to the corners – one tree in each quadrant (NE, NW, SE, SW) at section corners – recording the distance, direction, species, and stem diameter of each tree (Foreman 1882). Four witness trees were used at section corners and two bearing trees were used at quarter corners (Foreman 1882). Starting in the southeastern section, surveyors moved north and west, collecting what they called 'interior' tree data (Fig. 3). Surveyors also collected 'exterior' tree data along the boundary between two townships by the same methodology, i.e., recording four trees at section corners and two at quarter corners.

Methods to robustly reconstruct tree density from PLS records exist (Levine et al. 2017, Cogbill et al. 2018). PDEs rely on tree-to-tree, point-to-tree, or point-angle-tree distances to determine density in an efficient sampling scheme. Many PDEs have been used, but distance-based PDEs developed by Cottam, Pollard, and Morisita have been most frequently applied to PLS data (Cottam and Curtis 1956, Pollard 1971, Morisita 1957). A full explanation of the historical development and mathematical foundations of the PDE equations are detailed in Cogbill et al. (2018).

In fact, the PDE format was inspired by the public land survey sampling design. Important properties of the survey, however, are not inherent in some PDE models, and therefore only certain PDEs should be applied to PLS data (Cogbill et al. 2018). One problem arising from PLS sampling design is the low sampling density (minimum separation is 0.8 km, i.e., 0.5 mile), which results in regionally non-stationary mean densities and regional heterogeneity (Cogbill et al. 2018). Moreover, the performance of the models depends on the spatial arrangement of trees (Grimm 1984), and trees are often non-randomly dispersed at the local level. Hence, PDEs that assume complete spatial randomness (CSR) or are highly sensitive to non-randomness are not suitable for PLS data (Engeman et al. 1994, Kronenfeld and Wang 2007, Bouldin 2008, Hanberry et al. 2011). Lastly, PLS data have an unknown level of surveyor bias (Bourdo 1956, Grimm 1984, Bouldin 2008, Liu et al. 2011, Kronenfeld 2015).

Of the available PDEs, those in the family of non-CSR models are the most applicable to public land survey data, specifically, the Morisita PDEs. Morisita IV uses the nearest tree in each of the four sections and responds to local spatial patterns. Morisita II, however, uses only two trees and is therefore less responsive than Morisita IV to local spatial patterns. Morisita II increases variability but lowers bias such that it is preferred for PLS datasets and was used in this work (Picard et al. 2005, Cogbill et al. 2018). Using the Morisita II (Morisita 1957), density is calculated:

$$\lambda = K * \left[\frac{1}{\pi N}\right] \cdot \left[\sum_{i=1}^{N} \frac{2}{\sum_{j=1}^{2}(r_{ij}^2)}\right] \qquad (1)$$

Where λ = tree density in trees/ha, N is the total number of points, and r is the distance from point j to tree i. K is the scaling coefficient. Since r_{ij} is measured in meters and density is reported in trees/ha, K = 10,000.

2.2 Six Rivers PLS data
All surveys in Six Rivers were carried out between 1872 and 1884. Data collection was typically conducted by one compass man, two chainmen, two axe men, and a flagman in a standardized way across each township in their charge. Of the 90 townships encompassed by the Six Rivers management area, data from 76 townships were available (Fig. 4). PLS records were obtained from scanned copies of the original field notes, which are stored in the Bureau of Land Management's cadastral survey office in Sacramento, California.

Witness tree data were extracted from the handwritten archive into digital datasets for this analysis. Surveyors commented sporadically about rock type, soil texture, land features, and shrub cover in the original notes, but these details were not transcribed. Although the vast majority of trees was recorded with distance, direction, species, and stem diameter information, surveyors' notes contained three distinct types of omitted/absent data. Surveyors reported 'no trees within limits' when trees were present but were too far away for measurement. They reported 'pits impractical' when field conditions prevented physical demarcation of witness trees. Lastly, some entries were blank without explanation. These distinctions were recorded into as 'NTWL', 'PI', and 'NA', respectively.

Species identifications were inconsistent across surveyor crews (Appendix S1: Table S1) for some taxa categories. Five surveyor deputies – Brunt, Foreman, Haughn, Holcomb, McCoy – signed off on 92% of the records in the dataset, although they were not the ones collecting the data (crew names are unknown). The crews under Brunt, Holcomb, and McCoy recorded more species than Haughn and Foreman. Crews from Brunt, Holcomb and McCoy made distinctions between oaks (Black, White, Live), and Holcomb separated tanoak (*Notholithocarpus densiflorus)* and chinquapin *(Chrysolepis chrysophylla)* from true oaks *(Quercus spp.)*. In contrast, Foreman's crews did not differentiate oaks; instead, they lumped them into a generic 'Oak' category that included tanoak and chinquapin; this crew also used a generic 'Fir' for both *Pseudotsuga* and *Abies*. Pine, madrone, and cedar (the latter category including both *Calocedrus decurrens* and *Chamaecyparis lawsoniana* [Port Orford cedar]) were consistently separated across surveyor crews, however.

Given these findings, we created seven taxa categories to account for the variation in taxonomic resolution. They were Douglas-fir, oak, pine, cedar, madrone, other conifers, and other hardwoods. Our Douglas-fir category includes all original 'Spruce' identifications as well as original 'Fir' identifications below 1,370 m. True *Picea* is restricted to a very few sites at high elevations in the study area, and 'Spruce' was used extensively as a common name for *Pseudotsuga menziesii* (Peattie 1950). We used 1,370 m elevation to discriminate between Douglas-fir and true *Abies* because at that elevation there is a dramatic shift in dominance from *Pseudotsuga* to *Abies* in the modern forest (Appendix S1: Fig. S1a). We kept the generic oak category of Foreman's surveyors because the elevation ranges of tanoak and true oaks overlap significantly, making elevation-based discrimination impossible (Appendix S1: Fig. S1b).

2.3 PDE methods
Before analysis, we addressed missing and inconsistent information in the records. Any point with an NA was deleted. Like NA, all PI points were deleted. For NTWL, a maximum distance of 100.5 meters (500 links) was inserted. Since no trees were present at NTWL, basal area was always set equal to zero with a default density = 0.3 tree/ha, the density estimate when the distance to the nearest tree is the 100.3 m from the point. In rare cases (3%), corners had three or one tree recorded, instead of the expected four (section corners) or two (quarter corners), without explanation from the surveyors; these data points were removed. Also, 41 corner points had multiple entries. For these replicated points, we systematically selected the witness tree data from the interior (i.e., first) measurement unless there were missing data.

The clean dataset was analyzed using Morisita II (Eq. 1, Cogbill et al. 2018). First, section corners with four witness trees were reduced to two trees. Care was taken to ensure the closest tree on either side of the survey line was selected. Specifically, the closest tree in the east and west semicircle were included for surveys running N/S (most points). For surveys running E/W, the nearest tree in the north and south semicircle were included. Density in trees/ha (TPH) were calculated for each point using Eq. 1. Basal area per tree (m^2/ha) was calculated as the basal area of the individual tree (m^2, calculated with DBH) multiplied by the point estimate of TPH/2. Basal area per point was calculated as the sum of the basal area of the two neighboring trees. To calculate relative abundance by taxa, the basal area of trees was summed and divided by the total basal area in each vegetation type.

The calculated density and basal area assume that surveyors used a fixed sampling design of the nearest tree on each side of the section line. Surveyors had three documented reasons for bypassing the nearest tree: spatial geometry of less than equal halves; azimuthal censoring; and elimination of trees very near the corner (Manies et al. 2001, Kronenfeld and Wang 2007, Liu et al. 2011, Goring et al. 2016, Cogbill et al. 2018). The base metric was adjusted for these surveyor biases by a multiplier derived from the empirical witness tree bearing and distance measurements recorded by the surveyor. Corrections for surveyor bias followed procedures outlined in Goring et al. (2016). The union of these surveyor biases yields a single correction factor that increases the base density and basal area due to surveyor biases not sampling the nearest tree (Appendix S1: Table S2).

Density estimates were further corrected to account for the ambiguity in the minimum diameter of witness trees. Many studies have noted the logical absence of very small witness trees. Given their size and longevity, small trees make poor monuments and thus tend to be under sampled (e.g., Bouldin 2010, Hanberry 2012a, Goring et al. 2016). To adjust for this bias, we set a lower diameter limit of 20 cm and adjusted the raw density measurement by the proportion of witness trees > 20 cm DBH (Goring et al. 2016, Appendix S1: Table S2).

2.4 GIS methods
In ArcMap (10.6.1, ESRI 2011), Six Rivers' boundary was obtained from the USDA Forest Service Administrative Forest dataset (USDA Forest Service 2019). All datasets used the North American Datum of 1983 (NAD 83). Vector data of townships and ranges were obtained from BLM California cadastral PLS standardized data (USDOI 2019). A digital elevation model for Six Rivers was built from seven 1/3 arc-second tiles with a resolution of 10 meters (US Geological Survey 2013). Vegetation data from Cal-Fire Fire and Resource Assessment Program (called 'FVEG,' hereafter) was used (California Department of Forestry and Fire Protection, 2015). The wildlife habitat relationship class code in FVEG (Appendix S1: Table S3) was used to distinguish forest cover types at 30 x 30 m resolution. (Note that forest cover types, e.g., Klamath Mixed Conifer or Montane Hardwood, were capitalized in descriptions from FVEG and capitalization is preserved in this document (USDA Forest Service2010). Douglas Fir refers to the cover type from FVEG, whereas Douglas-fir refers to *Pseudotsuga menziesii*)

The spatial location of witness trees was determined by linking the unique point identifier from BLM's cadastral PLS standardized dataset to the historical data. Each PLS point code incorporates the meridian, township, section, and section/quarter corner and comes with latitude and longitude and elevation information (BLM 2006, USDOI 2019). PLS codes were created for 13,600 witness trees and FVEG vegetation polygon data were matched to those points.
The contemporary composition and structure of the forests in the Six Rivers management area were quantified using the most recent 10 years (2008-2017) of Forest Inventory and Analysis (FIA) data from the database version 1.8.0.0.1. FIA plots were clipped to the Six Rivers' extent and matched to FVEG classification types (Fig. 4). There was a total of 184 FIA plots sampled in Six Rivers. For trees > 20 cm in diameter, we calculated density, basal area, and aboveground live tree biomass by FVEG vegetation type. To ensure a sufficient number of samples in each vegetation type, we combined the two chaparral habitat types present in Six Rivers, namely Mixed Chaparral and Montane Chaparral, into one. While the Mixed Chaparral tends to be floristically richer than Montane Chaparral, these two broadly defined types overlap and shrub

species from two genera, *Ceanothus* and *Arctostaphylos,* are common constituents (CDFW 2020). We also merged the red fir and white fir alliances into one True Fir alliance (Appendix S1: Table S3).

Fire and harvest spatial information were obtained from state and federal agencies, respectively. Fire perimeter data from 1908 to 2018 were obtained from Cal-Fire's ArcGIS geodatabase file, grouped by decade, and clipped to Six Rivers' boundary. Harvest and salvage spatial information in Six Rivers began as Ecological Unit inventory (EUI) classification and mapping starting in the late 1980s. (FACTS data were not available for Six Rivers National Forest and data from the Ukonom region were unavailable). EUI's purpose was multi-pronged and included: estimating land productivity, understanding plant communities, determining long-term landscape processes, and identifying renewable products. In 1995, Six Rivers' office obtained ArcInfo and the ability to digitally map on the fly using geo-referenced Digital Ortho-photo quads (USDA Forest Service 2001). Between 1994 and 1999, Six Rivers' vegetation was mapped based on seral stage and potential natural vegetation type using aerial photography and ortho photograph quadrangles (USDA Forest Service 2001). An estimated 25% of the survey areas were ground-truthed (USDA Forest Service 2001).

2.5 Analyses
We evaluated the differences in forest composition and structure between the two periods by comparing means. Significant differences were defined as non-overlap in 95% confidence intervals. A drawback with the Morisita II is that variance is not defined (Cogbill et al. 2018). Thus, we estimated confidence intervals using resampling methods (Crowley et al. 1992). Specifically, we resampled with replacement our point estimates of density and basal area 1,000 times. For each vegetation type, we reported the mean and 95% confidence interval of these 1,000 realizations. For FIA results, we reported the mean and calculated 95% confidence intervals using the t-distribution.

To estimate aboveground live tree biomass (AGL) for the 1880s, we developed a plot-level basal area to AGL transfer function from the contemporary FIA data. We explored several different functional forms to predict AGL as a function of basal area. We also tested for differences by vegetation type. We compared our candidate models using the Akaike Information Criterion corrected for small sample sizes (AICc). The linear log-log functional form with a single equation for all forest types best fit the data (ΔAICc = 7.1). Specifically,

$$\ln(AGL) = 0.997 * 1.234 * \ln(Basal\ Area) \tag{2}$$

with AGL measured in Mg/ha and Basal Area in m^2/ha (p < 0.001 and R^2_{adj} = 0.97). We used Equation 2 to calculate AGL for each point based on the bias-corrected basal area. We then summarized AGL by vegetation type using the resampling approach described above. These analyses were conducted using R statistical software (R Core Team 2018; version 3.5.1).

3. Results
3.1 Changes in forest structure
The contemporary forest in Six Rivers contains three times more trees than in the 1880s: 255 trees/ha vs 81 trees/ha. For four of the six vegetation alliances studied, the mean density

(trees/ha) was significantly lower (± 2 se) during the 1880s than in contemporary forests (Fig. 5, Appendix S1: Table S4 and Table S5). These alliances included Douglas Fir, Klamath Mixed Conifer, Montane Hardwood-Conifer, and True Fir. The mean densities of Chaparral and Montane Hardwood, however, did not change over time. The vegetation alliance with the largest significant increase in density was Klamath Mixed Conifer with a mean change of 300%. The greatest increase in basal area since 1880 occurred for Klamath Mixed Conifer with a seven-fold increase. These changes in basal area translated into a net increment in aboveground live tree biomass of 175 Mg/ha since the 1880s (Table 1). The increases in biomass over time by vegetation type ranged from a doubling (Montane Hardwood, Montane Hardwood-Conifer, and True Fir) to a tripling (Douglas Fir) to a nine-fold increase (Klamath Mixed Conifer).

3.2 Changes in forest composition by relative basal area
Forest composition during the 1880s was predominantly Douglas-fir (34.4%), though pine (24.2%) and oak (21.9%) comprised high percentages of the forest vegetation, with moderate levels of madrone (7.0%), low levels of true fir (6.5%), and less than 5% containing cedars, other conifers and other hardwoods (Fig. 6, Appendix S1: Table S6). Contemporary forests are increasingly Douglas-fir dominant (45.2%), although the pine and true fir alliances also slightly increased (Fig. 6, Appendix S1: Table S7). Oaks, however, decreased by more than half since the 1880s and now make up a similar percentage of the forest similar as true firs. The compositional changes observed across Six Rivers were consistent within alliance types. For example, the relative abundance of Douglas-fir increased in Chaparral and Douglas Fir types, and the proportion of pines increased in Klamath Mixed Conifer, Montane Hardwood, Montane Hardwood-Conifer, while the proportion of oaks decreased (Appendix S1: Table S6 and S7).

3.3 Drivers of change
During the twentieth century, particularly in the late 1940s, 50s, and 60s, major harvest and logging efforts took place in Six Rivers (Table 2, Conners 1998). Although almost certainly an underestimate, geospatial data indicate that management activity (Fig. 7) occurred on 25% of the total forest area (Appendix S1: Table S8). Of the known harvested areas, three seral stages – 'pole harvest', 'shrub harvest', and 'early harvest' – accounted for 80% of the total (USDA Forest Service 2001). Based on assessments in the mid-1990's, stands classified as pole and shrub harvests were considered the result of clearcutting while the early harvest category referred to stands with less intensive methods of harvesting (USDA Forest Service 2001). Extensive logging during the twentieth century was not accompanied by re-planting (Conners 1998) and therefore did not contribute to densification.

Mid-century was also a period of active fire suppression. Fire perimeter data show a marked decrease in fire activity, with nearly total cessation between 1940 and 1969 (Fig. 8). Spatially, large recent fires (2000-2018) tended to occur in areas where harvests were not recorded, such as the Ukonom area in eastern Six Rivers and along the California-Oregon border (Fig. 7). The acreage burned gradually increased through the 1970s, 80s and 90s, then quadrupled in the 2000s to 325,000 ha. Compared to the 2000s, fewer hectares burned in the 2010s, but the decadal average was greater than any other decade between 1908 and 1999. Between 2000 and 2018, over 500,000 ha burned, compared to nearly 200,000 ha during the entire previous century (Table 3). Fire rotations (Heinselman 1973) are the number of years needed to burn an area the size of the study area given the extent of burning in that period (Heinselman 1973, Agee 1993).

Fire rotations, correspondingly, varied between 1908-1995 and 1908-2018; the fire rotation was three times longer during the twentieth century compared to the last 110 years (Table 3). Underlying the effects of fire suppression were changes in climate that were consistent with warming trends (Fig. 9). Precipitation trends, however, did not change substantially, suggesting that this region did not experience the pronounced drought that impacted much of the Western U.S. during 2012-2015.

4. Discussion

Our comparison of PLS data to modern vegetation data indicates stark changes in forest structure – namely statistically significant increases in tree density and basal area – as well as changes in composition. Densification was expected. It has been observed in several locations near Six Rivers: Hayfork in Shasta-Trinity National Forest (Taylor and Skinner 2003), Blacks Mountain Experimental Forest in the Southern Cascades (Dolph et al. 1995, Ritchie et al. 2008), and Lassen Volcanic National Park (Taylor 2000, Skinner and Taylor 2018). However, the magnitude of change shown by this reconstruction was considerable: the contemporary forest in Six Rivers contains three times more trees than the forest of the 1880s, with a comparable increase in basal area (Appendix S1: Table S4, Table S5). Densification has occurred elsewhere in California, but not to such a degree. For example, a comparison of 1911 inventory data to the contemporary forest revealed a near doubling of live basal area in the central Sierra Nevada (Collins et al. 2017). On the other hand, the density of historical mixed conifer forests in the Oregon Cascades are comparable to the density of Six Rivers' forests from the 1880s. A reconstruction of a 1920s timber inventory showed an average of 14 ± 7 m^2 ha^{-1} (mean $\pm$ standard deviation, Hagmann et al. 2014) compared to our average of 13.3 ± 0.6 m^2 ha^{-1}.

Absent direct causal evidence, fire suppression is the most likely explanation of the widespread differences in forest structure and composition since 1880 in Six Rivers. This conclusion is consistent with other historic forest reconstructions from the Oregon Cascade Range and the Sierra Nevada that suggest fire exclusion played a dominant role in forest densification (Collins et al. 2011, Hagmann et al. 2013, 2014, Collins et al. 2015, Stephens et al. 2015, Collins et al. 2017). The onset of forest changes in Six Rivers coincides with the start of fire suppression (i.e., between 1903 and 1905; Crawford 2012, Shrader 1965). Fire scar studies from the Klamath Mountains indicate a fire regime characterized by small, low-intensity, frequent fires and occasional large, intense burns before Euro-American colonization (Crawford 2012). The pre-Euro-American fire rotation of 19 years increased to 238 years after 1905 (Taylor and Skinner 2003). Fire perimeter records, too, show a near cessation of fire activity over a 29-year period (1940-1969) in an area where frequent fire from Native burning and lightning ignitions was common over the last millennia, according to fire scar and charcoal records (Crawford et al. 2015, Skinner et al. 2018).

Fire suppression is also consistent with observed compositional changes in Six Rivers. For example, pollen records from two lakes in Six Rivers indicate a compositional shift to shade-tolerant Douglas-fir and tanoak at the expense of shade-intolerant taxa such as oaks during the last century (Engber et al. 2011, Crawford 2012, Crawford et al. 2015). Closed-forest indicators such as Douglas-fir strongly increased over the last century, during which time charcoal and fire peak magnitudes sharply declined (Crawford et al. 2015). We found similar compositional change – that is, an increase in Douglas-fir abundance and a reduction in oaks – which aligns

with a pollen record that shows a 3,000-year historic high of Douglas-fir and coinciding oak decline in modern times (Crawford et al. 2015). In contrast to the more open Klamath forests in the 1880s, a study that used PLS data for canopy cover reconstruction in southwest Oregon found a late nineteenth century landscape mostly covered by closed forests and woodlands, with a minor amount of open plant community types (Duren et al. 2012). However, this study differs from ours in both its analysis and location. Duren et al. (2012) calculated density (trees/ha) by using "an alternative point-centered quarter method that requires random distribution around a section corner," in place of Morisita's equation. Additionally, they reconstructed canopy cover in valleys and foothills across a greater elevation gradient (280 to 1480 m) than this study.

Timber harvesting and climate warming are also drivers of vegetation change, but they are likely not the dominant forces shaping the observed shifts in forest structure and composition. The type of timber harvests undertaken in Six Rivers would likely have lowered density. Harvest and salvage data (USDA Forest Service 2001), though incomplete, generally aligned with written records of timber extraction for the forest (Conners 1998). Although some silviculture treatments might increase forest density (e.g., removal and replanting at high density), extensive replanting programs following clearcutting were specifically not undertaken in Six Rivers, according to timber records (Conners 1998). Extraction would therefore be consistent with net forest thinning -- the opposite of the trend reported (Fig. 5). Interestingly, areas without historical harvests were also areas with large recent fires (Fig. 7), possibly because these areas supported extremely dense forests with a high fuel load. Although regional climate warming has occurred in the study area since the end of the Little Ice Age in 1860, the expected impacts of climate warming are not consistent with our results. Under a warming climate, a greater number of fire events and more open forest structure would be expected (Miller and Urban 1999), but the pollen and fire scar record has shown a decrease in fire events and an increasingly closed forest structure (Crawford 2012, Crawford et al. 2015).

Although we showed that forest structure was substantially less dense during the 1880s, the montane hardwood and chaparral vegetation alliances did not follow this trend. The lack of structural changes in the montane hardwoods might be related to widespread timber improvement efforts that favored conifer recruitment. For example, in the 1970s, hardwoods were systematically killed to support commercial conifers in the Shasta-Trinity National Forest, particularly in areas where conifer regeneration had started in the understory (pers. comm. Carl Skinner 2019). This effort may have occurred in Six Rivers and would be consistent with reduced montane hardwood densification compared to other alliances.

Chaparral in the Klamath are described as persistent shrub-dominated communities with the stability attributed to edaphic conditions (e.g., moisture limitations), frequent fires that constrain tree encroachment, and the ability to rapidly resprout after fire (Detling 1961). Given the mix of *Ceanothus* and *Arctostaphylos* cover (Appendix S1: Table S3) and the relative abundance of trees in both the 1880s and contemporary Chaparral (Appendix S1: Table S6, Table S7), the Chaparral alliance in Six Rivers appears to be what Cooper (1922) describes as the conifer forest chaparral association. This association is a mix of what Cooper terms "broad-sclerophyll" shrubs and "narrow-sclerophyll" (i.e., needled-leaved) trees. The structure of this alliance has remained notably consistent since the 1880s, a result that suggests these associations are maintained more by edaphic conditions than the fire regime. However, we cannot explicitly exclude the role of

fire given the absence of definitive evidence that fire did not occur in the chaparral zones. In contrast to the constancy in tree density, tree composition has switched from one dominated by pine in the 1880s (40.2%, Appendix S1: Table S6) to Douglas-fir in the contemporary era (39.6%, Appendix S1: Table S7).

Currently, Six Rivers is Douglas-fir and pine dominated. During the 1880s, Douglas-fir and pines were present at high percentages, but oaks were also a dominant feature, in part because they were an important cultivar for Native use. Severe oak decline has been known to follow European settlement in northern and southern California (Mensing 1999, Scholl and Taylor 2010, Stahle et al. 2013, Cocking et al. 2012, Cocking et al. 2014). This decline has been attributed to fire suppression that resulted in composition shift from shade-intolerant, fire-resistant pines and oaks to fire-intolerant and shade-tolerant firs and cedars (Taylor and Skinner 2003, Scholl and Taylor 2010). We also found this trend. Even though Douglas-fir and mixed conifers (pines) were targeted by logging efforts, their densities still increased.

Debates concerning historic forest density in dry, fire-prone, pine-dominated and mixed-conifer forests are ongoing and unresolved (e.g., Hagmann et al. 2018, Baker and Williams 2018). These discussions have focused on the fire regime that could support reconstructed forest conditions, namely whether the landscape before Euro-American colonization had low- to moderate-severity wildfires that maintained a low-density forest dominated by large trees (e.g., Hagmann et al. 2013, Collins et al. 2011), or whether mixed-severity and high-severity wildfires supported medium- to high-density forests (e.g., Baker and Williams 2018). An important element of this debate is the method used to reconstruct forest conditions from PLS data. Although our structural estimates are considerably lower than historic estimates from the Sierra Nevada, our PLS approach nonetheless broadly corroborates other findings, such as 1911 inventory estimates (Collins 2017), tree ring reconstructions that were calibrated with a 1911 timber inventory (Scholl and Taylor 2010), and other western PLS studies (e.g., Hagmann et al. 2018) and inventory reconstructions (Hagmann et al. 2013, 2014). Additionally, our methodology was consistent with the methodology used in the vast majority of PLS reconstructions (Bouldin 2010, Goring et al. 2016, Hanberry et al. 2019). That is, we applied methods proven to be accurate for California conifer forests (Levine et al. 2017), supported by PDE sampling theory (Cogbill et al. 2018).

Within the PLS research community, many previous studies concerning PDE reconstruction have assumed estimates are accurate (meta-analysis from Cogbill et al. 2018), while other studies have focused on developing statistical techniques to account for known PLS sampling biases (Bourdo 1956), as well as providing a means to correct for surveyor biases (e.g., Kronenfeld and Wang 2007, Kronenfeld 2015, Goring et al. 2016, Cogbill et al. 2018, Cogbill et al. 2020 *in prep*). In a comparison of mapped forest stands in California, the Morista II was consistently the most accurate PDE despite a wide range of tree densities and spatial distributions (Levine et al. 2017). We also used empirically-derived bias corrections (Cogbill et al. 2018) to increase the reliability of our historical estimates. Together these methods accommodate the complexity of the vegetation and limitations of the data.

Correcting for surveyor biases in witness tree selection in PLS datasets is an active area of research. The four corrections employed in this study (Appendix S1: Table S2) provide a

detailed picture of the mechanics of the original survey, as well as an estimate of impact of these mechanics on the results (Goring et al. 2016, Cogbill et al. 2018). Compared to uncorrected results (Appendix S1: Table S9 and S10), bias corrected density was an average of 12.7% lower across all alliances due to fewer trees meeting the > 20 cm DBH cutoff. In contrast, the corrected basal area was 28.3% larger since the exclusion of smaller trees has little impact on total basal area. The overall small error in witness tree placement (i.e., less than equal halves correction = 1.14 for all points, Appendix S1: Table S2) had the benefit of authenticating Six Rivers field data, an important conclusion in the wake of fraudulent land surveys found in the eastern United States. Surveyor discrimination against large trees (>35 cm DBH) has also been postulated (Bourdo 1956, Manies et al. 2001, Schulte et al. 2007, Rhemtulla et al. 2009, Bouldin 2010). The comparison of fitted size frequency functions (e.g., Bouldin 2010) and the observed number of large trees (e.g. Bourdo 1956, Williams and Baker 2010, Tulowiecki 2014) are consistent with a quasi-reverse J distribution of trees and not necessarily bias. In any case, bias against small trees is much more important than any large tree bias that would require bypassing a larger tree in order to use a smaller farther tree. In this study, the density of trees $\geq$ 50 cm DBH was 11 trees/ha. When using the definition of "large" tree for Douglas-fir (trees $\geq$ 92cm, Lutz et al. 2009), the density was 1 tree/ha; the density at the next largest cut-off ($\geq$ 61cm, Lutz et al. 2009) was 7 trees/ha. The 95th percentile of tree size for our data was $\geq$ 76 cm (5 trees/ha).

We also made corrections to improve taxonomic resolution. We found that some surveyors were careful taxonomists who identified species with similar forms (e.g., true oaks from tanoaks), while other surveyors lumped taxa. We corrected for Douglas-fir/true fir aggregation using an elevation cut-off (Figure S1a) but kept the generic oak category because the elevation ranges of tanoak and true oaks overlap, making elevation-based discrimination impossible (Figure S1b). Knowledge of common names used during the 1880s allowed us to correct Douglas spruce to Douglas-fir. We encountered incomplete data and noted three types of omissions, which were treated differently (see methods) in accordance with previous reconstructions (Cogbill et al. 2018). Fire perimeter and harvest data are also likely underestimates of landscape-scale management strategies, but they constitute the best available information for the last century.

Lastly, all methodologies used to reconstruct historic forest conditions have tradeoffs. For example, a major strength of PLS reconstruction lies in its regional coverage and replicated methodology (Bourdo 1956), compared to twentieth century inventory data which are not as extensive (Collins et al. 2011, 2017), or dendrochronological reconstructions, which provide great detail about stand dynamics but are spatially restricted (Taylor and Skinner 2003, Scholl and Taylor 2010). The type of reconstruction method greatly influences not just the research question that can be answered, but also the management implications of the findings. The basis for management decisions can be greatly strengthened by combining multiple corroborating historic or paleo records from different spatial resolutions (Maxwell et al. 2014). The reconstructions in this study are geographically extensive but coarse, which may have masked important historic structural or compositional variation. Given that Six Rivers is a highly diverse region – indeed it is unique in California for its floristic diversity – our results should be integrated with other landscape-specific reconstructions (e.g., the Hayfork study, Taylor and Skinner 2003) to inform management decisions.

Reconstructed baselines have contributed to debates about restoration by illuminating conditions considered to be ecologically resilient (Swetnam et al. 1999), particularly for fire-suppressed forests in western North America (Larson and Churchill 2012, Churchill et al. 2013). Restoration priorities already exist for other California landscapes, such as the Sierra Nevada, but different targets may be needed for northwestern California. Although Six Rivers has greatly densified over the past century, its historical baseline likely supported a more open, smaller-tree landscape, compared to the open, large-tree landscape of the Sierra Nevada forests. Hardwood decline since the 1880s may also factor into the design of restoration treatments for the area. Management objectives must also meet societal demands for ecosystem services and can be informed by understanding forests of the past. For instance, a better understanding of forests from the 1880s could inform engaged citizens about the structural diversity of iconic landscapes.

Our findings indicate a doubling of aboveground live biomass in Six Rivers since Euro-American colonization and are important in the context of climate change mitigation goals. California is one of the few jurisdictions in the world to mandate limits to greenhouse gas emissions and therefore has an urgent need to track and quantify forest carbon (AB-32 2006, Forest Climate Action Team 2018). Fire exclusion in California forests has led to a reduction in large trees and an increase in smaller trees (Taylor et al. 2014, McIntyre et al. 2015). This increase in density boosts carbon stores above that of frequently burned forests, but small-tree carbon storage is unstable in the long-term (Hurteau et al. 2019). Quantitative reconstructions of past forest carbon stocks can impart crucial ecological information – including tempering expectations around forests' ability to sequester carbon in fire-prone forests – as the state endeavors to meet its climate mitigation goals.

5. Conclusion

Our work reconstructs a large, forested area and provides a landscape-level structural description. For Six Rivers National Forest, we found clear differences between forest conditions during Euro-American colonization and the modern period. We also demonstrated a reconstruction methodology that deals with spatial complexity and is accurate under PLS conditions (Levine et al. 2017), correcting for biases (Cogbill et al. 2018). These analytical steps are generalizable and can be applied to future PLS datasets in western landscapes. This work also elucidates the drivers of change in Six Rivers. Fire suppression likely increased forest density despite widespread timber extraction. The area has been actively managed to varying extents for centuries and probably longer, and this snapshot in time captures the rapid transitional era from Native management to Euro-American colonization. It is one of many potential baselines.

Baselines provide an understanding of relative change: how much did a system change relative to a reference state in the past? For California ecosystems, which have undergone vast change since active fire suppression policies, the 1880s represents a useful historical baseline when restoration targets are predicated on fire regimes from before Euro-American colonization (Churchill et al. 2013). By building a continuum of baselines, ecologists can determine how the current landscape has deviated from previous points in time and impart context for current tree populations, which has implications for ecosystem services and societal demands.

Acknowledgements

Figures

Figure 1. Historical photo from the Sawyer's Bar area shows the spatial complexity of late nineteenth century vegetation along the Salmon River in the Klamath National Forest, which borders Six Rivers to the east (Eldridge 1910).
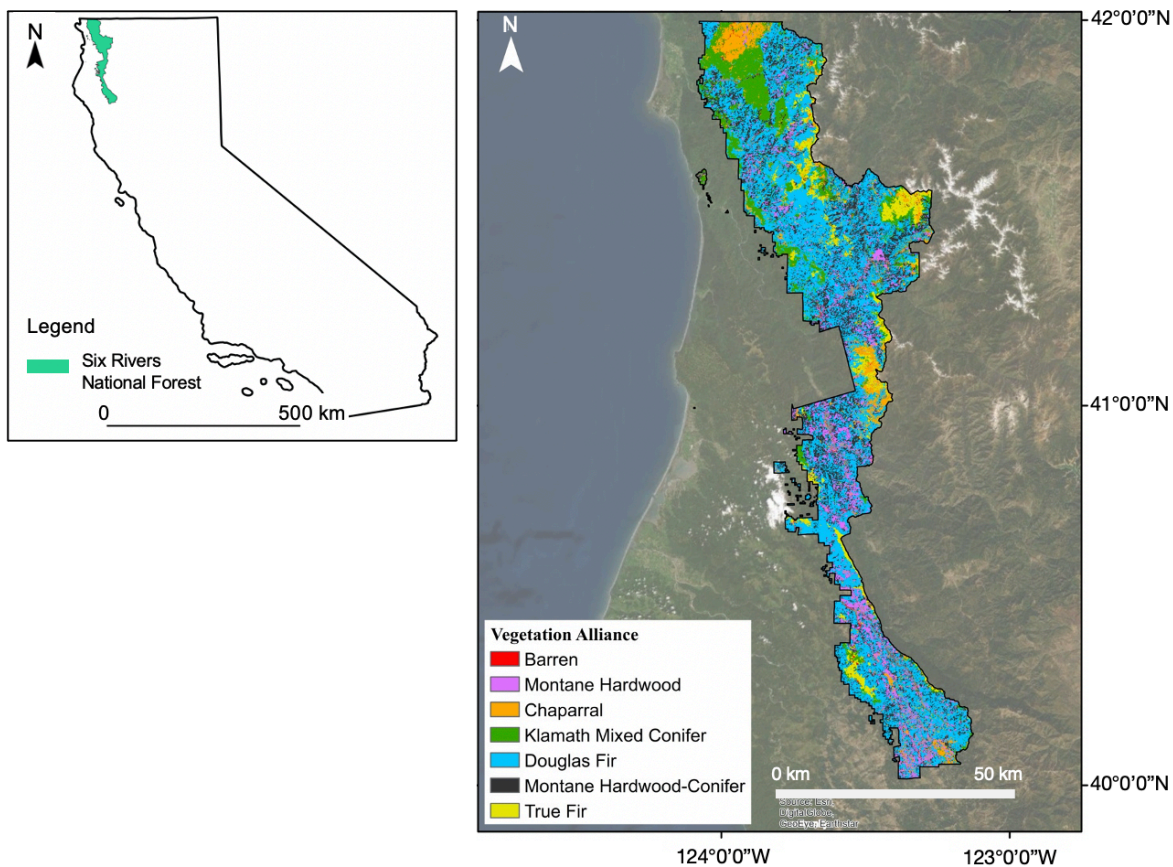
Figure 2. Six Rivers National Forest covers nearly 400,000 ha (~1 million acres) across Del Norte, Humboldt, Trinity, and Siskiyou counties (above). Vegetation alliances (right) include Montane Hardwood (purple), Chaparral (orange), Klamath Mixed Conifer (green), Douglas Fir (blue), Montane Hardwood-Conifer (black), and True Fir (yellow).

Figure 3. Township field note index for 13N5E of the Humboldt Meridian in California is a representative example of the surveying pattern used for PLS data collection (Foreman 1882). Sections are marked in black type. Surveyors marked the direction and sequence of their surveying paths with handwritten numbers (pencil); surveyors started in the southeast section and moved north and west collecting witness tree data.
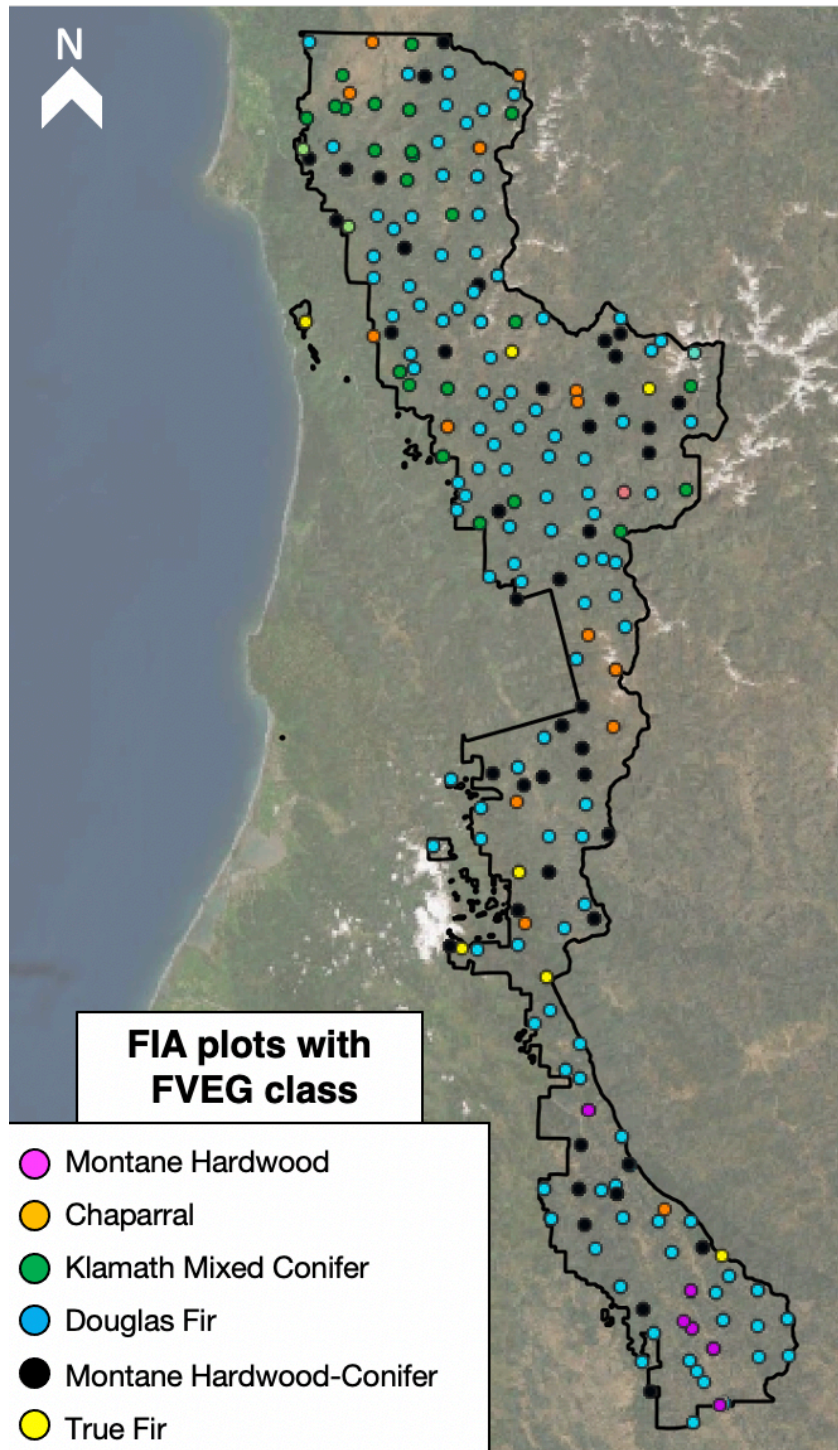
Figure 4. Witness tree data (green points) collected between 1872-1880 within the modern boundaries of Six Rivers National Forest. FIA plots (colored circles) in the Six Rivers boundary that have been matched to underlying modern FVEG data classifications.
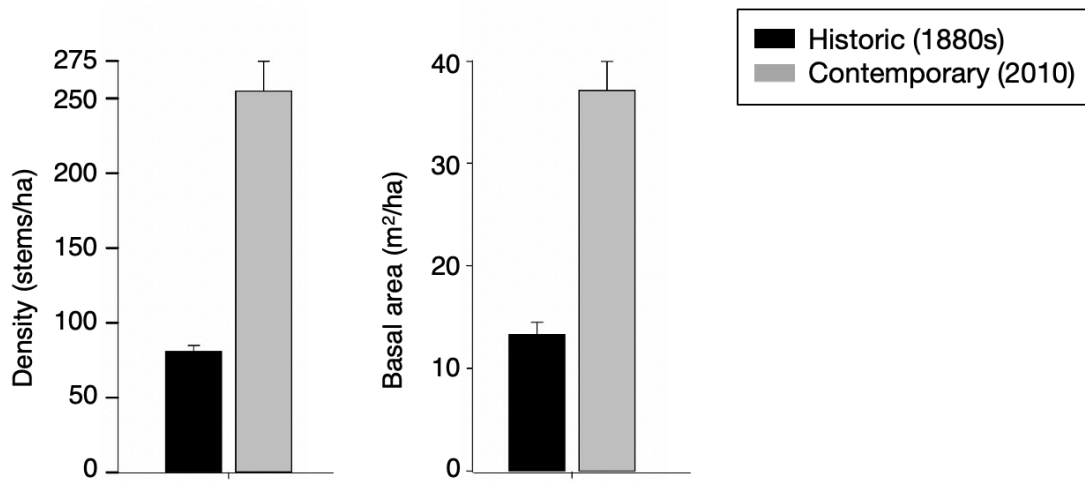
Figure 5. Changes in forest structure for Six Rivers National Forest. Historic estimates (bias-corrected) from General Land Office survey data (1880s). Contemporary estimates from FIA Phase 2 inventory plots (2008-2017). Results include only trees > 20 cm DBH. Means ± 95% confidence interval reported.
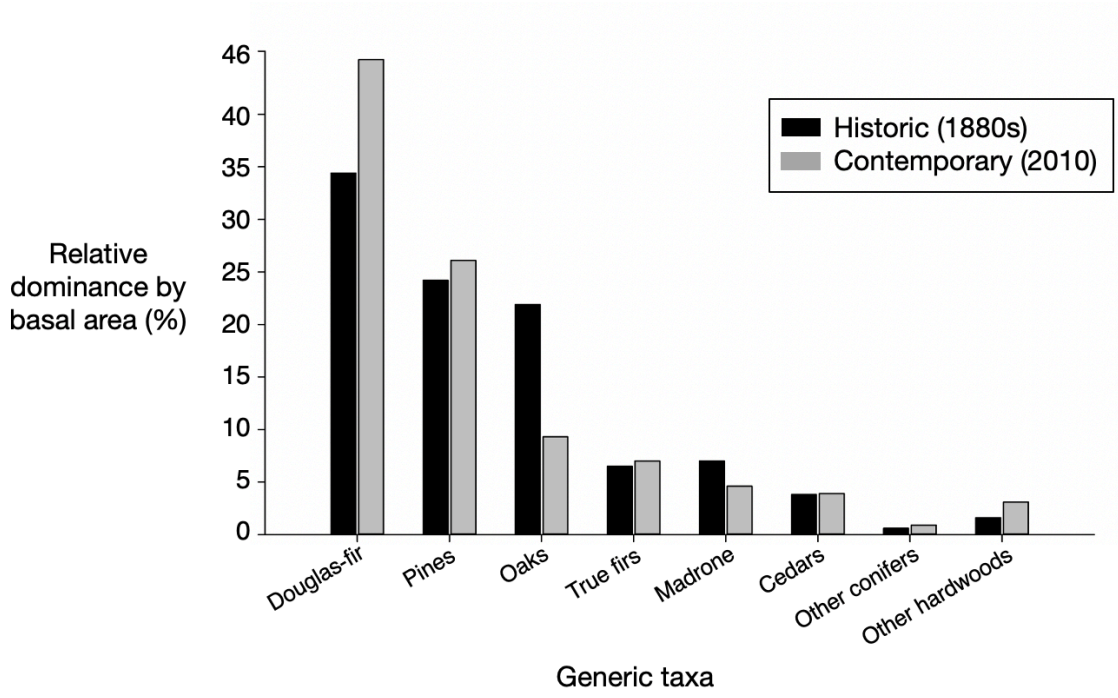
Figure 6. Changes in forest composition in Six Rivers National Forest. Historic estimates from General Land Office survey data (1880's). Contemporary estimates from FIA Phase 2 inventory plots (2008-2017). Compositional information based on generic taxa; relative dominance defined as relative basal area.
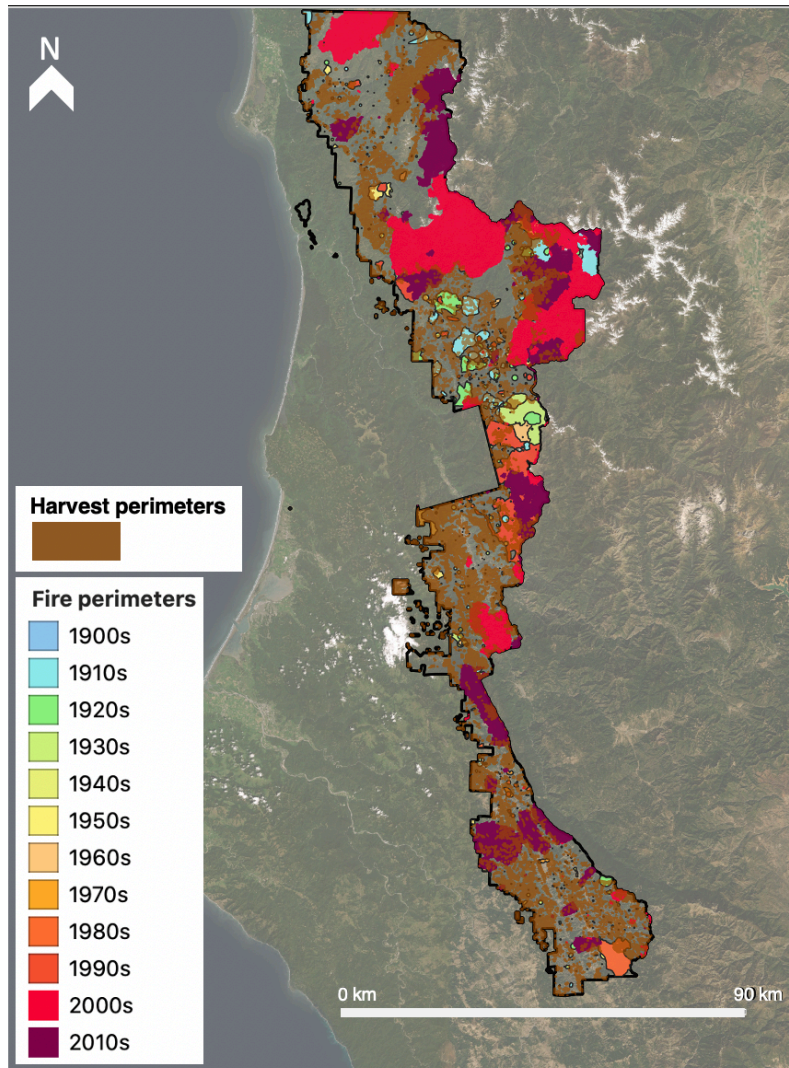
Figure 7. Harvest and salvage perimeters in Six Rivers (USDA Forest Service 2001) overlaid on fire perimeter data, which has been grouped by decade.

Fires in Six Rivers National Forest (1908-2018)
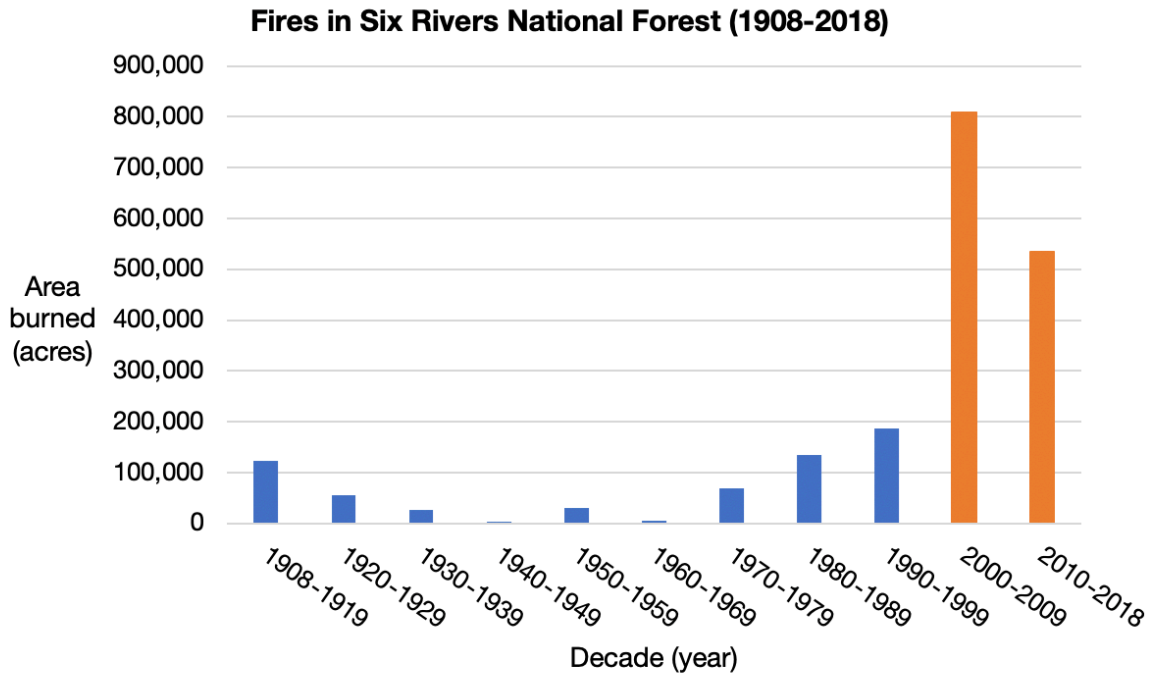
Figure 8. Area burned (ha) by decade in Six Rivers National Forest from 1908 to 2000 (blue bars) and 2000-2018 (orange bars).
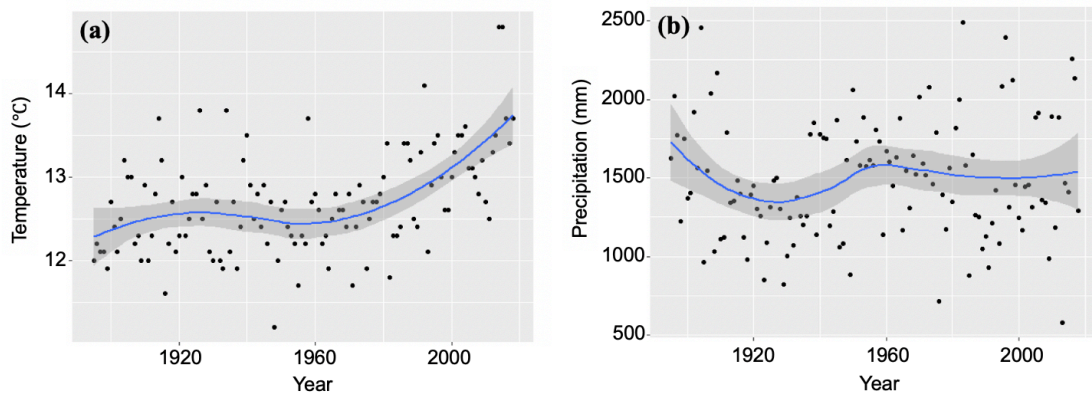
Figure 9. Trends in **(a)** mean annual temperature (°C) and **(b)** total precipitation (mm) at Lake Ogaromtoc, a lake in Six Rivers. Data are from PRISM 4km database from 1895 to 2018. Blue trend lines represent linear splines fit by locally estimated scatter plot smoothing. Gray buffers represent the standard error of the estimate.

24

Tables

Table 1. Comparison of aboveground live tree biomass (Mg/ha) at Six Rivers National Forest. Results for the six most common contemporary vegetation types (alliances). Two types (Chaparral and True Fir) represent higher order aggregations of two alliances. Results include only trees > 20 cm DBH. Means and standard errors (SE) reported for each vegetation alliance. Confidence interval (CI) defined as the range of values between the 2.5% and 97.5% percentiles (Euro-American colonization: calculated from resampled estimates; Contemporary: calculated using a t-distribution).

Contemporary Vegetation Alliance	Euro-American colonization (1880s)			Contemporary (2007-2018)		
	Mean	SE	CI	Mean	SE	CI
Chaparral	80	13.0	57-107	70.2	25.8	21-119
Douglas-fir	103	10.7	82-124	291.3	20.6	257-326
Klamath Mixed Conifer	42	6.8	29-57	397.8	97.1	202-593
Montane Hardwood	149	26.2	104-203	105.4	37.5	41-170
Montane Hardwood-Conifer	129	24.5	88-181	354.4	47.3	271-438
True Fir	46	9.2	30-66	290.1	32.7	235-346
Other	88	32.9	38-168	120.9	27.4	72-170
All	100	7.1	87-115	261.0	14.7	237-285

Table 2. Total timber harvest estimates for 1920, 1945, 1954, and 1955 in the in Six Rivers region. Note: Estimates are presented in million board feet to match original reports (Conners 1998) and to avoid confounding harvest estimates by any changes in the scaling system over time (Spelter 2002).

Date	Harvest estimates (million board feet)
1920	0.384
1945	0.480
1954	48.1
1955	76.6

Table 3. Fire rotations (year) in Six Rivers National Forest (394,420 ha) during two different time windows in the era of active fire suppression.

Time period	Years in observation interval	Area burned (ha)	Fire rotation (year)
1908-1995	87	194,157	176.7
1908-2018	110	801,236	54.1

Transition between chapter 1 and chapter 2

In chapter 1, I found significant changes in forest composition and structure from the 1880s to the present day. Using plotless density estimation on public land survey data, I quantified the extent of these changes for Six Rivers National Forest. The structure of the contemporary forest contains an estimated three times more trees than the 1880s forest. Forest composition also changed over time. In the 1880s, the dominant taxa were Douglas-fir, pine, and oak, but the modern forest contains relatively more Douglas-fir and pine but half as much oak. The increases in tree abundance since the 1880s occurred even though Six Rivers was extensively logged during the twentieth century. Historical records of fire perimeter data indicate that fires were successfully suppressed in Six Rivers throughout the 1900s, which likely contributed to the densification of the modern forests.

In sum, my quantification of changes in forest conditions in chapter 1 highlighted the profound effect of fire suppression on the forests of this region. The magnitude of changes in forest conditions since the 1880s prompted additional questions about the area's historical ecology over longer time horizons. In chapter 2, I build on this probing of historical conditions by developing novel pollen influx to forest biomass models from lake sediment data and vegetation abundance data. Such models are powerful means of reconstructing past forest conditions, but the conversion from pollen influx to forest biomass must first be determined through spatially explicit models. Hence, chapter 2 concerns the development of model methodology in detail using sediment-derived pollen influx data from lake sites in Six Rivers.

CHAPTER TWO

Linking modern pollen accumulation rates to biomass:
Quantitative vegetation reconstruction in the Klamath Mountains*

Abstract

Quantitative reconstructions of vegetation abundance from sediment-derived pollen systems provide unique insights into past ecological conditions. Recently, the use of pollen accumulation rates (PAR, grains cm^{-2} yr^{-1}) has shown promise as a bioproxy for plant abundance. However, successfully reconstructing region-specific vegetation dynamics using PAR requires that accurate assessments of pollen deposition processes be quantitatively linked to spatially explicit measures of plant abundance. Our study addressed these methodological challenges. Modern PAR and vegetation data were obtained from seven lakes in the western Klamath Mountains, California. To determine how to best calibrate our PAR-biomass model, we first calculated the spatial area of vegetation where vegetation composition and patterning is recorded by changes in the pollen signal using two metrics. These metrics were an assemblage-level relevant source area of pollen (aRSAP) derived from extended R-value analysis (*sensu* Sugita 1993) and a taxon-specific relevant source area of pollen (tRSAP) derived from PAR regression (*sensu* Jackson 1990). To the best of our knowledge, aRSAP and tRSAP have not been directly compared. We found that the tRSAP estimated a smaller area for some taxa (e.g., a circular area with a 225 m radius for *Pinus*) than the aRSAP (a circular area with a 625 m radius). We fit linear models to relate PAR values from modern lake sediments with empirical, distance-weighted estimates of aboveground live biomass (AGL_{dw}) for both the aRSAP and tRSAP distances. In both cases, we found that the PARs of major tree taxa – *Pseudotsuga*, *Pinus*, *Notholithocarpus*, and TCT (Taxodiaceae, Cupressaceae, and Taxaceae families) – were statistically significant and reasonably precise estimators of contemporary AGL_{dw}. However, predictions weighted by the distance defined by aRSAP tended to be more precise. The relative root-mean squared error for the aRSAP biomass estimates was 9% compared to 12% for tRSAP. Our results demonstrate that calibrated PAR-biomass relationships provide a robust method to infer changes in past plant biomass.

1. Introduction

Quantitative reconstruction of past plant abundance has been an important goal in paleoecology since the field's inception (Von Post 1918) and a major research frontier spanning decades (Davis and Deevey 1964, Likens and Davis 1975, Davis et al. 1984, Hicks 2001, Seppä et al. 2009, Matthias and Giesecke 2014, Marquer et al. 2014). The research community lacks a complete understanding of how the pollen signal reflects plant population parameters (e.g., biomass), and therefore past population change (Fagerlind 1952, Davis et al. 1984, Prentice 1988, Seppä et al. 2009). Developing methods to quantitatively reconstruct past plant populations would aid climate science and restoration ecology. In climate science, for example, quantitative reconstructions of past plant populations would allow better understanding of long-term ecosystem dynamics (Gaillard et al. 2000) and provide past analogues to test complex climate models that account for the effects of landcover on the climate system (Gaillard et al. 2010). Restoration ecology would benefit from an improved understanding of the impact of disturbances (natural and anthropogenic) on landscapes and ecosystems (Broström et al. 1998, Crawford et al. 2015) and from the increased participation by paleo-ecologists in the debates of modern restoration ecology (Swetnam et al. 1999, Hellman et al. 2009).

Approaches to quantitative reconstruction mostly fall into three broad classes: 1) biomisation, which relates pollen types to plant functional types, then uses proportions of functional types to identify the most likely biome (Prentice et al. 1996); 2) the modern analogue technique, which compares fossil pollen samples to modern pollen samples collected from the modern landscape where vegetation, climate, and other landscape characteristics are known (Overpeck et al. 1985); and 3) algebraic models of the pollen vegetation relationship, which involves applying pollen-vegetation conversion factors that are estimates from modern pollen spectra in conjunction with quantitative vegetation data from the pollen sampling sites (Davis 1963, Parsons and Prentice 1981). The main strength of algebraic pollen vegetation models (PVMs) over other methods is their ability to reconstruct vegetation from landscapes with no modern analogue (for details about linear PVMs, see background section 2.2). PVMs have also been widely tested against empirical data in quantitative reconstruction research (Davis 1963, Andersen 1970, Prentice 1985, Sugita 1993, Bunting and Middleton 2005, Bunting and Hjelle 2010) and have been successfully validated in at least one region (southern Sweden, see Sugita 2007a, b; Hellman et al. 2008a, b).

Palynologists often use pollen percentage data in pollen-vegetation models to reconstruct landcover and understand past plant populations, but this approach does not provide separate reconstructions for each taxon's population change (Davis 1963, Prentice 1988). Relative changes in abundance of species have been inferred form Bayesian hierarchical spatio-temporal pollen-vegetation models (Dawson et al. 2019). In contrast, pollen accumulation rates (PAR) – a measure of the rate of pollen deposition at the sediment surface per unit area during a given time period (e.g., grains cm^{-2} yr^{-1}, Davis and Deevey 1964) – depend on the abundance of the plant taxa producing that pollen type around the collection site. That is, the PAR for each taxon is independent of all other taxa. PAR allows results from different regions to be directly compared, irrespective of other taxa in the investigations (Hicks and Hyvärinen 1999, Giesecke and Fontana 2008). PAR has been used to reconstruct not only landcover, but also population dynamics and plant biomass (Seppä et al. 2009, Theuerkauf et al. 2012, Matthias and Giesecke 2014). For example, PAR has been used to reconstruct past population growth rates (Bennett 1983, 1986,

MacDonald 1993, Giesecke 2005) and to reconstruct Holocene biomass records in at least two areas: the Finnish boreal zone (Seppä et al. 2009) and a sub-alpine forest in Utah (Morris et al. 2015).

PAR is not a simple reflection of vegetation abundance because the pollen signal is a distance-weighted measure of taxa abundance in the surrounding vegetation, responding to the structure of the plant community as well as the species abundance of reproductively active members (Jackson 1990). Modern PAR values must be quantitatively correlated with modern plant population data from the lake surroundings in order to parameterize the PAR-population relationship before fossil PAR records can be interpreted in terms of past plant population change. This correlation step requires accurate vegetation data from forest inventories (Seppä et al. 2009, Matthias and Giesecke 2014), careful field surveys (Bunting et al. 2013), or well-resolved spatial imagery coupled with ground-truthing (Han et al. 2017) that encompasses the relevant source area of pollen ('RSAP', discussed below and in section 2.3, *sensu* Sugita 1993). Previous work has shown a linear relationship between PAR and distance-weighted biomass across a range of lake sites in northeastern Germany (Matthias and Giesecke 2014).

In addition to quantitative vegetation data, reliable PAR data require a robust chronology of the pollen system being studied. Ideally, a sedimentary core for PAR data collection has two features: it is obtained from an undisturbed lake environment where sediment accumulates evenly over time, and the resulting sediment is dated at high resolution. Where lakes are found to have stable sedimentary conditions, reliable PAR datasets can be obtained (e.g., Ritchie 1969, Hyvärinen 1975, Seppä and Hicks 2006). The recent development of Bayesian tools has improved the construction of chronologies from isotopic data such as ^{210}Pb activity measurements, giving more probable age models and reliable measures of uncertainty (Aquino-López et al. 2018).

Lastly, all sedimentary basins have a relevant source area of pollen (RSAP), which is sometimes referred to as the "pollenshed" of the basin (*sensu* Sugita 1993). The basic premise is that vegetation within a certain distance of the basin corresponds to the quantity and type of pollen deposited at the site. With distance from the lake shore, correlations between plant abundance and pollen loading are expected to improve, then approach an asymptote at some distance because source vegetation of pollen far from the basin should have much less influence on the pollen representation than vegetation closer to the basin. Estimating the RSAP is a key step for quantitative calibration because it provides information about the spatial extent of any subsequent vegetation reconstruction (Sugita et al. 1999, Bunting et al. 2004, Hellman et al. 2009). To our knowledge, the distinction between an assemblage-level RSAP (aRSAP, Sugita 1993) and taxa-specific RSAP (tRSAP, *sensu* Jackson 1990, Matthias and Giesecke 2014) has not yet been drawn within the same basin (Table 1). Comparing these estimates provides insight about how pollen assemblages "sense" vegetation, which is critical to the extraction of vegetation information from pollen data.

Given the methodological challenges, the application of calibrated PAR-biomass transfer functions to any ecosystem is not routine. This paper develops PAR-biomass models using short cores from seven small lakes in the western Klamath Mountains, California, and follows the general approach used in previous studies (e.g., Seppä et al. 2009, Matthias and Giesecke 2014)

whilst critically evaluating each step in the process. The Klamath bioregion contains numerous small lakes and is an area where Holocene-length paleoecological records have already provided a portrait of ecological change (Fig. 1). We measured modern PAR from lake sediments and acquired vegetation abundance data to achieve three goals: 1) to understand the spatial relationship between pollen flux in small lakes and surrounding vegetation cover, through modeling of the aRSAP and tRSAP, 2) to calibrate a PAR-biomass model using distance-weighted biomass for major tree taxa, and 3) to assess the potential of this model to reconstruct past changes in assemblage-wide biomass from the region.

2. Background

Below, we describe the study area's physical features (2.1), our pollen-vegetation modelling approach (2.2), and the methodology used to estimate aRSAP and tRSAP (2.3).

2.1 Study Area

The Klamath bioregion, a physically and floristically diverse area in northwestern California (Whittaker 1960, Cheng 2004), contains hundreds of small lakes. Many lakes are found at high elevations and are glacial in origin, but there are also landslide-created lakes at low- and mid-elevations in the western portion of the region (Wahrhaftig and Birman 1965). The landscape has deep catchments and steep mountains (Irwin 1981), and the climate is Mediterranean, consisting of cool, wet winters and warm, dry summers (Skinner et al. 2006). Prior to 20th century fire suppression, the landscape had a mixed-severity fire regime characterized by mostly small, low-intensity, frequent fires, and infrequent large burns of mixed-severity (Taylor and Skinner 2003).

Our study focused on the western Klamath Mountains where low-elevation forests (<600–800 m) are dominated by *Pseudotsuga menziesii* (Douglas-fir). Multiple *Pinus* (pine) species including *Pinus lambertiana* (sugar pine), *Pinus jeffreyi* (Jeffrey pine), and *Pinus ponderosa* (ponderosa pine) are also common but less frequent than Douglas-fir. The most common broadleaf tree species in the low-elevation forests are *Notholithocarpus densiflorus* (tanoak), followed by *Arbutus menziesii* (Pacific madrone), *Chrysolepis chrysophylla* (golden chinquapin), and *Quercus kelloggii* (California black oak). *Chamaecyparis lawsoniana* (Port-Orford-cedar) is mainly found in riparian areas but can be found on slopes. Higher-elevation montane forests are dominated by *Abies concolor* (white fir) and *Abies magnifica* (red fir; Sawyer and Thornburg, 1977), whereas sub-alpine (above ~1700 m) zones include *Tsuga mertensiana* (mountain hemlock) and *Picea breweriana* (Brewer spruce) (Sawyer and Thornburg 1977). On areas of ultramafic soils derived from serpentinite and peridotite bedrock, Jeffrey pine, *Pinus monticola* (western white pine) and *Calocedrus decurrens* (incense-cedar) are the dominant forest taxa (Whittaker 1960; nomenclature follows Greenhouse et al. 2012).

We selected seven small lakes in the Six Rivers National Forest with small basins, minimal stream inputs, and shallow slopes (Table 2, Fig. 1). Vegetation around the lakes is representative of the diverse mixed conifer forest of the Klamath bioregion (Hudiburg et al. 2009) although the dominant overstory varies at each lake site. Holocene-length pollen records (percentage and PAR) already exist for three of the seven lakes and suggest that the modern forest structure and composition have been relatively stable for the last 2,000 years (Wanket 2002) but also imply a 3,000-year high of Douglas-fir in the contemporary forest (Crawford et al. 2015).

2.2 Pollen-vegetation models

There are two main types of pollen-vegetation models (PVMs): non-hierarchical and Bayesian hierarchical models. Both PVM types use the relationship between pollen assemblages and vegetation to infer past vegetation composition or structure from fossil pollen data. Linear pollen-vegetation models (PVMs) have a long history of use in palynology (Davis 1963, 2000; Andersen 1970; Prentice 1985, 1988; Sugita 1993, 1994; Bunting and Middleton 2005, Bunting et al. 2013) and are the sole focus of this study. Linear PVMs use the relationship between pollen assemblages and vegetation to infer past vegetation composition or structure from fossil pollen data. We did not explore more recent Bayesian hierarchical models because 1) they are designed for regional scale reconstructions (see Paciorek and McLachlan 2009, Dawson et al. 2016) and 2) they require a high number of regional pollen records for calibration (>50) (Dawson et al. 2019). Unlike the eastern U.S. where Bayesian methods were developed (Paciorek and McLachlan 2009), the western U.S. does not yet have a sufficiently dense network of high-resolution paleo-ecological data (Anderson et al. 2020).

Linear PVMs must account for differences in pollen dispersal and pollen productivity. Empirical evidence has shown that pollen dispersal distances – the distance from the point of emission to the point of deposition – typically follow a leptokurtic distribution from the pollen source. This curve is characterized by a steep rate of decline from the origin (Janssen 1973, Levin and Kerster 1974). Because pollen source contribution to an assemblage declines with increasing distance between the source and the sample point (Prentice and Webb 1986), plants further away from the sampling point contribute less pollen compared to plants closer to the sampling point. Thus, a distance weighting scheme must be applied to spatially explicit vegetation data to approximate pollen dispersal. Early versions of linear models did not apply distance-weightings (e.g., Davis 1963; Webb et al. 1981), but more recent versions do. Two main classes of distance-weighting are widely used.

The first class uses geometric functions, such as stepwise inverse distance-weighting, of the form $1/d$, where d = midpoint distance of vegetation sampling ring (Prentice and Webb 1986) or $1/d^2$ (Webb et al. 1981, Calcote 1995). In these models, vegetation data are arranged either in one dimensional rings ("ring-source method," Sugita 1994) with the assumption that pollen dispersal is equally likely in any direction, or in a grid (via HUMPOL, Bunting and Middleton 2005), which allows differential weighting in two dimensions. Geometric functions assume all grains move in the same way – that is, differences in pollen grain size, weight, and density are negligible. The only biological parameter that needs to be estimated for the PVM is the relative pollen productivity.

In contrast, the second class of functions assume pollen grain differences *do* affect pollen dispersal, and these models aim for greater biological realism by parameterizing dispersal characteristics. The main choices are Sutton's empirically derived model of airborne particle dispersion (Sutton 1947), or the simulation based Lagrangian Stochastic models (Andersen 1991). In Sutton's equations (1953), weighting factors are generated using a combination of distance with climatological (wind speed, turbulence/stability) and taxon-specific parameters (fall speed). Lagrangian Stochastic models directly simulate the movement of individual particles using a climatological approach, assuming a thicker atmosphere than in Sutton's model, as well

as overt differences in the properties of atmospheric layers (Andersen 1991, Kuparinen et al. 2007, Theuerkauf et al. 2012).

In this work, we used a version of Sutton's original PVM model (Sutton 1947, 1953) inverted by Prentice (1985) and modified by Sugita (1994) for lake environments. This model's form – called Prentice-Sugita-Sutton – assumes that pollen could land anywhere on the lake surface and would be perfectly mixed in the water column before being deposited on the lakebed. The Prentice-Sugita-Sutton model also assumes that pollen transport is largely via wind above the canopy and gravity beneath the canopy, and that the sampling basin is circular with uniform wind in every direction (Sugita 1994, full list of assumptions in the supplement). Under this approach, we a) divide the vegetation into rings, b) distance-weight each ring, and c) compare the PAR from the basin with the summed distance weighting from one or more rings, working out from the edge of the basin. This model calculates the total pollen influx from each source across the whole lake. Its simplest linear form is:

$$Y_{ik} = \alpha_i \cdot \psi_{ik} \tag{1}$$

where,

    Y_{ik} = pollen influx for a taxon i at site k

    α_i = pollen productivity of taxon i

    ψ_{ik} = the distance-weighted plant abundance (DWPA) of taxon i around site k with the weighting term reflecting the pollen dispersal of taxon i (weighting term calculation shown in Eq. 3).

DWPA (ψ_{ik}) is defined as:

$$\Psi_{ik} = \int_R^\infty X_{ik}(z)\, g_i(z)\, dz \tag{2}$$

where,

    R = the radius of the canopy opening in which the sample site is located

    $X_{ik}(z)$ = the plant abundance measure consisting of the contribution of taxon i to the pollen assemblage formed at site k from plants located distance z from sampling location k, and $g_i(z)$ is the distance weighting term for taxon i at distance z from any sampling location.

    The Prentice-Sugita-Sutton weighting term g_i for taxon i at distance z is calculated using:

$$g_i(z) = b_i \gamma z^{\gamma-1} e^{b_i z^\gamma} \tag{3}$$

$$\text{where } b_i = \frac{4v_g}{nu\sqrt{\pi}C_z} \tag{3a}$$

and,

z = distance

γ = a coefficient of 0.125 (Prentice 1985)

v_g = approximated by v_s (fall speed, m sec^{-1})

C_z = the vertical diffusion coefficient (m$^{1/8}$)

n = a dimensionless turbulence parameter equal to 2

u = windspeed (m sec^{-1}), set equal to 3.

Note that C_z and n depend on atmospheric stability.

Equation 2 can be re-written as a sum with two addends: 1) the unique contribution of the vegetation close to site k where ζ is the pollen source area for site k, and 2) the long-distance pollen transport ('background pollen,' which is uniform beyond ζ), giving:

$$\Psi_{ik} = \int_R^\zeta X_{ik}(z) g_i(z) \, dz + \int_\zeta^\infty X_{ik}(z) \, g_i(z) dz \tag{4}$$

Which can be written as

$$Y_{ik} = \alpha_i \psi_{ik} + \omega_i \tag{5}$$

$$\text{Where } \psi_{ik} = \int_R^\zeta X_{ik}(z) g_i(z) dz$$

2.3 Spatial area represented by the pollen record
We estimated the spatial extent of our sites' source area of pollen in two ways (definitions in Table 1). We calculated the standard assemblage-specific metric – the relevant source area of pollen (aRSAP) – which is defined as the area beyond which the correlation between pollen and vegetation does not improve (Sugita 1993). Estimates of aRSAP can be extracted from extended R-value (ERV) analysis using pollen percentage data (Parsons and Prentice 1981). ERV analysis is the process of solving n equations for 2n unknowns in order to extract the parameter estimates, where ERV sub-models 1, 2 and 3 are the underlying vegetation-pollen relationship models. The three sub-models define background pollen differently (Sugita 1994). Whereas models 1 and 2 use pollen data and vegetation percentages (Parsons and Prentice 1981), model 3 uses pollen percentages and plant abundance data in absolute units (e.g., biomass per area) (Sugita 1994). Using the maximum likelihood method, ERV models iteratively fit the relationship between pollen and vegetation percentages (Bunting and Hjelle 2010). Maximum likelihood function scores measure the goodness of fit between pollen percentages and distance-weighted plant abundance. The aRSAP can be estimated from visual inspection of the likelihood function score plotted against distance; it is the point at which scores approach an asymptote (Sugita et al. 1999, Bunting et al. 2005).

We then calculated a taxon-specific metric of the relevant source area (tRSAP) to compare to the aRSAP. We call the tRSAP the distance beyond which the correlation between PAR and DWPA summed to that distance does not improve (Jackson 1990). We fit a linear equation (equation 5) for each individual taxon because both y and ψ are measured in independent terms. We again used the ring source model, which converts the integral into a summation. That is, we summed the value for each of the rings and $g_i(z)$ includes ring area in this formulation. As with aRSAP, tRSAP can be estimated from visual inspection of the R^2 value against the distance from the lake shore (m) (Matthias and Giesecke 2014).

3. Methodology

Fitting PAR-biomass relationships requires a number of steps shown in a flowchart (Fig. 2) with numbers matching the following sections.

3.1 Lake selection and core sampling

We used the following criteria to determine suitable lake sites: small size (radius approximately 100 m), no permanent outflow, simple basin, and core length greater than 25cm. Ten such lakes were identified from topographical maps and satellite imagery as promising, but each was assessed in the field. Out of this collection, seven lakes were viable and selected for ^{210}Pb dating. During the summer of 2018, one core per lake (~50 cm) of 7 cm diameter were taken from each lake's center using either a gravity corer (Ogaromtoc, Fish Lakes) or a piston corer (all other lakes). The sediment-water interface was immobilized by sodium polyacrylate for transport. Cores were later split and sectioned in the laboratory.

3.2 Sediment dating, age-depth model, and sediment lithology

We used lead-210 (^{210}Pb; 22.3 yr half-life) to assign ages to sediment deposited in the last 150 years. Surface bulk sediments from 0 cm to a maximum of 45 cm were taken from each core and dried to 105°C (see Tables S1-S7). ^{210}Pb activity was determined by alpha spectrometry (see SI for complete dating methodology). We used the Bayesian-based Plum software to develop age models from excess (unsupported) ^{210}Pb data (Aquino-López et al. 2018). Plum uses a self-adjusting Markov Chain Monte Carlo (MCMC) algorithm called the t-walk (Christen and Fox 2010). Plum uses millions of MCMC iterations to model the accumulation of sediment, using a gamma autoregressive semiparametric age-depth function (Blaauw and Christen 2011). This algorithm results in a probability envelope around the mean age model. Supported ^{210}Pb activities were determined from the direct measurements of ^{226}Ra by gamma-ray spectrometry.

3.3 Pollen analysis

Pollen samples – one from each lake site – were extracted from 0.63 cm^3 of wet sediment from the top 0.5 cm of each core and were processed according to standard pollen preparation procedures (Faegri and Iversen 1989) but modified to include two steps: 1) sieving with 5- and 153-micron mesh under vacuum and 2) swirling, with the less dense fractions retained. These steps draw on Doher's palynomorph methodology and current United States Geological Survey procedures (Doher 1980). One *Lycopodium* spore tracer tablet containing 20,848 spores was added to each sample to calculate pollen concentration (Stockmarr 1971, Faegri and Iversen 1989). Acetolysis and sieving steps were repeated for samples containing high amounts of organic material. Pollen samples were mounted in silicone oil and examined at 500×

magnification. At least 400 terrestrial grains per sample were counted and identified using the UC Berkeley Museum of Paleontology modern pollen reference collection, as well as pollen atlases (Knapp 1969, Halbritter et al. 2018).

Seven wind-pollinated taxa were identified at all sites: *Pinus, Pseudotsuga, Quercus, Notholithocarpus, Alnus,* TCT (Taxodiaceae, Cupressaceae, and Taxaceae families)*,* and *Abies*. The corresponding plant taxa from the study area were sugar pine, Jeffrey pine, ponderosa pine (*Pinus*); Douglas-fir (*Pseudotsuga*); California black oak, canyon live oak (*Quercus*); tanoak, golden chinquapin (*Notholithocarpus*); white alder (*Alnus*); Port-Orford-cedar, incense-cedar (TCT); white fir, red fir (*Abies*). We only encountered Port-Orford-cedar and incense-cedar in the vegetation survey at the study sites and assume all TCT originating within the surveyed vegetation area came from these species. Counts of *Pinus*, *Quercus*, *Notholithocarpus* and *Abies* reflect all the pollen grains from their respective genera (i.e., we report total *Pinus* which likely contained sugar pine, Jeffrey pine, and ponderosa pine grains). *Pseudotsuga* and *Alnus* counts represent the species *Pseudotsuga menziesii* (Douglas-fir) and *Alnus rhombifolia* (white alder). Other wind-pollinated tree pollen present in trace amounts includes willow (*Salix*), buckthorn (*Rhamnaceae)*, hazel (*Corylus*) and silk tassel (*Garrya*). This group of "other hardwoods" accounted for only 0.35% of the woody species. Given their rarity, we omitted them from the determination of pollen source area and subsequent PAR-biomass modeling.

3.4 PAR determination
Pollen concentrations (grains cm^{-3}) and PAR (grains cm^{-2} yr-^{1}) were determined using the *Lycopodium* marker grains, the number of pollen grains counted for each taxon, the volume of the pollen sample (e.g., 0.63 cm^3) (Stockmarr 1971), and the sediment accumulation rate (Davis and Deevey 1964), which differed by lake site and was determined by the Plum age model in increments of 0.5cm (see SI for equations used).

3.5 Forest inventories
We used cruising prisms (wedges of glass with a known size/angle) to determine the basal area of the dominant pollen-producing taxa within 750 m from each lake's shoreline (USDA Forest Service 2000). The prism method employs variable plot radius sampling at the stand level. Transects in eight directions (N, S, E, W, NE, NW, SE, SW) from the lake shore were sampled. The basal area of live trees was measured using the prisms every 50m along the transects, following Han et al. 2017 (Fig. 3).

We used aboveground live tree biomass (AGL) as the specific measure of abundance that is distance weighted. To estimate AGL from basal area measurements, we developed species-specific allometric equations using contemporary data from the US Forest Service Forest Inventory and Analysis program (FIA). From the FIA plots inventoried in Six Rivers National Forest between 2001 and 2017 (FIADB 2020), we calculated plot-level basal area (m^2 ha^{-1}) for every species in the plot and linked it to the estimate of plot-level aboveground live biomass (Mg ha^{-1}) for each species (n = 3,428 plot-by-species observations). AGL was estimated using the regional model of tree biomass (Zhou and Hemstrom 2009). For every species, we predicted AGL as a function of basal area using a linear log-log (natural) equation (*sensu* Knight et al. 2020).

Specifically,

$$\ln(AGL_{ij}) = \beta_{0_i} + \beta_{1_i} * \ln(Basal\ Area_{ij}) \qquad (6)$$

where $\ln(AGL_{ij})$ is the natural log of aboveground live biomass for species i in plot j, $\ln(Basal\ Area_{ij})$ is the natural log of tree basal area for species i in plot j, β_{0i} is the intercept for species i, and β_{1i} is the slope coefficient for species i. For the six most abundant species that accounted for 90% of the basal area, fits ranged from a low of 0.85 for sugar pine to a high of 0.97 for Port-Orford-cedar (Table S8). With these equations and field measurements of species basal area, we calculated the AGL of each species in the prism sample.

3.6 ERV analysis and estimation of aRSAP

The aRSAP values were extracted from conventional ERV analysis using model 3. We used PolERV from the software suite HUMPOL (Bunting and Middleton 2005) which has the same core code (erv-v6.exe and polsim-v3.exe) as other ERV software, e.g., POLLSCAPE (Sugita 1994). In order to meet the requirement that the number of sites is at least twice the number of taxa used in ERV analysis (Soepboer et al. 2007), we analyzed sub-sets of three taxa across the seven sites using the same reference taxon (TCT) every time. For example, one such sub-set combination was TCT, *Pseudotsuga*, and *Pinus*. We selected TCT as the reference taxon (i.e., specified that TCT has a relative pollen productivity of 1.0) for several reasons. First, a scatter plot of TCT pollen values and unscaled distance weighted plant abundance is positive and linear (Fig. S1). Second, TCT has an estimated relative pollen productivity in the middle of the dataset upon ERV analysis with all seven taxa. Lastly, TCT is well-represented in pollen data at all sites (unlike *Abies, Alnus,* or *Quercus*), and is present in vegetation close to the coring site. aRSAP was estimated by plotting the likelihood scores for each distance across all taxa combinations and pooling the results.

3.7 Distance weighting and estimation of tRSAP

AGL results were first averaged by the number of plots in each concentric ring and then each ring was weighted using the Prentice-Sugita weighting under stable conditions, which affect parameters C_z and n (Eq. 3, 3a). We assumed stable atmospheric conditions because simulation experiments comparing unstable and stable models demonstrate little difference in estimated aRSAP and pollen productivity (Broström et al. 2004). The pollen-specific fall speeds (m sec^{-1}) of *Abies, Alnus, Pinus, Pseudotsuga,* and *Quercus* have been determined in previous work (Table S9). For TCT, Stoke's Law (Gregory 1973) was used to calculate fall speed using the average grain size of each taxon and weighted by relative abundance of the contributing species Port-Orford-cedar and incense-cedar (both Cupressaceae family). For subprolate grain *Notholithocarpus*, major and minor axes were measured from reference slides in UC Berkeley's collections, and then Stoke's Law with Falck's (1927) correction was used. Lastly, we determined the coefficient of determination (R^2) of the linear model predicted from AGL$_{dw}$ at distance z (AGL_{dw_z}) as a function of PAR. The R^2 between PAR and summed AGL$_{dw}$ for each ring distance was plotted against the distance. The tRSAP occurs where the line reaches an asymptote.

3.8 PAR-biomass transfer equations

We developed transfer equations to predict taxon-specific contributions to the distance-weighted AGL (AGL$_{dw}$) as a function of taxon-specific PAR. Although biomass "predicts" pollen

accumulation rates in a functional sense, our aim was to apply calibrated transfer functions to predict biomass in the past. Consequently, we fitted regression lines with PAR values as the independent variable. This reasoning has been used for needle accumulation rate as a predictor of Holocene-era basal area (Blarquez et al. 2011).

In this analysis, each lake represented a sample with the source area defined by either aRSAP or tRSAP. We included seven pollen-producing taxa, namely *Pseudotsuga, Pinus, Notholithocarpus,* TCT*, Alnus*, *Quercus,* and *Abies*, that collectively account for greater than 99% of the pollen-producing trees present in the surrounding landscape. Using the assigned source area distances, we calculated AGL_{dw} for the taxa present at each lake and regressed it against PAR using linear models (see Fig. 8a,b). Specifically, we evaluated three model forms: a linear model with an intercept term and slope term, a linear model with only a slope term, and segmented linear model with one breakpoint. In the linear models with intercepts, the intercept represents the "background" pollen component; because we treated PAR values as the independent variable, these intercepts are negative. So, we included an origin-forced model as an option because negative-intercept models are not biologically meaningful for biomass reconstruction given that very low PAR values would yield negative biomass. We included the segmented model to potentially capture threshold responses in the relationship between AGL and PAR (Muggeo 2008). We ranked the models by the Akaike Information Criterion for small samples (AICc) in order to compare performance. AICc imposes a stronger penalty on model complexity than AIC and was chosen in order to avoid fitting models which were overly complex given the size of the dataset (Burnham and Anderson 2002).

To evaluate the uncertainty introduced by the PAR transfer functions, the AGL_{dw} predicted from PAR at each lake (predicted AGL_{dw}) was compared to the AGL_{dw} calculated from the observed AGL_{dw}. Error was propagated using a resampling method (Crowley et al. 1992). Specifically, we estimated the error in predicted AGL_{dw} for each iteration as a random sample from a normal distribution with the mean equal to zero and the standard deviation equal to the standard error of the regression estimate (SEE) for each taxon. Results were based on 10,000 iterations and reported as means and standard errors of the predicted AGL_{dw} for each lake. Bias between the predicted and observed AGL_{dw} was calculated as:

$$Bias = \frac{Predicted\ AGL_{dw} - Observed\ AGL_{dw}}{Observed\ AGL_{dw}} \tag{7}$$

4. Results
4.1 Chronology
The seven lakes' chronologies were established using at least 20 ^{210}Pb measurements at each site (see Table S3-S9 for exact number of samples for each core). Blue Lake is shown as an example (Fig. 4). The chronologies for Fish, North Twin, Ogaromtoc, Onion, Red Mountain, and South Twin lakes followed the same procedure (Fig. S2). The lakes are characterized by rapid sedimentation rates, with rates in the upper sediments in the range of 0.14-0.33 cm yr $^{-1}$ (3-7 yr cm^{-1}). Therefore, the model indicates that surface samples (upper 0.5cm) contain pollen from 2018 (collection date) to 2011 at the oldest. Core lithology results are provided in the supplement (Figs. S3-4).

4.2 PAR

Highly abundant tree taxa included *Pseudotsuga*, *Pinus*, *Notholithocarpus*, and TCT, which were reflected in high PAR values (> 2,000 grains cm^{-2} yr^{-1}) in most samples (Fig. 5, Table S10). For example, *Pseudotsuga* values were above 5,000 grains cm^{-2} yr^{-1} at all sites except Onion Lake. The highest overall PAR value was *Pinus* at Onion Lake which exceeded 10,000 grains cm^{-2} yr^{-1}. High PAR values reflect the Douglas-fir and pine-dominant composition of Six Rivers National Forest. Onion Lake is the only lake situated in the True Fir alliance zone and, unsurprisingly, the *Abies* PAR value was the highest compared to all other sites (5,000 grains cm^{-2} yr^{-1}). PAR values for *Notholithocarpus* and TCT varied across sites and were between 1,000-4,000 grains cm^{-2} yr^{-1}.

Less abundant arboreal taxa included *Alnus*, *Abies*, and *Quercus* which were present in most samples with PARs of less than 2,000 grains cm^{-2} yr^{-1} (Fig. 5). *Alnus* values were generally around 1,000 grains cm^{-2} yr^{-1}, although values above 2,000 grains cm^{-2} yr^{-1} were observed at Ogaromtoc and Fish Lakes. *Abies* values were low (< 1,000 grains cm^{-2} yr^{-1}) at all sites except North Twin and Onion Lakes. Although pollen from *Alnus*, *Abies*, and *Quercus* were found at all sites, the taxa themselves were not recorded from the transect sampling at several lakes. This could be due to low abundance such that they were not captured in the survey or due to their absence in the sedimentary basin in which case their PAR contributions are background deposition. Pollen from the "other hardwood" category (defined as willows, buckthorn, hazel, and silk tassel) was detected in trace amounts (< 100 grains cm^{-2} yr^{-1}).

4.3 aRSAP and tRSAP

Using the sub-setting approach for the aRSAP calculation, a coherent pattern was exhibited in the likelihood function scores from model 3. The values were high at short distances and then decreased rapidly until 175 m where they begin to flatten out. For all taxa combinations, we inferred via visual inspection that the curves reached their asymptotes at a distance of 625 m and thus the aRSAP of these lakes is 625 m from the lake shore. The likelihood function scores in relation to the distance from the lake shore are shown for one of the three sub-set examples: TCT, *Pseudotsuga*, and *Pinus* (Fig. 6).

Based on tRSAP calculations for the four dominant tree taxa, maximum R^2 values were reached before the maximum distance surveyed (750 m) from the shoreline (Fig. 7). The R^2 values for *Pinus* and TCT were high (> 0.75) at only 25 m from the shore and stabilized around 225 m, the tRSAP. The R^2 values for *Pseudotsuga* and *Notholithocarpus* continued to improve for some distance from the lake shore. For *Pseudotsuga,* the tRSAP was 625 m; for *Notholithocarpus,* it was 525 m. Sample sizes were insufficient to estimate tRSAP values for the minor taxa. For these taxa, we used the aRSAP value in AGL$_{dw}$ calculations (i.e., 625 m).

4.4 Transfer functions: PAR to AGL$_{dw}$

PAR was a statistically meaningful and reasonably precise estimator of contemporary AGL$_{dw}$ for most of the pollen taxa present (Fig. 8). Based on the aRSAP distances, the linear model without intercept was the best performing model (ΔAIC$_c$ > 4.0) for the four most abundant taxa (Fig. 8a). For these taxa, the no-intercept regressions were not only significantly better than the null model (p < 0.001) but also explained most of the variation. R^2 ranged from 0.87 for TCT to 0.96 for *Pseudotsuga* (Table S11). The model results for the three less abundant species (i.e., *Alnus*, *Abies* and *Quercus*) were more complex (Fig. 8b). Based on ΔAIC$_c$, the segmented regression

model best fit the *Alnus* and *Abies* data. However, both species were rare and found in abundance at only one lake (Fig. 5). The existence of this one abundant point exerts extraordinary leverage in the segmented regression. To avoid relying on a single point in these two transfer functions, we used the second-best regression model. For *Alnus*, it was a linear model; for *Abies,* it was a linear model without intercept (Table S11). For *Quercus,* none of the regression models were superior to the null (Fig. 8b, Table S11), so we used the mean and standard error to predict *Quercus* contribution to AGL_{dw} estimates for each lake. We recalculated the biomass transfer functions using the tRSAP weighted AGL_{dw} estimates for all taxa. Both the functional forms and fits were similar to aRSAP-based results (Table S12). However, the coefficients varied with changes in the source area distance.

The transfer functions based on aRSAP distances provide robust means to estimate contemporary AGL from PAR (Table 3). The coefficient of variation (COV) in predicted AGL_{dw} ranged from 13-17% for six lakes with Ogaromtoc being the exception with a COV = 24%. The standard error of the estimate varied little among lakes and averaged 32 Mg ha^{-1}. In terms of accuracy the relative root mean squared error (rRMSE) between predicted and observed AGL_{dw} was 9.2%. There was a small tendency for predicted AGL_{dw} to overestimate the observed. The mean bias was 4.8% with two lakes, Red Mountain and South Twin, contributing the most to the positive bias (Table 3). The predictions of AGL weighted using tRSAP distances (Table 4) tended to less accurate (rRMSE = 12.7%) and more biased (10.1%).

5. Discussion
5.1 Source areas of pollen: aRSAP and tRSAP
Calibration of pollen-vegetation relationships is only effective when the scale of the vegetation sampling is close to or exceeds the scale of the relevant source area of pollen (Bunting et al. 2004). Therefore, being able to specify the source area of pollen in a given basin is an important step towards quantitative reconstruction of past vegetation (Sugita et al. 1999, Hellman et al. 2009). A primary aim of this work was to understand the spatial extent represented by the pollen assemblage. We addressed this aim by determining the assemblage-level relevant source area of pollen (aRSAP) obtained from pollen percentage data and ERV analysis and comparing those estimates with the taxon-specific source area of pollen (tRSAP) for four main taxa. Both metrics estimate the extent of vegetation that requires surveying for a subsequent reconstruction step but are seldom compared.

aRSAP values have been estimated for lakes similar in size to those presented here (i.e., 100 m radius), in different settings including simulated landscapes. Reported aRSAP values have ranged from: 300 m in a simulation of a hemlock-hardwood forest in the US (Sugita 1994), to 800-1,000 m in a simulation of spruce forest in Sweden (Sugita et al. 1999), to 1,700 m in varying landcover types in Denmark (Nielsen and Sugita 2005), to 1,500-2,000 m in semi-boreal forests of Estonia (Poska et al. 2011), and to 2,200 m in the upper Tibetan Plateau (Wang and Herzschuh 2011). Within this list, all aRSAP estimates were derived from Prentice-Sugita-Sutton distance-weighted models and are thus comparable to our estimate. Our aRSAP value of 625 m falls in the range (300-2,200 m), though on the lower end.

The aRSAP is unique to a given set of lakes and is sensitive to numerous factors such as lake size and basin shape (Sugita 1993), vegetation patch size (Sugita 1994, Broström et al. 2005),

vegetation patterns (Bunting et al. 2004), and taxa spatial distribution (Hellman et al. 2009). For example, aRSAP values tend to increase with landscape openness defined as the extent of the vegetation cover in the basin's watershed. For example, the aRSAP for small ponds in a closed forest was simulated to be 300 m (Sugita 1994) and empirically verified by Calcote (1995), whereas the aRSAP for small ponds in an open Swedish landscape was 1,000 m (Sugita et al. 1999). However, expectations based on landscape openness can be complicated by vegetation heterogeneity. Higher vegetation diversity and complex spatial distribution of taxa are associated with larger aRSAPs (Hellman et al. 2009). The presence of rare taxa in a landscape can also increase the aRSAP, other factors being held constant (Bunting et al. 2004). For example, Commerford et al. (2013) observed the effect of rare taxa empirically: small lakes in a 'very open' grassland in Kansas had a large aRSAP of 1,060 m, which they attributed to scattered tree taxa in the tallgrass prairie.

The contemporary forests around our lake sites are dense, closed, and heavily dominated by Douglas-fir (Skinner et al. 2018). Taxa like black oak (*Quercus*), white alder (*Alnus*), and white fir (*Abies*) are present but not common. These rare taxa in the area contributed little to the overall biomass (2.3%) but make the landscape more heterogeneous. This heterogeneity can result in a larger aRSAP than if there were no rare taxa present. All else being equal, longer distances from each sampling site are required to get a sufficient cover of all taxa within the landscape to reach the regional average. These greater distances produce larger aRSAP estimates (Hellman et al. 2009).

tRSAPs have been estimated at small lakes and ponds. For example, the tRSAP for *Pinus* was 200 m from the lakeshore in northeastern Germany (Matthias and Giesecke 2014), and other tRSAP values in that study ranged from 50 m (*Quercus*) to 300 m (*Fagus*) to 1,000 m (*Betula*). Jackson (1990) found small tRSAP estimates from ponds in New York: *Acer* (< 20 m), *Betula* (> 1,000 m), *Fagus* (> 1,000 m), *Picea* (< 100 m), *Quercus* (> 1,000 m) and *Pinus*/*Tsuga* (< 500 m). In this study, the tRSAP value for *Pinus* was 225 m, a near match to Matthias and Giesecke (2014) and comparable to Jackson (1990). The other tRSAP values in this study ranged from 225 m (TCT) to 525 m (*Notholithocarpus*) to 625 m (*Pseudotsuga*). Like Matthias and Giesecke's results, the tRSAPs are inconsistent with expectations based solely on the respective fall speeds of the taxa. For example, *Pinus* has one of the assemblage's lowest fall speeds and was expected to travel longer distances and have a large tRSAP; in fact, it had one of the shortest tRSAPs.

Unexpectedly small source areas of highly dispersible taxa have been observed in simulated landscapes (e.g., *Betula*, Sugita 1994) and have been attributed to vegetation patterning. The estimated RSAP reflects the minimum distance at which the regional vegetation composition is attained. For example, if *Betula* is uniformly spread in a forest, the regional distribution signal of *Betula* will be captured closer to the sampling point than in a forest where *Betula* is heterogeneously spread across the forest. In this case, tRSAP reflects the distance at which regional vegetation composition is reached, instead of being predominantly controlled by the taxon's pollen dispersal ability and depositional properties (Sugita 1994). The vegetation patterns in the Klamath area are complex and heterogeneous (Skinner et al. 2018). Within the sampling area, Douglas-fir (*Pseudotsuga*) is the dominant species with large amounts of tanoak (*Notholithocarpus*) at most lake sites, with pines (*Pinus*) intermixed and some cedars (TCT). The small "patches" of pines and cedars within a Douglas-fir dominant overstory could effectively

shrink the tRSAPs of *Pinus* and TCT, following the logic presented in Sugita (1994). Thus, the finding of relatively small tRSAPs for *Pinus* and TCT, despite their fall speeds, and relatively large tRSAPs for *Pseudotsuga* and *Notholithocarpus*, aligns with the study area's vegetation patterning.

Our estimated aRSAP (625 m) and tRSAP values (all 625 m or less) suggest consistent, though not identical, interpretations of the source area of pollen. Both estimates indicate that the pollen deposition pattern captures a local view of about the same spatial scale of the surrounding vegetation. Given that vegetation surveying must meet or exceed the scale of the relevant source area of pollen for quantitative reconstruction (Bunting et al. 2004), vastly different aRSAP and tRSAP estimates would potentially be consequential. If, for example, we had estimated an aRSAP << tRSAP, it would imply that our assemblage-level view was in some way blind to taxa in the assemblage, and thus missing important landscape patterning or other features of the area from which pollen originated. On the other hand, if we had estimated an aRSAP >> tRSAP, it would imply the subsequent reconstruction represents a larger area than is potentially being recorded by the pollen system.

This consistency between the aRSAP and tRSAP results was reflected in the similarity of the AGL_{dw} reconstructions (Table 3, Table 4). On average, observed AGL_{dw} for each lake was 10.1 Mg ha^{-1} (5.2%) larger using aRSAP with the differences ranging from 2.6 Mg ha^{-1} (1.1%) larger at North Twin Lake to 22.2 Mg ha^{-1} (10.3%) larger at Onion Lake. The differences in terms of predictive ability were equally modest with aRSAP estimates producing somewhat more accurate and less biased results.

5.2 The potential of calibrated PAR as a bioproxy
Establishing the relationship between contemporary biomass and modern PAR values is contingent upon obtaining accurate sedimentation rates in cores. We are confident in our estimated sedimentation rates for two key reasons. First, we used a state of the art, robust Bayesian model to develop age models from ^{210}Pb dates (Aquino-López et al. 2018). Our results showed low uncertainty in the modeled ages in all cores, particularly in the top 20cm. Second, we were able to compare our upper sedimentation rates representing the last decade to estimates from two of the same lakes (Ogaromtoc and Fish lakes) that were collected in 2008 and 2009 (Crawford et al. 2015). We found similar sedimentation rates in the upper sediments: 2.0-4.0 mm yr^{-1} compared to 2.0-3.3 mm yr^{-1}. Our modern PAR values are also in agreement with PAR values from the youngest sediments in Crawford et al. (2015).

The ultimate goal of this research was to assess whether PAR be used to predict distance-weighted biomass for major tree taxa in the Klamath area, and therefore generate models suitable for reconstruction of past biomass dynamics. The fact that contemporary pollen influx is a reasonably precise predictor of contemporary distance-weighted AGL at these sites suggests that PAR can be used to infer changes in plant biomass for these sites. But even with apparently statistically sound modern models, it may not be reasonable to apply the models for reconstruction in all contexts. In an ideal situation, the calibration dataset would include sites with a wide range of population sizes of the main taxa to allow any time in the fossil record to be reconstructed. Our model had less skill in estimating low levels of forest biomass because we were unable to find lake sites that both met our selection criteria and supported sparse forest

cover. Other modern quantitative vegetation reconstruction models have been restricted at the upper end of the calibration. Trees growing in dense forest stands produce less pollen than an exposed tree in a field, which suggests that increased forest density could result in reduced net pollen productivity (Andersen 1970, Fægri and Iverson 1989, Feldman et al. 1999). For example, Blarquez et al. (2011) found that the relationship between needle accumulation rate and forest basal area tended to saturate above 40 $m^2 ha^{-1}$ for conifer-dominated sites. However, despite the high biomass-density of the contemporary forest at our sites (Knight et al. 2020), there was no evidence of saturation in the PAR-biomass functions for the major taxa. Even at the maximum PAR values, the biomass values increase at pace following the log-linear fits (Fig. 8a).

Long-term PAR records from lakes in the area provide insight into time periods where our calibrated models will be able to capture past conditions. Comparable taxa-specific PAR values from lake sites in the region were only available for *Pinus,* and they suggest time periods of agreement with our *Pinus* PAR measurements and our total *Pinus* PAR-AGL model, which covers a range between 1,500 and 11,000 grains $cm^{-2} yr^{-1}$. For example, Briles et al. (2008) reported *Pinus* PAR between 2,000 and 8,000 grains $cm^{-2} yr^{-1}$ at Sanger Lake in the western Klamath Mountains over 15,000 years. Likewise, a 3,000-year PAR record from Fish Lake (a lake also examined in this study) shows agreement with our total *Pinus* PAR range during some time periods. Fish Lake's record shows temporal variability in *Pinus* PAR values between 2,000 to 9,000 grains $cm^{-2} yr^{-1}$ during the last two hundred years (Crawford et al. 2015), which falls within our calibration. Lastly, total PAR values measured at eight lakes in the Klamath area since 15,000 BP range from 2,000 to 15,000 grains $cm^{-2} yr^{-1}$ (Briles et al. 2011) and are similar in size to lakes in this study and have a dense surrounding forest, although they are located in the white-fir vegetation zone.

In addition to selecting a range of forest conditions, researchers undertaking similar efforts will need to consider the number of lakes needed for statistical soundness for the calibration. The seven lakes presented here appear to have been sufficient to build robust models in terms of low coefficient of variation (Table 3), but it may be difficult in other locations to find enough suitable lakes using consistent selection criteria. If reconstructions of continuous Holocene-length biomass records are sought, using a high number of lakes has the downside of great expense (from radiometric dating) and labor (from pollen counting), unless accurate automated classification systems become widespread (Sevillano et al. 2020).

The calibration step we undertook required modern biomass data, which may be difficult to obtain empirically for a large number of lakes or in settings with challenging topography. For example, transects in this study ran 750 m from the shoreline, but steep topography and scree slopes occasionally prevented a complete survey. Because we studied small lakes and needed finely resolved biomass data, sparse inventory data with large geographic extent (e.g., FIA data) were not an appropriate substitute for field surveys. However, FIA data provided essential information regarding the basal area to biomass relationships for the common tree species in the region (Table S8).

5.3 Limitations of PAR and PVMs
Our results show the utility of calibrated PAR-AGL models for this study, and we have provided a robust process for including uncertainty in PAR-AGL models. However, PAR itself may vary

in ways that reduce its value for pollen-based reconstructions in all landscapes. For instance, net pollen deposition can vary spatially and temporally if sediment focusing or pollen redeposition occurs. While studies investigating PAR from modern sedimentary records did not find that redeposition and sediment focusing affected PAR (Seppä and Hicks 2006; Giesecke and Fontana 2008), other studies have documented the influence of these factors on PAR (Davis et al. 1984, Odgaard 1993, Matthias and Giesecke 2014). Additionally, between-lake differences in PAR values can arise from differences in pollen taphonomy due to basin size or stream inflow (Davis 1967b). Pollen monitoring studies have illustrated another known issue with PAR: the amount of pollen produced can change year to year and is related to the weather conditions of the preceding year (Hicks 2006). Lastly, one study has implied that PAR may depend on the net primary production of the pollen-producing taxa as well as overall plant biomass (Matthias and Giesecke 2014). Without long-term pollen monitoring studies across different biomes and accompanying detailed biomass data, true data validation will not be possible.

Pollen transport in mountain environments has been studied in Europe through the European Pollen Monitoring Programme, but, to our knowledge, has not been studied in the mountains of western North America outside of the present work. Several pollen monitoring studies with transects running through multiple vegetation zones in mountainous areas tend to show that pollen from lower forest zones is quite abundant in upper zones, and this effect appears more pronounced when high altitude zones have lower productivity (e.g., the Rila Mountains in Bulgaria, Tonkova et al. 2001). Unlike mountain transect studies, our sites are all within one vegetation zone, therefore reducing the significance of these effects, and we are not studying tree line position. The Douglas-fir dominated conifer forest in the Klamath Mountain is a relatively high productivity zone, and such zones typically show less of an "uphill" effect that impacts tree-line pollen assemblages (e.g., Swiss Alps tree line study, Sjögren et al. 2008)."

All PVMs, including PAR-biomass transfer functions, are based on assumptions that may not hold in a changing landscape. It must be assumed, for example, that taphonomic processes filtering pollen in lake sediments are constant over time and among lakes, unless taphonomic biases are precisely quantified (Allison and Bottjer 2011). Using our method, quantitative biomass reconstruction would also assume that the relevant source area of pollen is constant over time. We estimated the aRSAP of our seven sites as well as the tRSAP of abundant taxa, but these may apply to a landscape arrangement which is unique in the last 3,000 years. The present-day high PAR values of *Pseudotsuga* are not replicated in the fossil pollen record at any other time in three millennia (Crawford et al. 2015), suggesting that the dominance of shade tolerant *Pseudotsuga* is also not found elsewhere during this period. Deep-time reconstructions from lakes in this study have shown large changes in vegetation composition due to climate, Native land-use, fire disturbances, and, in the last century, fire suppression. In response, we anticipate that the relevant source areas of pollen will expand and contract over time. Because the spatial patterns of past vegetation are usually unknown, it is difficult to estimate past relevant pollen sources areas. However, the Multiple Scenario Approach (MSA, Bunting and Middleton 2009) can offer insight on this issue. Under MSA, hypothetical landscapes are created via rules for plant placement and environmental parameters, and then pollen assemblages are simulated and compared to known pollen signals to identify probable past vegetation mosaics. Another experimental method to estimate past relevant pollen source area has been explored through modeling (Hellman et al. 2009) where regional vegetation composition and available pollen

productivity estimates are available for multiple sites (Sugita 2007b). Hellman et al.'s (2009) simulations suggest relatively robust aRSAP estimates of 1,000 to 2,500 m for small lakes under hypothetical landscapes from southern Sweden where natural and anthropogenic disturbances have occurred during the Holocene. Such simulations provide a means to test the potential robustness of aRSAP in the Klamath area.

6. Conclusion

Although methodologically challenging, calibrating PAR-biomass models is an important step towards quantitative reconstruction of past vegetation. Our calibration steps included estimating the spatial extent represented by the pollen system, comparing two estimates of the RSAP, and evaluating PAR-AGL models. We found comparable aRSAP and tRSAP estimates that aligned with expectations given the modern forest's dense, closed conditions. We also demonstrated that PARs of major tree taxa derived from lake sediments are linearly related to distance-weighted AGL, and our PAR-AGL$_{dw}$ models accurately reconstruct modern lake-surrounding biomass. According to PAR values from local and regional lakes sites, our modern models are broad enough to capture a range of forest structures over the last 15,000 years. We therefore conclude that our results prove the utility of calibrated PAR-AGL models for quantitative reconstruction of past vegetation.
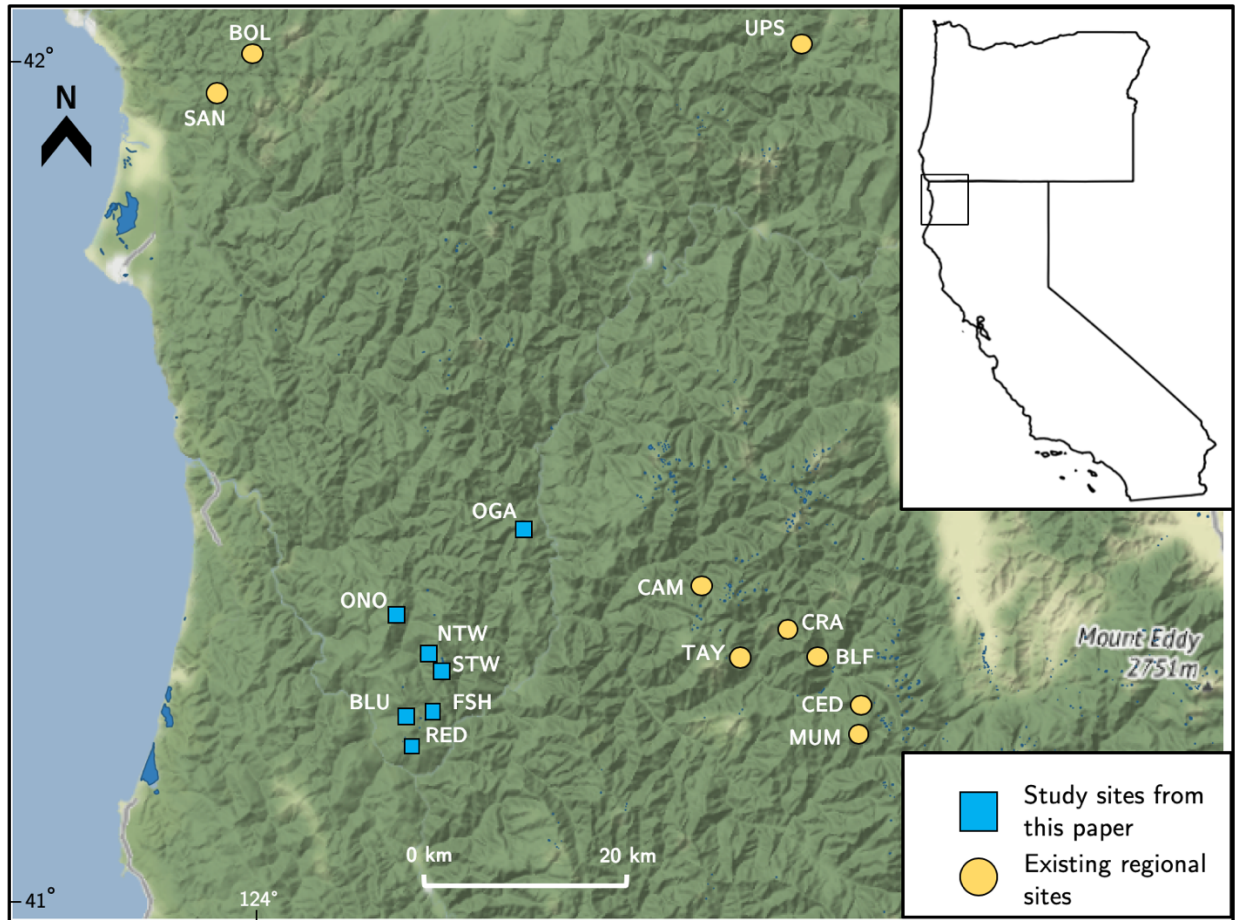
Figures

Figure 1. Map shows study sites (blue squares) in northwestern California: Blue Lake (BLU), Fish Lake (FSH), North Twin Lake (NTW), Lake Ogaromtoc (OGA), Onion Lake (ONO), Red Mountain Lake (RED), and South Twin Lake (STW). Note that Lake Ogaromtoc and Fish Lake were described in Crawford et al. (2015) and North and South Twin Lake were described in Wanket (2002) but were also studied in this project. Map also shows Holocene-era pollen records from other parts of the region (yellow circles): Bluff (BLF) and Crater (CRA) Lakes (Mohr et al. 2000); Sanger (SAN) and Bolan (BOL) Lakes (Briles et al. 2008); Upper Squaw Lake (USL; Colombaroli and Gavin 2010); Mumbo (MUM) Lake (Daniels et al. 2005); and Campbell (CAM), Taylor (TAY), and Cedar (CED) Lakes (Briles et al. 2011).
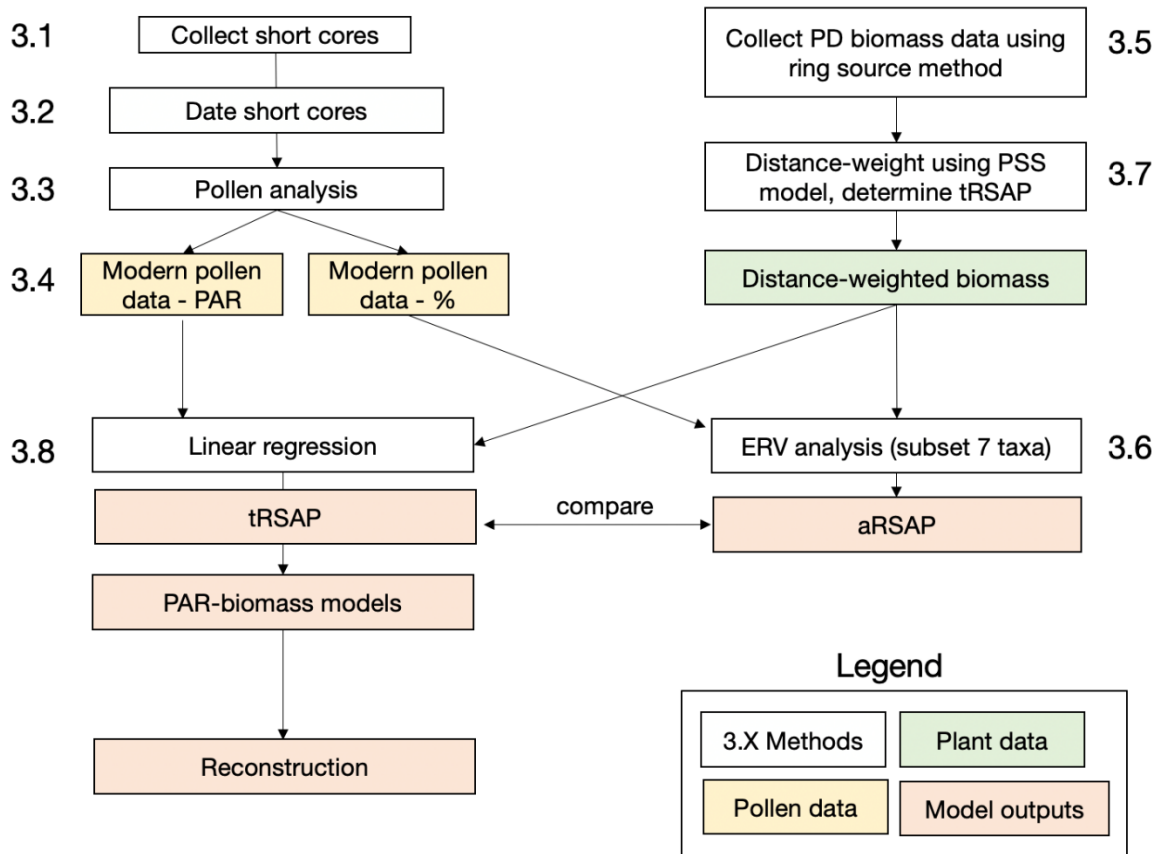
Figure 2. Flowchart of methodological steps leading to a calibrated PAR-biomass model.
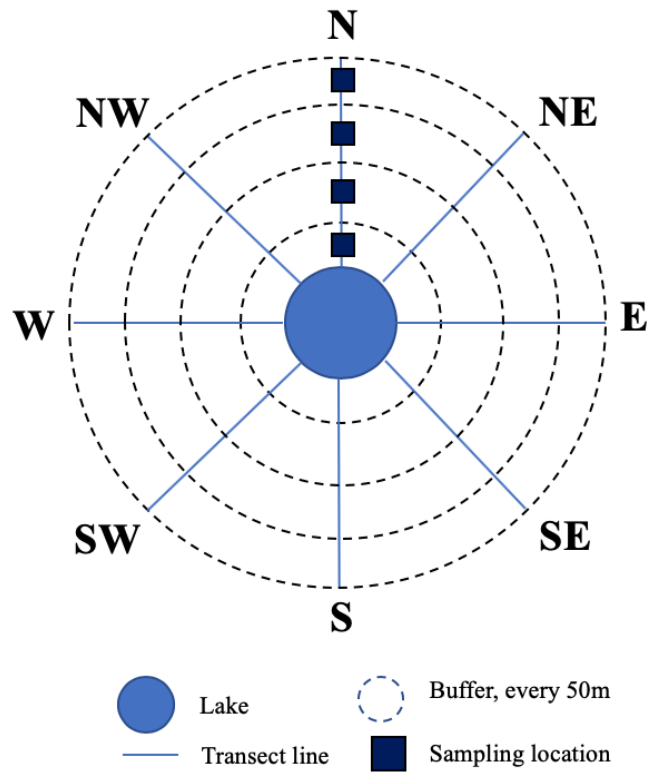
Figure 3. A schematic of the vegetation survey design (not to scale), following Han et al. (2017), that included eight transect lines along the cardinal and sub-cardinal directions where sampling occurred at the mid-point of each concentric ring (the schematic shows an example with only four rings). Sample locations (squares) are shown on the north transect for illustration.
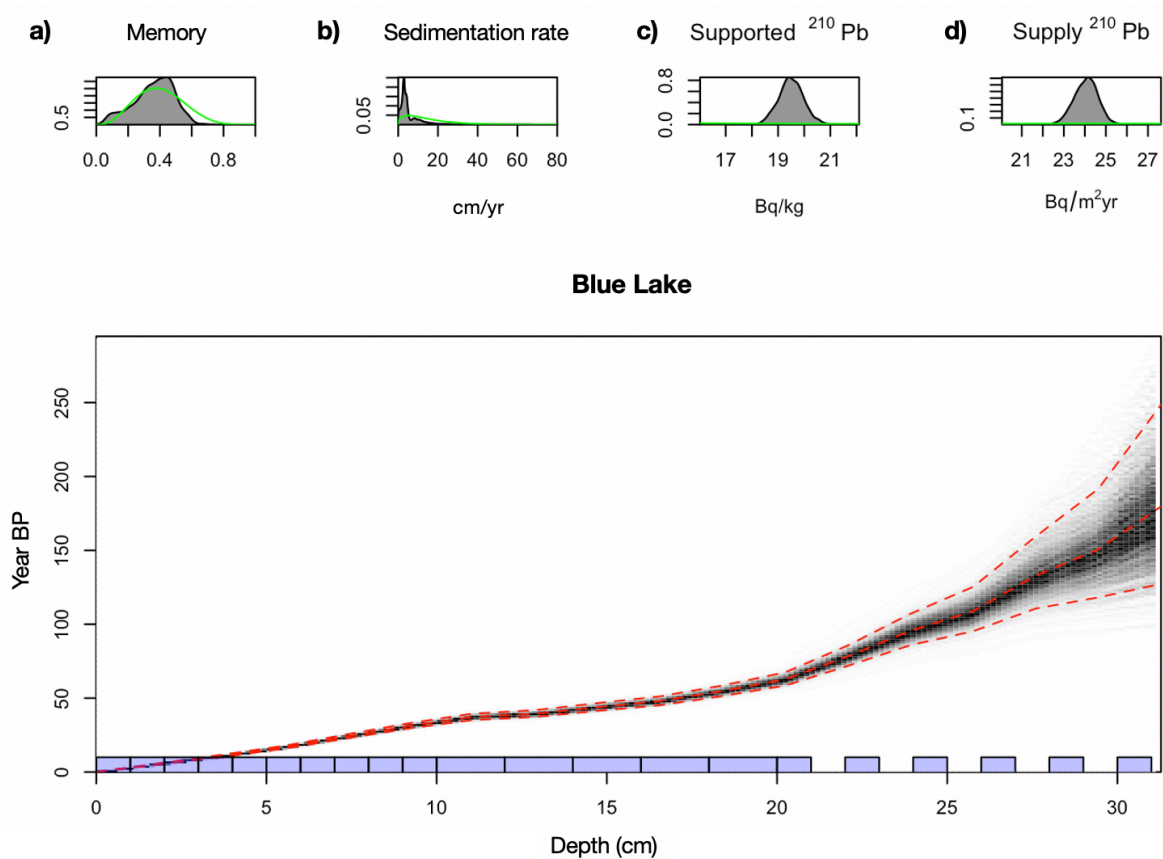
Figure 4. Example of Pb-210 age model construction. The age-to-depth results of the Plum modeling for Blue Lake. The grey lines are simulation from Plum and the dashed red lines represent the mean age and the 95% interval. The small panels at the top show the prior (green) and posterior (grey) distributions for **(a)** the memory (ω), which describes the coherence in sedimentation rates along the core **(b)** the sedimentation rate (α), **(c)** the supported ^{210}Pb (P^S), which is the background level of ^{210}Pb already present in the sediment, and **(d)** and the supply of ^{210}Pb (Φ). For other sites, see Supplementary Information.
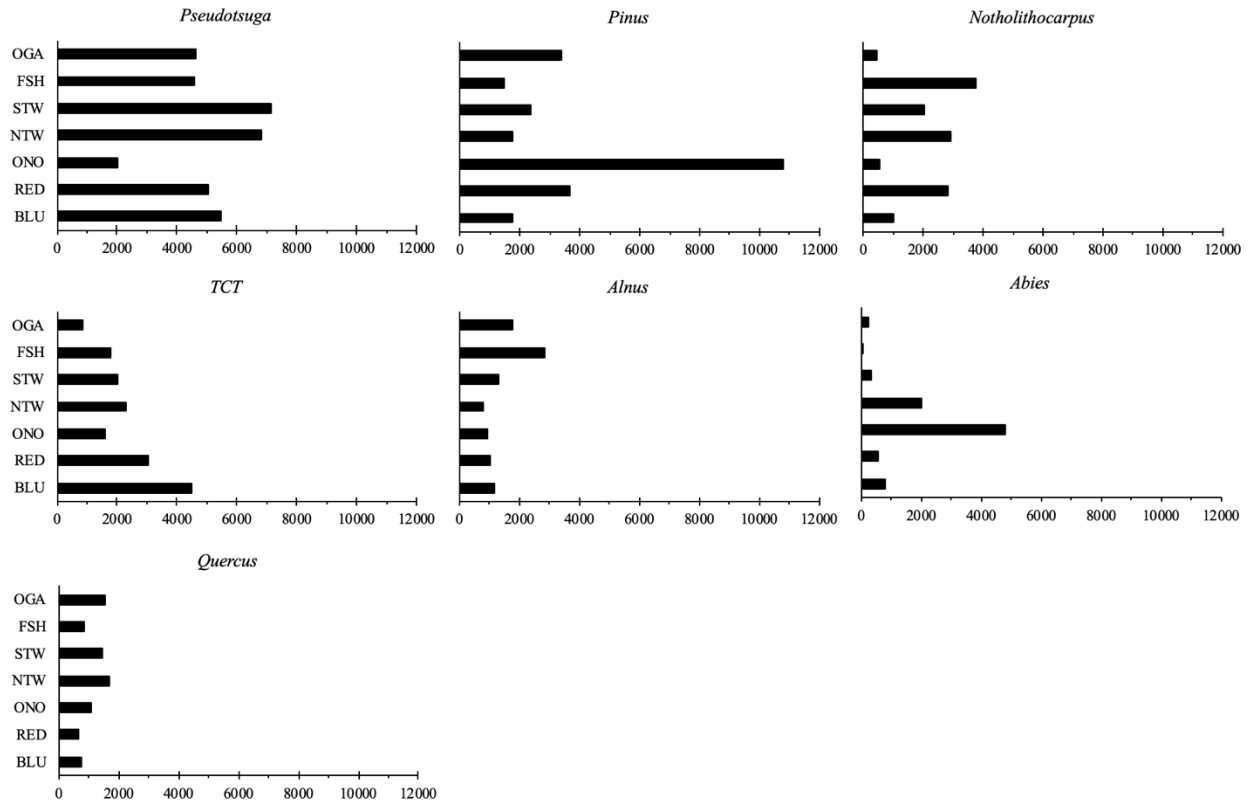
Figure 5. Pollen accumulation rates (grains cm^{-2} yr^{-1}) for the most important wind-pollinated taxa in 2018 in the Klamath Mountains. Lake sites are abbreviated: Ogaromtoc lake (OGA), Fish lake (FSH), South Twin Lake (STW), North Twin lake (NTW), Onion lake (ONO), Red Mountain lake (RED), and Blue lake (BLU). For the data's tabular form, see Table S10.
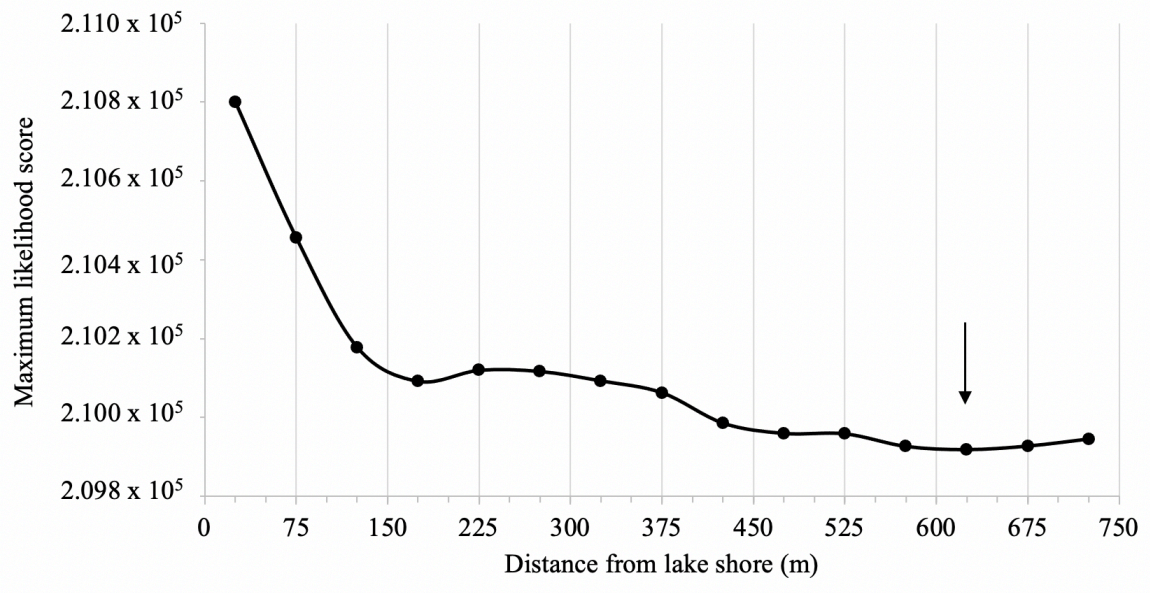
Figure 6. PolERV model 3 results of maximum likelihood scores compared to distance (m). Arrow indicates the aRSAP value (625m).
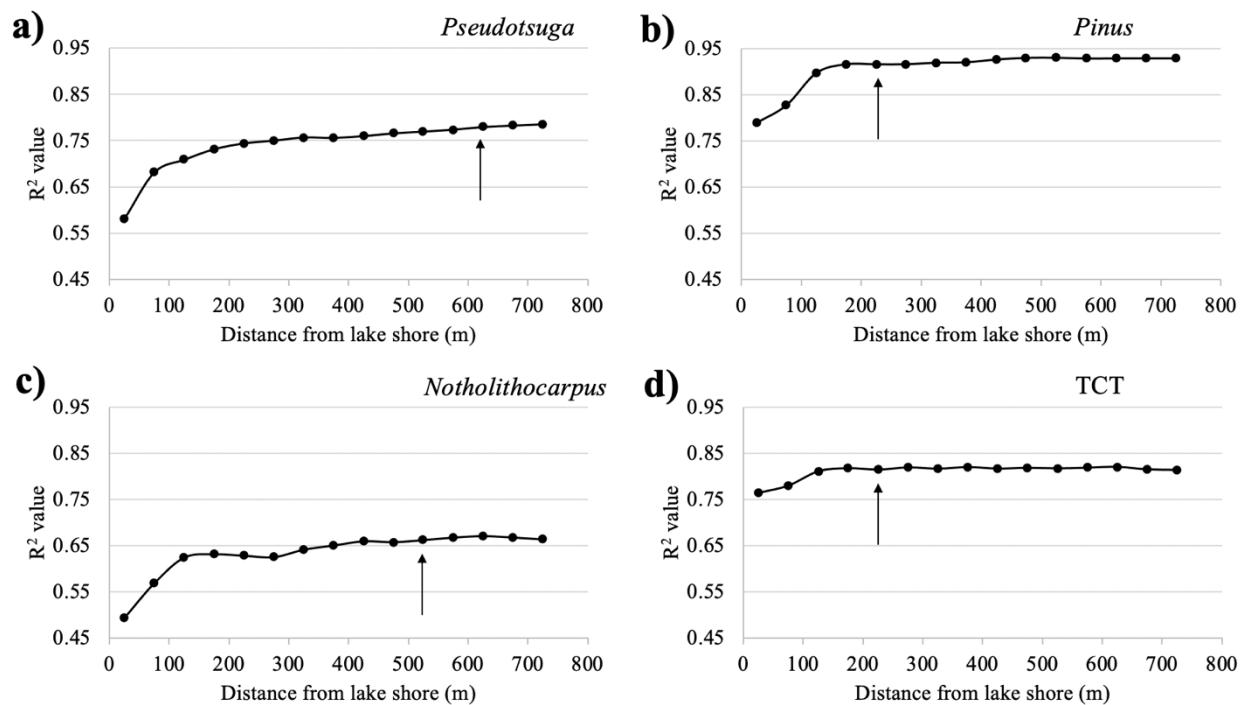
Figure 7. R^2 for regressions between AGL_{dw} and PAR at increasing distance from the lake shore to the furthest vegetation survey site. tRSAP is shown by the arrow: **a)** *Pseudotsuga* (625m), **b)** *Pinus* (225m), **c)** *Notholithocarpus* (525m), and **d)** TCT (225m).
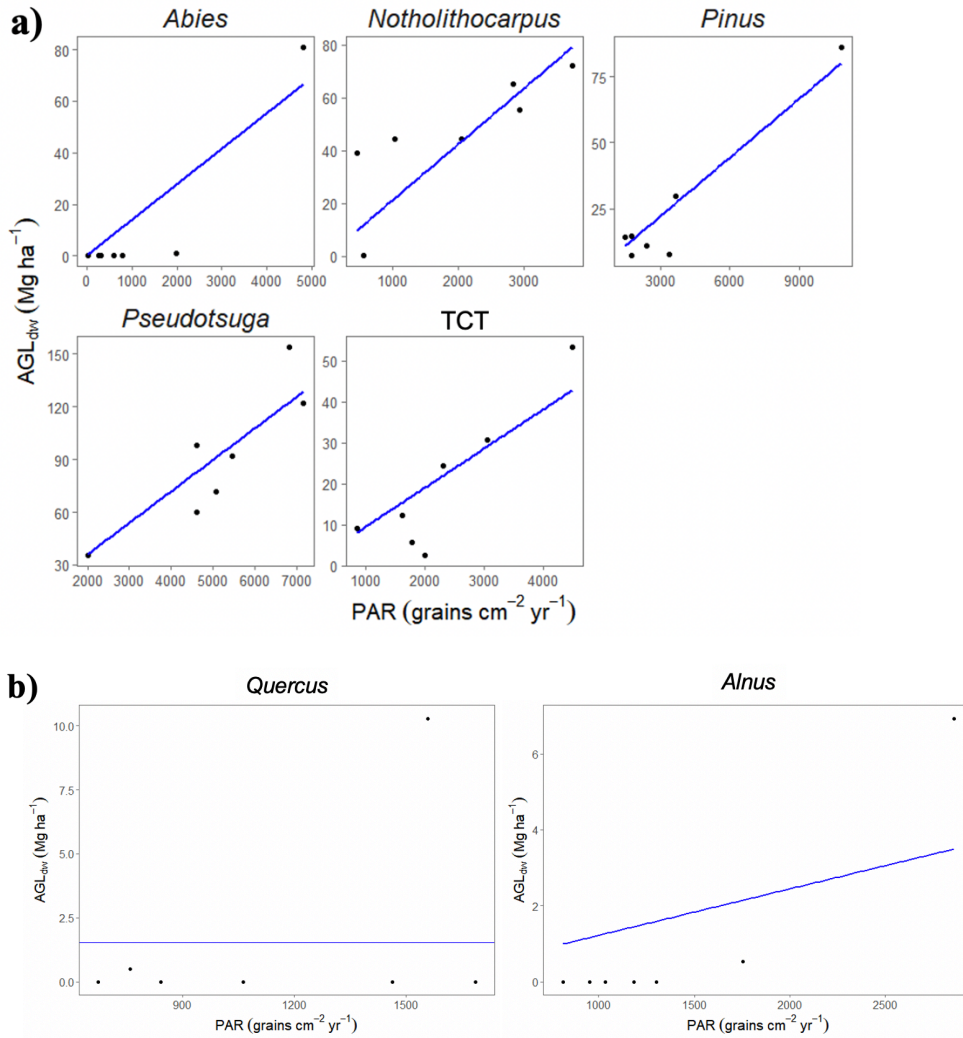
Figure 8. a) The relationship between distance-weighted aboveground live biomass (AGL$_{DW}$) and pollen accumulation rate (PAR) for five of the pollen taxa present at the seven lake sites in the Klamath Mountains. Lines represent linear regressions forced through the origin. The relevant source area of pollen (aRSAP) was defined as a circle with a radius of 625 m from the centroid of the lake. Note that the scales change for each pollen taxa. For summaries of the linear models, see Table S11. (Note: Although biomass "predicts" pollen accumulation rates in a functional sense, our aim is to eventually apply calibrated transfer functions to predict biomass in the past; thus, we fitted regression lines with PAR values as the independent variable.) **b)** The relationship between distance-weighted aboveground live biomass (AGL$_{dw}$) and pollen accumulation rate (PAR) for *Quercus* and *Alnus* at the seven lake sites in the Klamath Mountains. The line represents the intercept of the null model. The relevant source area of pollen was defined as a circle with a radius of 625 m from the centroid of the lake. For details on the linear model, see Table S11.

Tables

Table 1. Definitions of RSAP, aRSAP, and tRSAP.

Term	Definitional basis and relevant literature
RSAP	Originally described by Sugita (1994) as the "smallest area within which reliable estimates of parameter values and asymptotic r^2 or likelihood function scores can be obtained." The definition was refined as the "distance from a pollen deposition point beyond which the relationship between vegetation composition and pollen assemblage does not improve" (Bunting et al. 2004, with Sugita). Estimates are derived for the overall assemblage from extended R-value analysis (Parsons and Prentice 1981) through inspection of the likelihood function score plot. RSAP varies depending on which taxa and which sites are included in the analysis, thus is dependent on the assemblage chosen for analysis.
aRSAP	Identical to the standard RSAP, but with the addition of an "a" to denote that it is an assemblage-specific metric, in contrast to the tRSAP.
tRSAP	The RSAP concept can be extended to single taxa where pollen taxa are measured independently (e.g., PAR values rather than percentage values). In this situation, we define a taxon-specific Relevant Source Area of Pollen, the tRSAP, as the distance beyond which the correlation between PAR (Y) and distance-weighted plant abundance (ψ) summed to that distance for a single taxon does not improve (Jackson 1990).

Table 2. Lake site characteristics and overstory vegetation at each site.

Lake site and code	Lat and long (dec. degrees)	Elevation (m)	Depth at deepest point/sample location (m)	Surface area (ha)	Mature overstory vegetation
Blue (BLU)	-123.69, 41.24	822	4.6	1.4	*C. lawsoniana, P. menziesii, C. chrysaphylla, N. densiflora, A. menziesii, A. rhombifolia, P. lambertiana, T. brevifolia*
Fish (FSH)	-123.68, 41.26	541	13	9.6	*C. lawsoniana, P. menziesii, P. lambertiana,* *N. densiflora, A. menziesii, A. rhombifolia, C. chrysaphylla*
North Twin (NTW)	-123.67, 41.32	1142	0.5	3.4	*P. menziesii, P. lambertiana, C. lawsoniana, C. chrysaphylla, P. jeffreyi, T. heterophylla, C. decurrens, N. densiflora, A. menziesii*
South Twin (STW)	-123.67, 41.31	1137	1.2	3.5	
Onion (ONO)	-123.75, 41.38	1356	1.5	0.66	*P. ponderosa, P. menziesii, A. magnifica, C. decurrens, A. concour, P. lambertiana, T. brevifolia*
Ogaromtoc (OGA)	-123.54, 41.49	600	6.3	1.74	*P. menziesii, N. densiflora, P. lambertiana, A. macrophylla, A. rhombifolia, A. menziesii, U. californica, C. decurrens, Q. kelloggii, Q. garryana*
Red Mountain (RED)	-123.69, 41.25	768	1.6	1.2	*C. lawsoniana, P. menziesii, P. lambertiana, N.densiflora, A. menziesii, A. rhombifolia, C. chrysaphylla*

Table 3. A comparison of observed to predicted distance-weighted aboveground live biomass (AGL$_{dw}$) for each lake site using the assemblage-level relevant source area pollen (aRSAP) estimates. Predicted AGL$_{dw}$ is the mean from 10,000 resampling iterations; Standard Error is the standard deviation of the 10,000 samples; COV is the coefficient of variation (Standard Error/Predicted AGL$_{dw}$); Bias is the percent difference between predicted and observed AGL$_{dw}$.

Lake	Observed AGL$_{dw}$ (Mg ha^{-1})	Predicted AGL$_{dw}$ (Mg ha^{-1})	Standard Error (Mg ha^{-1})	COV (%)	Bias (%)
Blue	205	189	31.5	17	-7.8
Fish	197	195	31.8	16	-1.1
North Twin	242	251	32.0	13	3.7
Ogaromtoc	127	134	31.6	24	5.7
Onion	215	212	32.1	15	-1.1
Red Mountain	197	218	31.4	14	10.5
South Twin	180	217	31.6	15	20.5

Table 4. A comparison of observed to predicted distance-weighted aboveground live biomass (AGL$_{dw}$) for each lake site using taxon-specific source area pollen estimates (tRSAP). Predicted AGL$_{dw}$ is the mean from 10,000 resampling iterations; Standard Error is the standard deviation of the 10,000 samples; COV is the coefficient of variation (Standard Error/Predicted AGL$_{dw}$); Bias is the percent difference between predicted and observed AGL$_{dw}$.

Lake	Observed AGL$_{dw}$ (Mg ha^{-1})	Predicted AGL$_{dw}$ (Mg ha^{-1})	Standard Error (Mg ha^{-1})	COV (%)	Bias (%)
Blue	196	189	31.5	17	-3.7
Fish	185	195	31.8	16	5.2
North Twin	239	251	32.0	13	4.9
Ogaromtoc	121	134	31.6	24	10.6
Onion	193	212	32.1	15	10.3
Red	184	218	31.4	14	18.4
South Twin	173	217	31.6	15	24.9

Transition between chapter 2 and chapter 3

In chapter 2, I quantitatively linked spatially explicit measures of plant abundance to pollen influx data at seven lake sites in Six Rivers. I fit linear models of pollen influx values from modern lake sediments with empirical, distance-weighted estimates of aboveground live biomass. I found that the pollen from major tree taxa around the lake sites were statistically significant and reasonably precise estimators of modern aboveground live biomass.

The contributions of chapter 2 are two-fold. First, it demonstrates pollen influx-biomass relationships can provide a robust means of inferring changes in past vegetation biomass. Second, this insight was critical because it allowed a 3,000-year record of pollen influx data from this area to be converted into forest biomass values, which is the subject of chapter 3. Thus, chapter 2 serves as a methodological bridge that allowed me to tie findings about forest conditions in the 1880s (chapter 1) to forest conditions over the late Holocene (chapter 3). In chapter 3, I expand on the reasons for forest change over 3,000 years by incorporating multiple data sources including Native oral histories, fire scar and charcoal data, and other historical records. This chapter explores how Indigenous land stewardship affected forest conditions and provides context to current forest conditions over a long time horizon.

CHAPTER THREE

Land management explains major trends in forest structure and composition
over the past 3000 years in California's Klamath Mountains

Abstract

For millennia, forest ecosystems in California have been shaped by fire both from natural processes and Indigenous land management. Twentieth century fire suppression coupled with a warming climate has caused forest densification and increasingly large wildfires that threaten forest ecosystem integrity and the State of California's plan to manage forests as part of climate mitigation efforts. To put recent changes in a historical context, we elucidate anthropogenic influence on forest conditions over three millennia in the western Klamath Mountains – the ancestral territories of the Karuk and Yurok Tribes – by combining paleo-environmental data and Indigenous knowledge. Findings show tribal burning practices coupled with a lightning-based fire regime were associated with long-term stability of forest biomass. Before Euro-American colonization, the long-term median forest biomass at our study sites was between 104 Mg/ha (SE 33.5) and 128 Mg/ha (SE 24.4), compared to values over 250 Mg/ha today. Indigenous depopulation after 1800 AD coupled with 20th century fire suppression likely allowed biomass to increase, culminating in the current landscape: a closed Douglas-fir dominant forest unlike any seen in the preceding 3000 years. Findings are consistent with pre-contact forest conditions being influenced by Indigenous land management and suggest large-scale interventions would be needed to return to historic forest biomass levels.

1. Introduction

Fires ignited by lightning and Indigenous people have influenced the structure and composition of forest ecosystems in the American West for millennia (Wright and Heinselman 1973, Kimmerer and Lake 2001). Indigenous Knowledge from Tribal sources, historical ethnographic accounts by Euro-Americans, and ecological reconstructions all document landscape features consistent with a regime of frequent fire consisting of both lightning-based ignitions and Indigenous ignitions (Blackburn and Anderson 1993, Anderson and Moratto 1996). Over the past century, however, forests in the American West have been altered due to the removal of Indigenous stewardship, the imposition of fire exclusion, and the harvest of merchantable trees (Stephens and Sugihara 2006). As a result of this management history coupled with a warming climate, large fires increasingly threaten the ecological integrity of many conifer-dominated California forests (Serra-Diaz et al. 2018, Westerling 2018). Wildfire hazards also jeopardize the State of California's plan to manage forest ecosystems for carbon storage as part of climate mitigation efforts (Natural and Working Lands Climate Change Implementation Plan 2019). Successful management and conservation efforts partly depend on meaningful comparisons between modern conditions and long-term histories (Barnosky et al. 2017), as well as an understanding of how humans have shaped historical baselines (Long et al. 2020).

Because western North American forests are partly a product of Indigenous burning (Codding and Bird 2013, Taylor et al. 2016), these forests provide an ideal setting to study human-modified baselines with the goal of transferring information to land managers. The State of California has explicitly recognized the importance of historical perspectives – e.g., with 2018's Senate Bill 901 calling for the development of "a historic baseline of greenhouse gas emissions before fire suppression" (SB-901 2018). However, current wildfire and resiliency discussions still lack an understanding of how recurring fire impacted forest biomass over long time horizons. An accurate reference of ecosystem dynamics requires incorporation of data predating Euro-American colonization. Underestimation of Indigenous fire use on past landscapes may generate misleading inferences about the best way to conserve fire-prone ecosystems (Stephens et al. 2007). Thus, characterizing Indigenous effects on ecosystems – an Indigenous baseline – is a pressing scientific challenge with important implications for land management (Long et al. 2020, Armstrong et al. 2020, Lake 2007).

Quantifying the degree to which pre-colonial forests were a product of natural (e.g., climate) versus anthropogenic activities (e.g., Indigenous burning) is not straightforward. However, multidisciplinary methodology has successfully distinguished human-caused vegetation change from climatically-driven vegetation changes in California (Lake 2007, Ejarque et al. 2015, Bowerman and Clark 2011, Klimaszewski-Patterson et al. 2021). For example, previous research has identified paleo-ecological evidence suggesting open-forest conditions and shade-intolerant vegetation when the prevailing climate favored the development of a closed-canopy forest with shade-tolerant vegetation (Klimaszewski-Patterson et al. 2021). The underlying assumption was that the persistence of shade-intolerant taxa (e.g., *Quercus*) and their associated habitat during cool, wet periods when shade-tolerant taxa (e.g., *Pseudotsuga*) should climatically dominate (e.g., the Little Ice Age) is a signal of a human-modified landscape (Klimaszewski-Patterson et al. 2021). We built on that technique and also integrated multiple lines of evidence to answer socioecological questions about land use change and the links between forest biomass and fire. Specifically, we investigated the impacts of Indigenous management and biophysical controls on

forest ecosystems in two small watersheds in the western Klamath Mountains. Our main question is: what is the extent to which climate and/or human activity influenced major trends in reconstructed forest biomass over the past 3000 years? The 3000-year paleoecological record derives from sediment cores from two low-elevation sites, Fish Lake and Lake Ogaromtoc (Fig. 1)(Crawford et al. 2015); vegetation at both sites is comprised of montane hardwood-conifer forests with a diverse, well-mixed canopy of tree species (Table S1) (Sawyer and Thornburgh 1977). Fish Lake is an area of joint use between the Karuk and Yurok Tribes, and Lake Ogaromtoc is a cultural-use site in the Karuk's ancestral territory. We used a mixed methods approach, drawing from:

(1) Karuk and Yurok Tribe ethnographies (Lake 2007) and Karuk/Yurok-based Traditional Ecological Knowledge (section 2.1)
(2) Paleoecological records (biomass, charcoal, and fire scars) (section 2.2)
(3) Correlations among climate, vegetation, and fire proxies (section 2.3)
(4) Multiple independent cross-references (Birks and Birks 2006) to validate the biomass record with historical data from 1880 AD onward (section 2.4).

Our integrated approach demonstrates the magnitude of Indigenous influence on pre-contact forests, while independent cross-references enabled us to check estimates of our novel biomass reconstruction. Critically, these integrated results allow us to contextualize land ownership change and management decisions that have played out over centuries and discuss the implications for modern landscape interventions.

2. Results
2.1   Indigenous burning practices resulted in significant landscape modification
Indigenous peoples have inhabited the Klamath-Siskiyou bioregion for at least 9,000 years (King et al. 2016). Oral histories suggest that, for at least the last century, Indigenous people of the Klamath Mountains – the Karuk and Yurok – have intentionally ignited, and still ignite, fires for numerous reasons: production of food and fiber, ceremonial purposes, creation of travel corridors, promotion of hunting, and reduction of pest populations (Kimmerer and Lake 2001, Lake 2013, Halpern 2016). The Karuk describe fire as "crucial to who people are, and what they do," "enabl[ing] them to live" (Tripp et al. 2017).

The forest composition and structure encountered by Euro-American colonists in the mid 1800s was thus shaped by cultural burning practices developed over the last millennia (King et al. 2016). Specifically, in the watersheds encompassing Fish Lake and Lake Ogaromtoc, patch burning and broadcast burning altered the landscape. For the Yurok, the Fish Lake area was historically used for gathering hazelnuts, acorns, berries, basket materials, hunting game, camping, and other subsistence and ceremonial practices (Waterman 1920, see methods). The Karuk used Fish Lake and Lake Ogaromtoc for purposes similar to the Yurok, including as traditional gathering places for acorns from *Quercus kelloggii* (black oak) and *Notholithocarpus densiflorus* (tanoak), as well as mushrooms (Department of Natural Resources, Karuk Tribe 1999, see methods). Small patch burning facilitated pest control, berry and root harvesting, and trail maintenance, whereas broadcast burning often covered large extents and facilitated habitat conversion, nut/acorn harvesting, and hunting (Lake 2007). Patch burning was both seasonal and situational, and broadcast burning occurred during late winter/early spring and late summer/early fall (Zybach 2005). Broadcast burns were capable of altering vegetation succession at time scales

of decades to centuries (Lake 2007, Bonnicksen et al. 1999). In these watersheds, fire was applied in places where lightning fire was less common to achieve desired cultural conditions (Pullen 1996) and in places to preempt lightning ignitions. These burning practices were concurrent with, and influenced by, two distinct climate events: the warm, dry Medieval Climate Anomaly (MCA ~1100-600 calBP [calendar years before present, where 'present' is 1950 AD], Cook et al. 2004) and the cool, wet Little Ice Age (LIA ~600-100 calBP, Graham et al. 2007). For example, the greatest spatial extent of the Karuk's burning occurred around 250 calBP to maintain fire-tolerant assemblages (including *Quercus* spp.) that were promoted during the MCA's more xeric conditions (Skinner et al. 2018).

In addition to forest composition, Karuk oral history also indicates the occurrence of structural change before and after Euro-American colonization. Before contact, lower fuel levels and open forest were critical to the cultivation of acorns, nuts, berries, mushrooms, and weaving materials (Lake 2007, Tushingham and Bettinger 2013) that supported a population of tribal peoples (Chartfkoff and Chartfkoff 1975). The modern forest, in contrast, is overstocked and underburned: "We never had this much fuel on the ground," M. McCovey, a Karuk elder, said (Lake 2007). Members of the Karuk and Yurok Tribes recognize that their traditional lands are over-enriched in biomass; they characterize the current high biomass forest conditions as a "degradation" of subsistence land (Sowerwine et al. 2019, see methods). Additional ethnographic and historical evidence are in the supplement.

2.2   *Paleoecological data indicate frequent fire limited biomass*

Robust quantitative reconstruction of past plant abundance is possible using calibrated models of pollen influx (grains cm^{-2} yr^{-1}) and aboveground live biomass (Mg/ha) (Knight et al. 2021). Using models parameterized with data from Fish Lake and Lake Ogaromtoc, pollen influx values were transformed into aboveground live biomass using taxa-specific calibrated functions (Knight et al. 2021) and overlain with charcoal influx (particles cm^{-2} yr^{-1}) and fire scar records from both lakes. Total biomass trends at both sites track proxies for fire occurrence, namely charcoal influx trends (Fig. 2A,B, Fig. 3A,B) and fire scar records (Fig. 2C, Fig 3C). The fire scar record for Fish Lake and Lake Ogaromtoc indicates frequent fire with a median fire return interval for fire recorded by at least two trees of 8 and 15 years, respectively (Table 1). For the period of maximum sample depth (1700-1900 AD), the median return interval was 7 years for Fish Lake and 12 years for Lake Ogaromtoc. More samples were available at Fish Lake (n=35) compared to Lake Ogaromtoc (n=14). A majority of fire scars (Fish Lake=91%, Lake Ogaromtoc=81%) were recorded in the latewood or dormant position of the intra-annual tree ring, implying the majority of area burned in the fall. Dormant position fire scars could indicate winter and early spring (prior to radial growth) burns as well.

The charcoal and biomass records show site-specific variation. At Fish Lake, charcoal influx was relatively low, and biomass was above 150 Mg/ha before 1900 calBP. Between 1500–650 calBP, biomass dropped and remained under 100 Mg/ha, coincident with large increases in charcoal influx from 1500–900 calBP. Biomass started rising in 600 calBP and increased between 400–200 calBP, rising above 150 Mg/ha, then abruptly dropped, consistent with increasing charcoal influx and multiple fire scars 250 calBP onward. Several rapid increases and decreases in biomass occurred in the 20th century (see section 2.4). The highest predicted biomass values in Fish Lake's record occur in the present and are over 250 Mg/ha, which is accompanied by

sharply declining charcoal influx. During the baseline time period of ~2800–100 calBP, median tree biomass was 128 Mg/ha (SE 24.2) (Fig. S1A, Table S2).

Unlike Fish Lake, biomass at Lake Ogaromtoc was estimated to have been under 150 Mg/ha prior to Euro-American contact, except during a two-hundred-year interval around 2300 calBP and around 1100 calBP. Biomass fluctuated but generally remained around 100 Mg/ha from 2200–1200 calBP, during which time charcoal influx gradually increased. Charcoal influx increased throughout the MCA and LIA until the modern period when it sharply declined. Fire scars from 250–50 calBP track increasing charcoal influx from 250–100 calBP and generally low biomass values. The abrupt cessation of fire events in the last century coincided with rising biomass exceeding 300 Mg/ha by 2008, despite an abrupt drop and recovery between the 1950s and 1970s (see section 2.4). Median tree biomass was 104 Mg/ha (SE 33.5) between ~3300–150 calBP (Fig. S1B, Table S2).

2.3   Correlations suggest anthropogenic burning during the Little Ice Age
We applied a framework for detecting climatically anomalous fire and vegetation dynamics using the Palmer Drought Severity Index (PDSI), charcoal accumulation (CHAR), and a vegetation response index (VRI) (Klimaszewski-Patterson et al. 2021, Crawford et al. 2015). The premise is if climate and lightning-caused fires primarily drove vegetation response, then more open-canopy/shade-intolerant taxa during warmer/drier climatic periods and more closed-canopy/shade-tolerant taxa during cooler/wetter climatic periods are expected. If Indigenous burning played a major role in driving vegetation response, then the persistence of open-canopy/shade-intolerant taxa during cooler/wetter periods is expected. The pollen and charcoal records from Fish Lake and Lake Ogaromtoc are largely consistent with climatically controlled patterns of forest and fire dynamics, except during the LIA (Fig. 4). At Fish Lake during the LIA, PDSI suggests cooler and wetter conditions were accompanied by statistically significant increases in charcoal influx and forest opening. At Lake Ogaromtoc during the LIA, increasing charcoal influx was positively correlated (not significantly) with forest opening and significantly negatively correlated with cooling climate. For both sites, the modern period shows forest closure and sharply decreasing charcoal, consistent with widespread fire exclusion.

2.4   Cross-references show consistency in biomass records
We used independent archival evidence to check the consistency of our biomass record from ~150 calBP onward (Fig. 5). Predicted biomass values at both sites were generally low initially and then rose rapidly towards the present day (Fig. 5A,B). Density calculations derived from 1880 witness tree data in the area (Knight et al. 2020) indicate low aboveground live biomass (mean 100 Mg/ha SE 7.1) consistent with low predicted biomass at both lakes ~70 calBP. We detected reductions in pollen influx that temporally correspond to documented harvests of mature, pollen-producing trees (Fig. 5C). This further confirms the link between forest biomass and pollen influx at the lake sites (Fig. S2). Timber harvest data from the federal Forest Activity Tracking System (FACTS) database (US Forest Service Forest Activity Tracking System 2020) indicate patch clear cuts occurred at Fish Lake in 1968, 1977, and 1985 (Fig. S2A). A corresponding drop in predicted biomass was found at the modeled age 1982 (± 3 years). The FACTS database also shows patch and stand clear cuts occurred at Lake Ogaromtoc in 1961, 1972 and 1984 (Fig. S2B), the largest of which was 105-acre clear cut in 1972, and predicted biomass indicated a drop by 1974 (± 2.8 years). USDA Forest Service field notes from a 1993 re-

survey around the lake sites provide additional confirmation of clear-cuts recorded in FACTS, as well as a dense modern landscape (Wheeler and Doman 1995). For example, "old clear-cut areas" are noted adjacent to Fish Lake (e.g., sections 3,4,9,10) and the general description reads: "vegetation varies from dense brush, manzanita, chinkapin, and clear-cuts" (Wheeler and Doman 1995). Lastly, high modern biomass values in Klamath montane forests were confirmed by detailed field surveys showing modern forest biomass > 200 Mg/ha (Knight et al. 2021).

3. Discussion

These results bring the effects of human-modified disturbance regimes on forest biomass into sharp focus. By using a broad evidence base – including engagement with tribal knowledge, ethnographic history, and paleoecological records – this work provides a more robust understanding of Indigenous land management in the western Klamath Mountains than can be obtained from any single line of evidence (Lake 2013). The biomass record strongly suggests frequent fire limited biomass relative to the potential productivity of the sites. The anomalous vegetation-fire-climate correlations during the LIA, coupled with Karuk-Yurok ethnographic data about these watersheds, are suggestive that Indigenous stewardship contributed substantially to the fire regime. Because there was similar Indigenous presence, vegetation, and climatic conditions throughout the low-elevation areas of the Klamath Mountains (Lake 2007), these results are applicable beyond the two lake sites.

The most powerful way to assess the reliability of a proxy record – such as our biomass reconstruction – is to compare the reconstruction to independent archival records (Birks and Birks 2006). We are confident in the biomass reconstructions because they are consistent with multiple, independent lines of evidence. For example, low biomass values derived from 1880 public land survey witness tree data (Knight et al. 2020) align with predicted biomass from the same time period. Additionally, documented silviculture treatments since the 1960s translated into dips in the biomass record, as expected, and the regrowth after clear cut events were also captured by concomitant increases in biomass estimates. Qualitative descriptions from tribal members also link subsistence and open forest conditions to the low biomass environment predicted by the biomass reconstruction before Euro-American colonization. The lower pre-contact median biomass at Lake Ogaromtoc (104 Mg/ha SE 33.5) compared to Fish Lake (128 Mg/ha SE 24.2) could be due to the higher proportion of ultramafic (serpentine) substrate, as serpentine areas tend to have lower productivity (Briles et al. 2011). However, the large standard error from our biomass proxy method and slightly more mesic conditions at Fish Lake due to coastal summer fog (Skinner et al. 2018), which also might support higher biomass, cautions against overinterpretation. Two peaks in pre-contact biomass were noted at Lake Ogaromtoc around 2300 and 1100 calBP and are corroborated by temporally-consistent peaks in *Sequoia sempervirens* pollen and heightened fog reconstructed from a nearby high-resolution paleoclimate record (Barron et al. 2018). Increased fog ~2300 and 1100 calBP occurred due to changes in coastal currents and upwelling that may have lowered natural fire or limited the spread of fires, allowing biomass to increase.

In addition to the consistency between the biomass records and other evidence, the paleo fire record matched expectations from Karuk/Yurok-based knowledge about cultural burning. Both Fish Lake and Lake Ogaromtoc had lower long-term biomass pre-Euro-American colonization, which was likely maintained by the numerous fire events detected in the charcoal influx and fire

scar record. The Karuk and Yurok burned strategically and seasonally around the lakes to provide trail access and to promote desired resource qualities among their traditional gathering and hunting places (Lake 2013). Cultural use of fire and Indigenous fire technology also developed, evolved, and diversified over time (King et al. 2016). For example, the Tuluwat Pattern – a period from 1500 calBP onwards that characterizes the material culture of north coast tribes – marks a transition to more intense land usage and possibly increased tribal burning to support expanding populations driven by migration into northwestern California (Crawford et al. 2015, King et al. 2016). High charcoal accumulation around 1500 calBP and commensurate low biomass at Fish Lake are consistent with shifts in cultural subsistence patterns.

The relative contribution of past ignition from lightning versus cultural burns, however, is difficult to separate. One reason is the biology of fire-scar formation in regions with bimodal or year-round fire seasons is not completely understood (Harley et al. 2018). However, the intra-annual position of a fire scar within the annual growth ring can be linked to the seasonal timing of past fires. In this work, 81-91% of fire scars were detected in latewood or at the ring boundary, implying fall through early spring burns (prior to tree initiating growth), with a short median fire return interval (< 15 years). Lightning ignitions are more likely to be recorded in earlywood because, in the Klamath area, the highest number of lightning strikes occur between June and July (van Wagtendonk and Cayan 2008), a period during which trees are actively growing. A fire history from Happy Camp, Klamath National Forest shows similar fire scar timing (Taylor and Skinner 1998). Indigenous broadcast burns, and likely some patch burns, occurred in late summer/early autumn when latewood is added. The fire scar record suggests fire occurred later in the year than was typical for lightning ignitions. Additionally, lightning was less likely to strike and ignite fuels in riparian areas, wetlands, prairies, and mid- to low-elevation sites, like our lake sites. Taken together, these findings implicate cultural burning in those zones (Bonnicksen et al. 1999, Busam 2006). It is worth noting that our data almost certainly underestimate paleo fire, whether lightning-induced or anthropogenic, because fire scars and charcoal are inherently conservative recorders of past fire activity (Whitlock et al. 2004).

As expected, the lack of recent fire scars and limited charcoal influx from our record coincide with 20th century fire suppression. Federal and state-mandated fire suppression began after the Forest Reserve system was established in 1905. US Forest Service and Civilian Conservation Corps suppression efforts became effective in accessible areas of the Klamath Mountains in the 1920s and in remote areas after 1945 (Skinner et al. 2018). Greatly reduced fire perimeters in California Department of Forestry and Fire Protection's historical records demonstrate the effectiveness of this policy in Six Rivers National Forest (Knight et al. 2020, CAL FIRE 2020). While tribal burning declined during the mid-1800's gold rush period in other portions of the Klamath Mountains (Fry and Stephens 2006), the evidence of fire (i.e., two or more contemporaneously fire scarred trees) at Lake Ogaromtoc and Fish Lake continued until 1903 and 1911, respectively. The fact that fire continued despite Indigenous depopulation could be due to colonists using fire to clear vegetation (Lake 2013) or local resistance to federal fire suppression (Show and Kotok 1924). Nonetheless, this study is broadly consistent with Klamath area fire history studies indicating two distinct fire regime periods: one before fire suppression and one after (Taylor and Skinner 1998, Agee 1991).

If climate and climatically induced factors (such as fire disturbance) were the only drivers of forest change, we would expect changes in vegetation structure and fire to be consistent with changes in local climate reconstructions. For example, a shift to drier climatic conditions (+ PDSI) would bring about increases in fire (+ CHAR) and forest opening (+ VRI). As in other multidisciplinary paleo-ecological research (Klimaszewski-Patterson et al. 2021, Crawford et al. 2015), we found pollen assemblage dynamics were not always well-predicted by climate. We documented anomalous increases in charcoal coupled with increased shade-intolerant taxa at both Fish Lake and Lake Ogaromtoc during the climatically cooler and wetter LIA, during which fire should decrease if climate was the main driver. The cool-moist conditions of the LIA coincided with population growth and cultural expansion evidenced through increased trading between the coast and the interior (King et al. 2016). By 700 calBP, subsistence activity increased at mid-elevation, the foothills, and valley riverside sites, suggesting larger populations and/or territoriality pressures (West 1985). After the LIA, more fires, a more open landscape, and decreasing biomass would be expected. Instead, fire suppression and rising forest biomass driven by increasing abundance of fire-intolerant *Pseudotsuga* and *Notholithocarpus* at the expense of shade-intolerant taxa such as *Quercus* was pronounced, corroborating other records during the last century (Knight et al. 2021, Engber et al. 2011).

Climate is undoubtedly a key factor in past and present fire regimes, but humans are also important drivers of ecosystem change and respond to climate, producing complex vegetation dynamics (Stephens et al. 2019). Our biomass and fire history findings align with a growing body of literature corroborating ethnographic accounts of the influence of Indigenous land management on landscape-scale vegetation in California (Lake 2007, Klimaszewski-Patterson et al. 2021, Lake 2013) and North America more broadly (Delcourt et al. 2004). Debate about the extent of Indigenous landscape modification, however, still exists. In California and other North American landscapes, some have argued the impact of Indigenous burning at a regional scale was negligible, and the effects of climatically driven fires exceeded anthropogenic fires (Vale 2002) in the Sierra Nevada (Vachula et al. 2019) and northeastern US (Oswald et al. 2020).

Discrepancies between results of paleo studies stem, in part, from differences in spatial scale. In contrast to regional perspectives (Vachula et al. 2019, Oswald et al. 2020), this study relied on two small lakes which inherently reflect local vegetation and fire history (Whitlock et al. 2004). Additionally, the signal of Indigenous impact in the paleo record can range from slight to ecologically profound (Kimmerer and Lake 2001). Successful detection of an Indigenous signal can be obscured by several factors. For instance, these lakes were selected in part because the surrounding landscape has supported Indigenous inhabitants, and these localities remain culturally important to local tribes. Depending on the location of sedimentary deposits relative to Indigenous presence, Indigenous management may not be captured in the sedimentary record but could still have influenced forest composition (Thomas-Van Gundy and Nowacki 2013). Consulting local tribes who could gauge the potential detectability of their practices in the paleorecord is critical (Armstrong et al. 2020).

4. Conclusion

This research underscores the need to develop a more accurate and quantitative representation of past forest biomass that takes Indigenous influence on fire regimes and vegetation dynamics into account. To restore more resilient forests, managers often rely on historic conditions as a

baseline; these conditions are assumed to reflect a natural range of variation in the absence of human modification (Safford and Stevens 2017). By assuming historical forests were not highly managed, the long-term role of Indigenous people in ecosystem functioning before Euro-American colonization is discounted. A major drawback of this assumption is it understates the scale of intervention needed to achieve historical fidelity. Our work, in contrast, suggests Indigenous forest and fire management was critical to maintaining forest conditions before colonization. The study also illustrates the unprecedented level of contemporary forest biomass and puts the last century of fire suppression into its long-term context. Predictable carbon dynamics of forests are needed to achieve California's greenhouse gas emissions goals; yet carbon storage and emissions fluctuate in response to disturbance (e.g., fire, logging, and drought) making policy goals harder to achieve (Battles et al. 2014). Indigenous knowledge and cultural practices are rarely translated into land management plans despite their value (Armstrong et al. 2020). This work demonstrates the power of integrating paleo and ethnographic records to inform land management geared toward historical fidelity.

5. Materials and methods

5.1 Site Description
This study presents data from two small lakes with small watersheds and minimal stream inputs from the western Klamath Mountains (Fig. 1). We re-analyzed records from previously collected (2008-2009) sediment cores at Fish Lake and Lake Ogaromtoc (Crawford et al. 2015).

5.2 New chronology and laboratory analyses
Details about sediment coring, ^{14}C dating, and ^{210}Pb dating are previously published (Crawford et al. 2020). Using raw ^{210}Pb activity data and uncalibrated ^{14}C data (Crawford 2012), we constructed new age models for Fish Lake and Lake Ogaromtoc using Bayesian-based software Plum (Aquino-López et al. 2018) in R (R Core Team 2020). The 'rplum' package (Aquino-López et al. 2018) integrates age control data from ^{210}Pb and ^{14}C (Fig. S3). Deposition times (yr/cm) were quantified where pollen was sampled and converted to accumulation rates (cm/yr) for PAR calculations. Pollen samples were extracted from 0.625 cm^3 of wet sediment at approximately 10 cm increments down each core and completed previously (Crawford 2012). Additional samples were extracted from the Lake Ogaromtoc core to refine existing pollen data, but the Fish Lake core was not suitable for resampling. All samples were processed using the same standard methods (Fægri and Iversen 1989). *Lycopodium* spore tracer tablets were added to determine pollen concentrations (Stockmarr 1971).

5.3 Karuk/Yurok-based Indigenous Knowledge
We report ethnographic information from interviews conducted with Karuk tribal members (Lake 2007, Department of Natural Resources, Karuk Tribe 1999), as well as historical documents (Pearsall et al. 1928) and recent surveys of tribal members (Sowerwine et al. 2019). The supplement contains all relevant materials. Full quotes from section 2.1 presented here.

"Fire is crucial to who people are, and what they do. It enables them to live. It is a central component of that duty of care for the whole world, which is inherited form their common ancestry as Spirit People" (Tripp et al. 2017).

Fish Lake and Lake Ogaromtoc (Frog Pond), as described by Karuk tribal member, Charlie Thom in 1996 (Department of Natural Resources, Karuk Tribe 1999):

> "And there was an abundance of stuff. My family gathered at [nearby places]…and our gathering place for acorns at Frog pond [Lake Ogaromtoc]. Beautiful, beautiful acorn gathering place and mushroom gathering place."

Fish Lake was historically used as a gathering place by the Yurok (Pearsall et al. 1928):

> "Our first sleep…would be spent by the borders of a small lake to the north of Weitchpec, among the pine and fir timber. After we had followed a trail a mile or more up the river, we began to ascend the mountain…The lake, but few acres in extent, and almost covered with pond-lily pads, contained an abundance of trout, upon which we feasted."

The Karuk and Yurok have described modern forest conditions (Sowerwine et al. 2019):

> "…and degradation of the environment are reported as the strongest barriers to accessing native foods…"

5.4 Paleoecological records
a.   Predicted aboveground live tree biomass (AGL)
PAR values were calculated using:

$$PAR_i = C_i \times S \qquad \text{Eq. 1}$$

Where PAR_i is the pollen accumulation rate for taxon i, C_i is the pollen concentration (grains cm^{-3}) for taxon i, and S is the sedimentation rate (cm yr^{-1}) which was determined above in 2.2 (Davis and Deevey 1964). Knight et al. (2021) demonstrated that PAR values of major tree taxa derived from lake sediments are linearly related to distance-weighted aboveground live biomass (AGL_{dw}). Biomass trends were plotted using 'palyoplot' in R (Klimaszewski-Patterson et al. 2020). Error in the biomass estimate based on PAR measurements was propagated using a resampling method (Crowley 1992). We estimated error in predicted AGL as a random sample from a normal distribution with the mean equal to zero and the standard deviation equal to the standard error of the regression estimate (SEE) for each taxon. For each iteration, we included a taxa specific live biomass estimate based on its PAR value and summed results for each core sample (i.e., lake and time specific) to estimate AGL. Uncertainty was calculated from 10,000 iterations and reported as means and standard errors of the predicted AGL for each sample.

b.   Fire scars
Cross sections of stumps/downed logs with visible fire scars were collected around the lakes in 2008. Each cross section was sanded allowing tree rings and fire scars to be distinguished under a microscope then cross-dated against tree ring chronologies from nearby locations (Graumlich 2005, Carroll and Jules 2011) using standard dendrochronological methods (Stokes and Smiley 1968). The COFECHA program was used to identify most likely ring dates for samples difficult to cross-date (Grissino-Mayer 2001). Fire scar dates were plotted using FHAES (Brewer et al. 2016). To reduce the chance of including scars caused by very small (i.e., single tree) fires or wounding other than by fire, a composite of fire years was generated using only scars recorded by a minimum of two trees per site. The median fire return interval for each site was calculated

for the period from 1700 and 1900 AD – the time frame during which sample depth was maximized.

5.5 Correlations among climate, vegetation, and fire proxies
a. Independent climate analysis
Independent, annually resolved climate reconstructions for the Klamath bioregion over the last 2,000 years come from the North American Drought Atlas (NADA) tree-ring datasets (Cook et al. 2008). Tree-ring reconstructions were used to calculate annual paleo drought conditions based on the Palmer Drought Severity Index (PDSI). Annually reconstructed PDSI values from grid cell 035 of NADA were used as an independent measure of climate change at both lakes.

b. Vegetation response index
Changes in the percentage of pollen taxa over time are used to interpret changes in surrounding vegetation (Mensing 2001). When taxa respond inversely to climatic variability, a single variable vegetation response index (VRI) can be calculated from the ratio of different taxa to clearly illustrate change (Mensing 2001, Klimaszewski-Patterson and Mensing 2016). A shade tolerance scale of Northern Hemisphere trees and site-specific knowledge was used to determine which taxa to compare (Niinemets and Valladares 2006, Table S1). The VRI was calculated from pollen counts: ((*Pseudotsuga + Notholithocarpus*) – (*Quercus + Pinus*))/(*Pseudotsuga + Notholithocarpus + Quercus + Pinus*). Positive VRI indicated a greater proportion of shade tolerant to shade intolerant pollen and was inferred to show a more closed canopy, while a negative VRI indicated a greater proportion of shade intolerant to shade tolerant pollen and was inferred to show a more open canopy. Results from a non-metric multidimensional ordination (NMS) of tree abundance (as measured by AGL) at different sample dates supported the interpretation of the VRI (McCune et al. 2002, Fig. S4).

c. Charcoal influx data
Macroscopic charcoal preparation steps are detailed in Crawford et al. (2015) and followed standard procedures (Long et al. 1998). Charcoal influx data provides a qualitative reconstruction of fire activity (Anderson et al. 2021, *in review*). Char-Analysis charcoal "peak" methodology and results are described in the supplement (Fig. S5A,B; Higuera et al. 2009).

We interpolated PDSI, VRI, and charcoal influx every 20 years using a smooth spline to calculate correlations and explore relationships between all three proxies (Fig. 4). Pearson's correlations were calculated at the 95% confidence interval. Statistical correlations were based on pollen zones identified by CONISS (a stratigraphically constrained cluster analysis), using the 'rioja' package in R (Grimm 1987, Juggins 2015) where 6 breaks were identified. These breaks independently conformed to known climatic periods of the LIA and MCA.

5.6 Cross-references
In QGIS version 3.14 (2020), lake boundaries (California Department of Fish and Game 2012) and harvest records (US Forest Service Activity Tracking System 2020) were obtained and plotted. Federal public land surveys from 1882 and 1993 were obtained from the Bureau of Land Management (Knight et al. 2020). Detailed transect surveys between 0m and 750m from the lakes' shores were undertaken in 2018 (Knight et al. 2021).

67

Acknowledgments

Fig. 1 Map shows study sites in northwestern California and a shaded-relief map of the surrounding watershed. Lakes and streams are shown in blue, while white lines indicate forest roads. Fire scar samples (red circles) were taken near Fish Lake and Lake Ogaromtoc in 2008. Cores were taken from **(A)** Fish Lake in 2008 and **(B)** Lake Ogaromtoc in 2009.

A Fish Lake
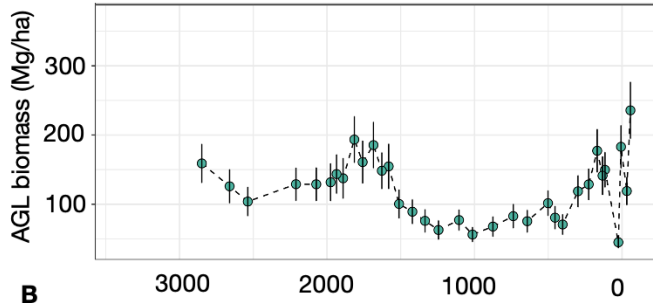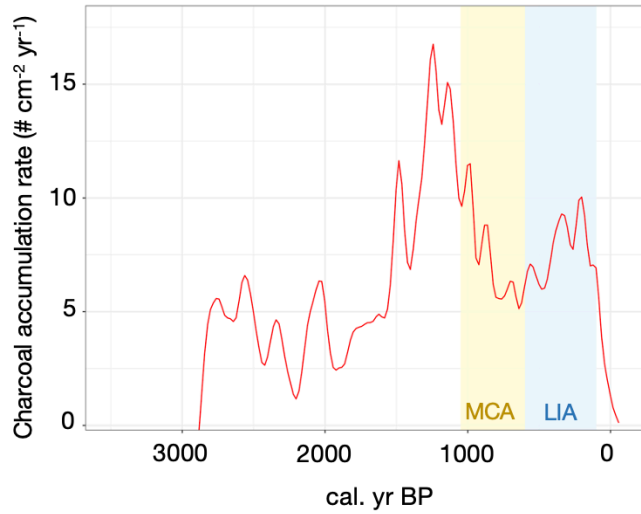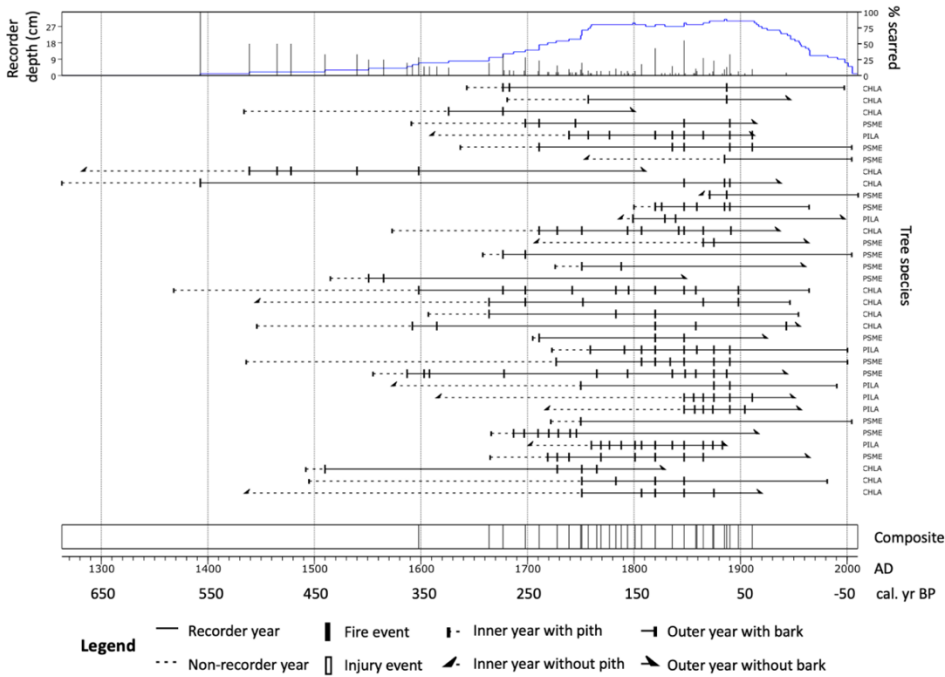
Fig. 2 (A) Reconstructed (or estimated) total aboveground live (AGL) biomass (Mg/ha, summation of major taxa, dots with standard error bars) at Fish Lake between 2850 and -58 cal. year BP. **(B)** Variation in charcoal influx (particles cm^{-2} y^{-1}) where the Medieval Climate Anomaly (MCA) is shaded yellow, and the Little Ice Age (LIA) is shaded blue. **(C)** Fire scar records for CHLA (*Chamaecyparis lawsoniana*), PILA (*Pinus lambertiana*), and PSME (*Pseudotsuga menziesii*) with legend at left; summary statistics are in Table 1. The composite record (bottom panel) is based on fire events and filtered by number of trees recording fires ≥ 2 with a minimum sample number ≥ 2.
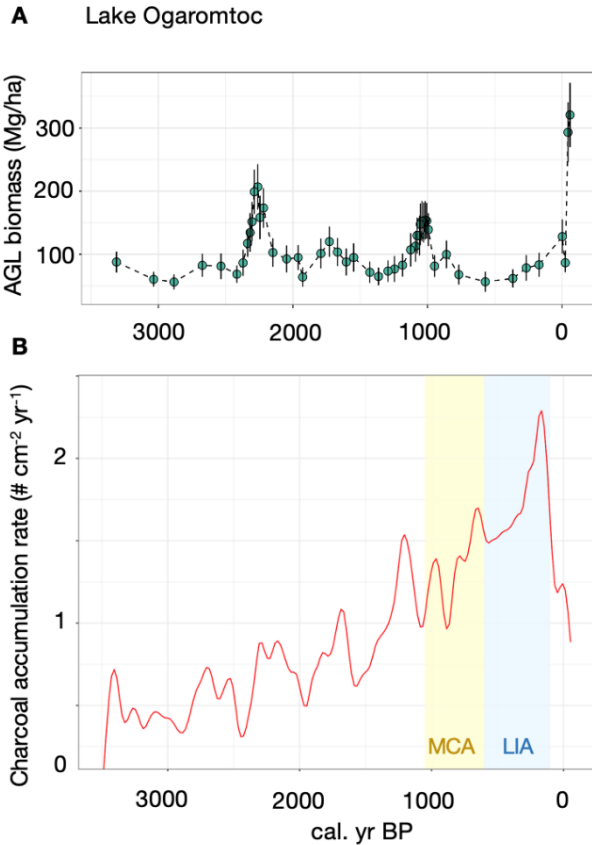
Fig. 3 (A) Total aboveground live (AGL) biomass (Mg/ha, summation of major taxa, dots with standard error bars) at Lake Ogaromtoc between 3312 and -59 cal. year BP. **(B)** Variation in charcoal influx (particles cm^{-2} y^{-1}) where the Medieval Climate Anomaly (MCA) is shaded yellow and the Little Ice Age (LIA) is shaded blue. Fire scar records for PILA (*Pinus lambertiana*), PIPO (*Pinus ponderosa*), and PSME (*Pseudotsuga menziesii*) with legend at bottom; summary statistics are in Table 1. The composite record (bottom panel) is based on fire events and filtered by number of trees recording fires ≥ 2 with a minimum sample number ≥ 2.

71
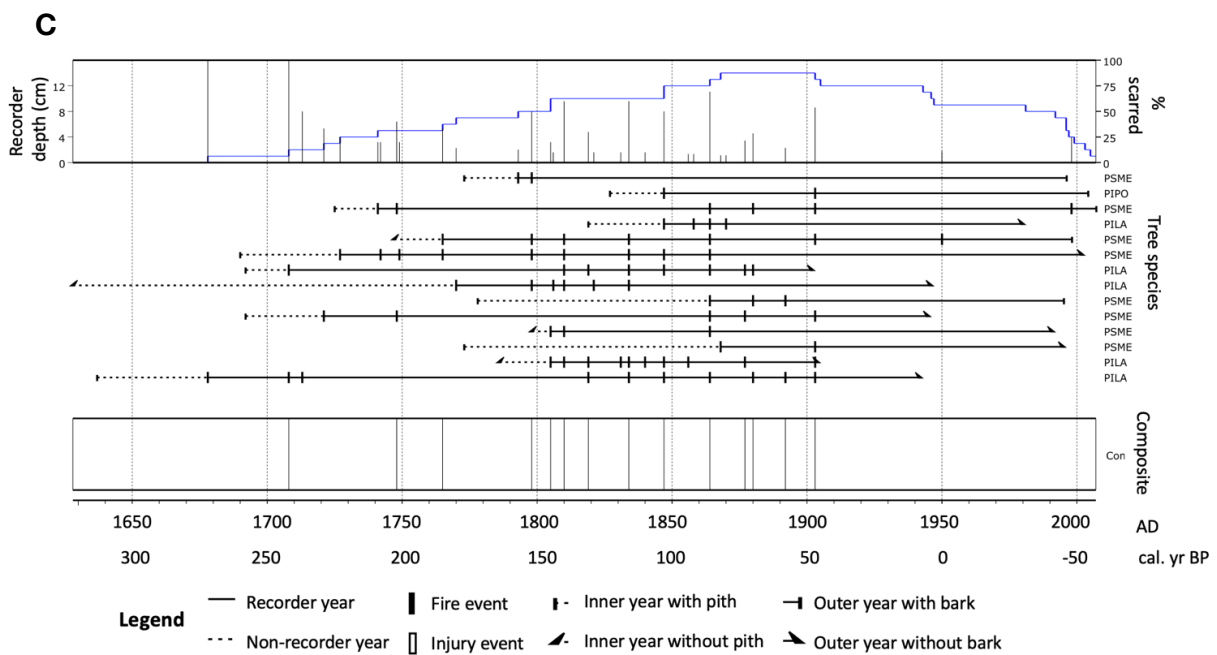
A. Fish Lake

Pollen zones	Zone 1	Zone 2	Zone 3	Zone 4	Zone 5	Zone 6
cal yr BP	2850-2190	2190-1560	1560-1110	1110-540	540-100	100 to -58
VRI v PDSI	--	--	-0.09	0.34	-0.32	0.40
VRI v Charcoal	-0.60**	0.30	0.33	0.28	0.40*	0.90
PDSI v Charcoal	--	--	-0.29	0.2	-0.27	0.30

*p-value <0.05, **p-value <0.01   Note: PDSI data does not extend through Zones 1-2
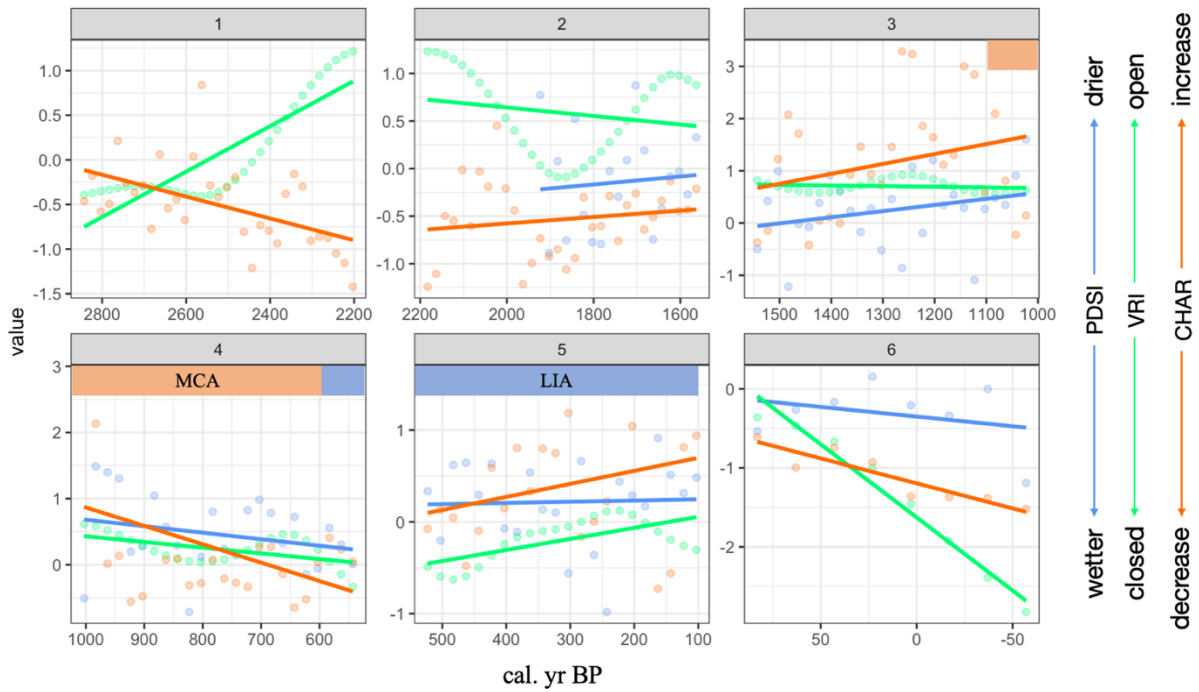
B. Lake Ogaromtoc

Pollen zones	Zone 1	Zone 2	Zone 3	Zone 4	Zone 5	Zone 6
cal yr BP	3340-1800	1800-1100	1100-600	600-200	200-25	25 to -59
VRI v PDSI	--	0.13	-0.04	-0.51*	-0.41	0.65
VRI v Charcoal	-0.44	0.43**	0.20	0.35	-0.43	0.65
PDSI v Charcoal	--	0.16	0.03	-0.16	0.87**	0.39

*p-value <0.05, **p-value <0.01   Note: PDSI data does not extend through Zone 1
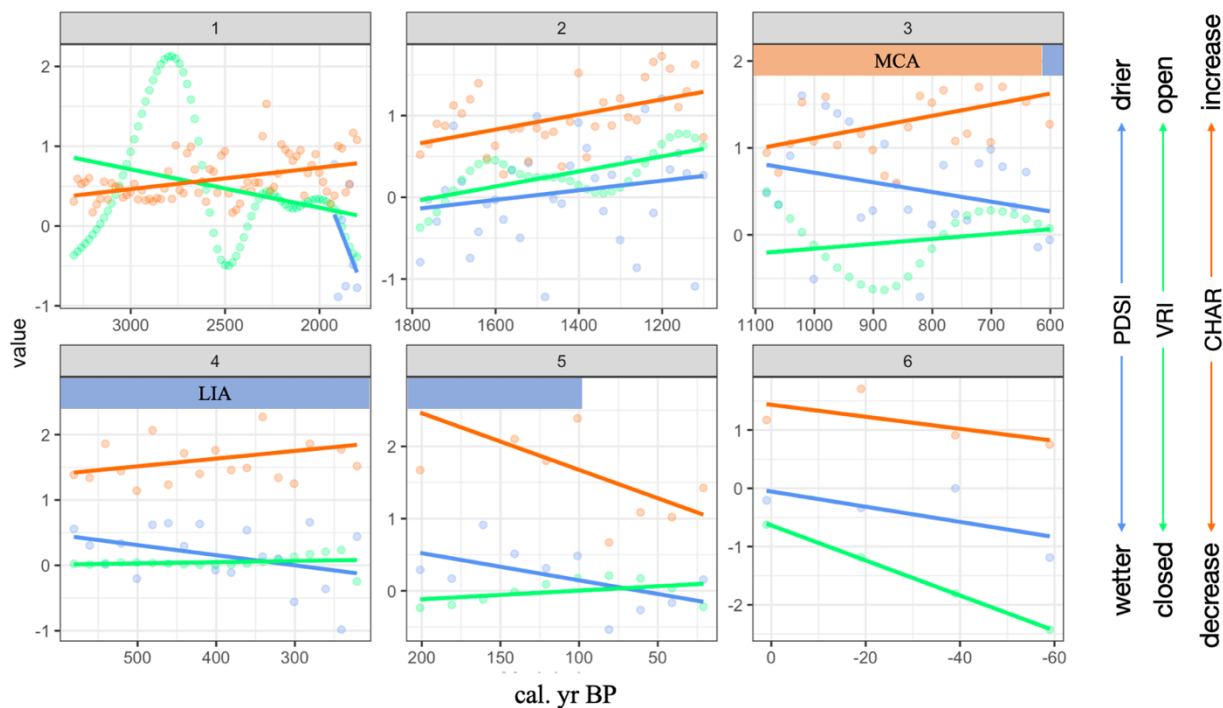
Fig. 4 Pearson's product moment correlation values between standardized sedimentary proxies and independent climate reconstructions were interpolated at 20-year intervals using a smooth spline at **(A)** Fish Lake and **(B)** Lake Ogaromtoc. In each table, red indicates negative correlation values; asterisks indicate significant p-values at different thresholds. In each graph, standardized, interpolated values for the Vegetation Response Index (VRI, green), Charcoal accumulation (CHAR, red), and Palmer Drought Severity Index (PDSI, blue) were plotted. Note that PDSI and VRI values were multiplied by negative one so that dry PDSI, open VRI, and increased CHAR matched direction on the axis (i.e., upwards). Pollen zones are shown at the top of each panel with their corresponding number. The orange bar under the pollen zones denotes the time span of the Medieval Climate Anomaly (MCA). The blue bar denotes the Little Ice Age (LIA).

A Fish Lake

Modeled age AD (BP)
a) 1894 (56)
b) 1943 (7)
c) 1982 (-32)
d) 2008 (-58)

B Lake Ogaromtoc

Modeled age AD (BP)
v) 1779 (171)
w) 1952 (-2)
x) 1974 (-24)
y) 1994 (-44)
z) 2009 (-59)

AGL biomass (Mg/ha)

cal yr BP

C

Cross-references				
Data source	**Information Provided**	**Time period**	**Age model**	
			Fish	**Ogaromtoc**
Federal public land survey (PLS) of townships covering the lakes	Witness tree data	1880s	a	v-w
Federal Forest Activity Tracking System (FACTS)	Timber extractions	1960s-1980s	b-c	w-x
Re-surveyed PLS townships	Ground-truthing of past clear-cuts	1993	c-d	y
Transect data from field surveys	Modern biomass values	2018	--	--

Fig. 5 Enlargement of **(A)** the period 300 to -58 cal. yr BP with modeled ages (small letters) and corresponding predicted biomass at Fish Lake and **(B)** 300 to -59 cal. yr BP with modeled ages (small letters) and corresponding predicted biomass at Lake Ogaromtoc. Data points (green circles) with small letters were cross-referenced against independent datasets **(C)**.

74

Tables

Table 1. Summary table of fire scar history at Fish Lake and Lake Ogaromtoc. Median fire return intervals are presented at two time periods and with different scar thresholds. Intra-ring scar positions are also summarized.

Site	Samples	Earliest scar (AD)	Last scar (AD)	Median fire return interval (all years, ≥ 2 scars/site)	Median fire return interval (1700-1900 AD, ≥ 2 scars/site)		
Fish Lake	35	1393	1943	8	7		
Lake Ogaromtoc	14	1678	1998	15	12		
Intra-ring scar position							
	Fire scars	Scars with position	% early wood	% middle earlywood	% late earlywood	% late wood	% dormant
Fish Lake	172	107	0.9	2.8	5.6	52.3	38.3
Lake Ogaromtoc	77	53	3.8	7.5	7.5	49.1	32.1

CONCLUSION

In its totality, the contribution of this dissertation is an extensive, quantitative investigation into the forest conditions in northern California, with emphasis on understanding the drivers of changes in aboveground live biomass over a long time horizon. To accomplish this, I leveraged 3000 years of fossil pollen data, historic survey data from the 1880s, fire scar and charcoal records, and spatial interpolations from contemporary forest inventories to create a biomass record of unprecedented depth for the fire-suppressed forests in Six Rivers. In line with my major aim, this work extends the baseline of quantitative information in Six Rivers and the Klamath bioregion. Forests of northwestern California are dissimilar enough from Sierra Nevada and southern Cascade forests – whose historical ecology has been studied (e.g., Collins et al. 2011, Taylor et al. 2014, Hagmann et al. 2018) – to warrant further investigation into their historic structure and composition. Specifically, baseline information from decadal- to millennial-scale records of disturbances and ecosystem responses is needed to properly evaluate the impact of altered disturbance regimes (McLauchlan et al. 2014), and this logic underpins all three dissertation chapters.

In chapter 1, I used quantitative archival data about tree populations immediately prior to active fire suppression to understand forest conditions in Six Rivers in the late 19th century. Federal public land survey data was systematically collected between 1872-1884 at 36mi^2 resolution across much of California. These surveys record witness tree data that, through robust plotless density estimation (Cogbill et al. 2018, Levine et al. 2017), provide a record of tree density at regional scales from the late nineteenth century. The 1850-1900 era is important because it represents a snapshot of forest conditions before active fire suppression policies began in the early 1900s. My work with witness tree data provides a regional portrait of ecological conditions, and I found that modern forests have more Douglas-fir and are substantially denser than forests from the 1880s. The magnitude of change shown by this calculation was considerable: the contemporary forest in Six Rivers contains three times more trees than in the historic forest and a comparable increase in basal area. Densification has occurred elsewhere in California, but not to such a degree. For example, a comparison of 1911 inventory data to the contemporary forest revealed a near doubling of live basal area in the central Sierra Nevada (Collins et al. 2017). Although Six Rivers has greatly densified over the past century, its historical baseline likely supported a more open, smaller-tree landscape, compared to the open, large-tree landscape of the Sierra Nevada forests. Thus, these results are important for management because they suggest different targets may be needed in northwestern California.

The witness tree records I presented in the previous chapter are only one of several data types available for reconstructing past forest conditions. In chapter 2, I tackled the first step in quantitative reconstruction of past vegetation via fossil pollen. The application of fossil pollen data to quantitative reconstruction has been a long-standing goal in paleo-ecology (Davis and Deevey 1964). A key first step in the methodology is determining the nature of the relationship between biomass surrounding lake sites and the pollen preserved in lake sediments. My goal in chapter 2 was to test whether modern pollen accumulation rates (PAR, pollen influx) could be used as a bioproxy for modern plant abundance (biomass) at seven lake sites in Six Rivers. Previously, PAR has been used to reconstruct past population growth rates (e.g., Giesecke 2005) and Holocene biomass in at least two areas (Seppä et al. 2009, Morris et al. 2015). Although data

collection and methodological challenges (e.g., the need for precise sediment age modeling) are barriers to widespread quantitative reconstruction, I was able to obtain critical data. I then used a linear pollen vegetation model and found that contemporary pollen influx is a reasonably precise predictor of contemporary distance-weighted aboveground live biomass at my sites. These results suggest that calibrated PAR-biomass models can be used to infer quantitative changes in past plant biomass, given a long-term record of PAR values.

Using the empirical foundation from chapter 2 that quantified the relationship between pollen influx and plant biomass, in chapter 3 I leveraged a previously collected 3000-year record of pollen influx data from two lake sites in Six Rivers (Crawford et al. 2015). My aim was to understand long-term forest carbon dynamics and fire history. A disturbance regime is fundamentally linked to biomass storage (Bormann and Likens 1971), but theoretical understanding is limited by a lack of empirical data. In particular, the research community lacks a long-term record of tree biomass to match the documented temporal variation in the fire regime for the Klamath (Taylor and Skinner 2003, Crawford et al. 2015). In this chapter, I provide a first assessment of tree biomass in mixed conifer forests over the late Holocene and show the connection between biomass fluctuation, fire history, and management activities.

Unlike other multidisciplinary paleo-ecological approaches (e.g., Vachula et al. 2019, Oswald et al. 2020), I started with the hypothesis that Native land management, particularly burning, strongly influenced forest structure and composition over millennia. This stance is justified because Traditional Ecological Knowledge from California tribes and anthropological scholarship has shown that Indigenous people in northwestern California (and elsewhere) were altering the landscape with fire (Anderson and Moratto 1996, Kimmerer and Lake 2001) and supporting considerable populations (Chartkoff and Chartkoff 1975). With collaborators from the Karuk and Yurok Tribes, I combined Native oral history and paleo-ecological data to explain anthropogenic influence on forest carbon (Lake 2007, Tripp et al. 2017). I also developed cross-references to check for consistency in my reconstruction and found corroboration among independent datasets (*sensu* Raiho et al. 2016). For example, I calculated pre-suppression estimates of tree biomass using the pollen accumulation rate from lake cores and then used witness tree information from the surveys to assess my results. The same cross-referencing tactic was used to understand fire reconstructions where there were overlapping records (i.e., charcoal data and tree fire scars, *sensu* Whitlock et al. 2004).

The results from chapter 3 suggest that pre-contact Indigenous peoples played a significant role in shaping the forest ecosystems of California. I found that the combination of Native burning practices and the lightning-based fire regime supported the long-term stability of forest carbon dynamics and an average biomass value of 100 Mg/ha for most of the past three millennia. Beginning around 1850 AD, significant socio-ecological land use change in the area – namely Native depopulation and fire suppression – led to forest densification, allowing biomass to climb to a contemporary peak of > 250 Mg/ha. My biomass record helps resolve uncertainty about the effect of fire suppression on forest carbon, which may be useful in the modern policy context. For example, these results suggest large scale interventions would be needed to manage California's forests for resiliency and effective forest carbon storage. Such insight may aid land managers who seek to move California forests closer to their long-term historical conditions.

My chapter 3 results also highlight the ahistorical features of the contemporary forest, which may contribute to debates about the best way to manage forests to store carbon and mitigate climate change – a highly contested topic in California (Bellassen and Luyssaert 2014). Currently, California's forest sector substantially contributes to efforts to reduce greenhouse gas emissions (Christensen et al. 2017); yet the interaction between a warming climate and increasing wildfire frequency and severity threaten California's forests carbon carrying capacity (Liang et al. 2017, Dass et al. 2018). The California Forest Carbon Plan, in recognition of this threat, outlines strategies to sustain the State's forests as reliable carbon sinks (Forest Climate Action Team 2018). Understanding long-term forest carbon dynamics under different stewardship scenarios and climatic conditions will be critical to the development of 'sustainable' land management policy.

The concept of 'sustainability' in land management implies a considerable time dimension (Davies and Bunting 2010). With this in mind, California's legislative goals are starting to incorporate historical perspectives in policy and management. For example, Senate Bill 901 from the 2018 legislative session instructs Cal-Fire and the Air Resources Board to develop "a historic baseline of greenhouse gas emissions from California's natural fire regime reflecting conditions before modern fire suppression" (SB-901). More generally, meeting California's goals regarding greenhouse gas emissions depends on predictable carbon dynamics of forests and other working lands (Sapsis et al. 2016). Yet, carbon storage fluctuates in response to disturbance (e.g., fire, logging, and drought) making policy goals harder to achieve (Battles et al. 2014, Battles et al. 2018). Understanding how fire has influenced past and present forest carbon is a key aspect of the California Forest Carbon Plan (Forest Climate Action Team 2018).

Although the potential for California's forests to sequester carbon makes them a critical component of the State's integrated climate change strategy (Natural and Working Lands Climate Change Implementation Plan 2019), a century of active fire suppression has transformed California's vast mixed conifer forests and potentially diminished their capacity for long-term carbon storage (Safford and Stevens 2017). The prospect of increasingly severe and frequent fires provides a strong motivation to obtain and evaluate long-term datasets about forest carbon and fire in California because that information could improve the evidence base for management decisions. Over three chapters, I have sought to broaden this evidence base using paleoecological techniques and trans-disciplinary approaches. A multidisciplinary tact allowed me to answer quantitative questions about forest structure and composition in northwestern California and provide a nuanced view of the area's ecology. I believe such research is useful in the development of land management actions. Taken collectively, these chapters provide a more comprehensive understanding of the area's historical ecology and point to management interventions needed to be consistent with historic forest conditions.

REFERENCES

Agee, J. K. 1991. Fire history along an elevational gradient in the Siskiyou Mountains, Oregon. Northwest Science 65:188–199.

Agee, J. K. 1993. Fire Ecology of Pacific Northwest Forests. Island Press, Washington, DC, p. 493.

Alagona, P. S., J. Sandlos, and Y. Wiersma. 2012. Past imperfect: using historical ecology and baseline data for contemporary conservation and restoration projects. Environmental Philosophy 9:49-70.

Allison, P. A., and D. J. Bottjer DJ. 2011. Taphonomy: Bias and process through time. In: Allison, P. A., and Bottjer, D.J. (eds) Taphonomy. Springer, pp. 1–17.

Andersen, S. T. 1970. The relative pollen productivity and pollen representation of north European trees, and correction factors for tree pollen spectra. Danmarks geologiske Undersogelse. 96:1–99.

Andersen, M. 1991. Mechanistic models for the seed shadows of wind-dispersed seeds. The American Naturalist 137:476–497.

Anderson, M. K., and M. J. Moratto. 1996. Native American land-use practices and ecological impacts. Aspen Bibliography. Paper 1815.

Anderson, L., D. B. Wahl, and T. Bhattacharya. 2020. Understanding rates of change: A case study using fossil pollen records from California to assess the potential for and challenges to a regional data synthesis. Quaternary International. *In revision.*

Appleby, P., and F. Oldfield. 1978. The calculation of lead-210 dates assuming a constant rate of supply of unsupported 210Pb to the sediment. Catena 5:1–8.

Aquino-López, M. A., J. Blaauw, A. Christen, and N. K. Sanderson. 2018. Bayesian Analysis of 210-Pb Dating. Journal of Agricultural, Biological, and Environmental Studies 23:317.

Armstrong, C. G., D. Lepofsky, K. Lertzman, A. C. McAlvay, and J. E. D. Miller. 2020. Re-evaluating "Conservation Implications of Native American Impacts" EcoEvoRxiv. February 11. doi:10.32942/osf.io/tgu65.

Assembly Bill Number 32 (AB-32). Air pollution: greenhouse gases: California Global Warming Solutions Act of 2006. https://leginfo.legislature.ca.gov/faces/billNavClient.xhtml?bill_id=200520060AB32

Baker, W. L. 2012. Implications of spatially extensive historical data from surveys for restoring dry forests of Oregon's eastern Cascades. Ecosphere 3:1–39.

Baker, W. L. 2014. Historical forest structure and fire in Sierran mixed-conifer forests reconstructed from General Land Office survey data. Ecosphere 5:79.

Baker, W. L. 2015b. Historical Northern spotted owl habitat and old-growth dry forests maintained by mixed-severity wildfires. Landscape Ecology 30:655–666.

Baker, W. L., and C. T. Hanson. 2017. Improving the use of early timber inventories in reconstructing historical dry forests and fire in the western United States. Ecosphere 8:e01935.

Baker, W. L., and M. A. Williams. 2018. Land-surveys show regional variability of historical fire regimes and structure of dry forests of the western USA. Ecological Applications 28:284–290.

Baldwin, W. C. 1990. A Fish Lake Odyssey. Humboldt Historian 38(6):14-20.

Barak, R. S., A. L. Hipp, J. Cavender-Bares, W. D. Pearse, S. C. Hotchkiss, E. A. Lynch, J. C. Callaway, R. Calcote, and D. J. Larkin. 2016. Taking the long view: integrating recorded,

archeological, paleoecological, and evolutionary data into ecological restoration. International Journal of Plant Science 177:90–102.

Barron, J. A., D. Bukry, L. E. Heusser, J. A. Addison, C. R. Alexander. 2018. High-resolution climate of past ~7300 years of coastal northernmost California: Results from diatoms, silicoflagellates, and pollen. Quaternary International 469:109–119.

Barnosky, A. D., E. A. Hadley, P. Gonzalez et al. 2017. Merging paleobiology with conservation biology to guide the future of terrestrial ecosystems. Science 355.

Baskaran, M., C. J. Miller, A. Kumar, E. Andersen, J. Hui, J. P. Selegean, C. T. Creech, and J. Barkach. 2015. Sediment accumulation rates and sediment dynamics using five different methods in a well-constrained impoundment: Case study from Union Lake, Michigan. Journal of Great Lakes Research 41:607–617.

Battles, J. J., P. Gonzalez, T. Robards, B. M. Collins, and D. S. Saah. 2014. Final Report: California Forest and Rangeland Greenhouse Gas Inventory Development. California Air Resources Board Agreement 10–778.

Battles, J. J., D. Bell, R. Kennedy, D. Saah, B. Collins, R. York, and J. Sanders. 2018. Innovations in Measuring and Managing Forest Carbon Stocks in California. California's Fourth Climate Change Assessment, California Natural Resources Agency. Publication number: CCCA4-CNRA2018-014.

Bellassen, V., and S. Luyssaert. 2014. Carbon sequestration: Managing forests in uncertain times. Nature 506:153–155.

Beller, E. E., L. McClenachan, E. S. Zavaleta, and L. G. Larsen. 2020. Past forward: Recommendations from historical ecology for ecosystem management. Global Ecology and Conservation 21: e00836.

Bennett, K. D. 1983. Postglacial population expansion of forest trees in Norfolk, UK. Nature 303: 164–67.

Bennett, K. D. 1986. The rate of spread and population increase of forest trees during the postglacial. Philosophical Transactions of the Royal Society of London, Series B 314:523–531.

Birks, H. H., and H. J. B. Birks. 2006. Multi-proxy studies in palaeoliminology. Vegetation History Archaeobotany 15:235-251.

Bjorkman, A. D., and M. Vellend. 2010. Defining historical baselines for conservation: ecological changes since European settlement on Vancouver Island, Canada. Conservation Biology 24:1559–1568.

Blaauw, M., and J. A. Christen. 2011. Flexible paleoclimate age-depth models using an autoregressive gamma process. Bayesian Analysis 6:457–474.

Blaauw, M., J. A. Christen, M. A. Aquino-Lopez, J. Esquivel-Vazquez, O. M. Gonzalez, T. Belding, J. Theiler, B. Gough, and C. Karney. 2020. Package 'rplum': Bayesian age-depth modeling of ^{210}Pb-dated cores. Version 0.1.4. CRAN Repository.

Blackburn, T. C., and M. K. Anderson. 1993. Introduction. In Before the wilderness: Native Californians as environmental managers, eds. T.C. Blackburn and K. Anderson, 15–25. Menlo Park, CA: Ballena Press.

Blarquez, O., C. Carcaillet, T. M. Elzein, and P. Roiron. 2011. Needle accumulation rate model-based reconstruction of palaeo-tree biomass in the western subalpine Alps. The Holocene 22:579–587.

Bonnicksen, T. M., M. K. Anderson, H. T. Lewis, C. E. Kay, and R. Knudson. 1999. Native American Influences on the Development of Forested Ecosystems in Ecological

Stewardship: A Common Reference for Ecosystem Management. Vol. II. W. Sexton, A Malk, R. Szaro, and N. Johnson (eds). Elsevier Science Press, Netherlands. Pages: 439-469.

Bormann, F. H., and G. E. Likens. 1971. The ecosystem concept and the rational management of natural resources. Yale Science Magazine 45:2–8.

Bouldin, J. 2008. Some problems and solutions in density estimation from bearing tree data: a review and synthesis. Journal of Biogeography 35:2000–2011.

Bouldin, J. 2010. Issues in estimates of relative metrics of historic forest conditions from bearing tree data. Ecological Applications 20:1183-1187.

Bourdo, E. A. 1956. A review of the General Land Office survey and of its use in quantitative studies of former forests. Ecology 37:754–768.

Bowerman, N. D., and D. H. Clark. 2011. Holocene glaciation of the central Sierra Nevada, California. Quaternary Science Reviews 30 (9–10):1067–1085.

Brewer, P.W., Velásquez, M.E., Sutherland, E.K. and Falk, D.A. 2016. Fire History Analysis and Exploration System (FHAES) version 2.0.2, [computer software], https://www.fhaes.org(link is external). DOI:10.5281/zenodo.34142

Briles, C. E., C. Whitlock, P. J. Bartlein, and P. Higuera. 2008. Regional and local controls on postglacial vegetation and fire in the Siskiyou Mountains, northern California, USA. Palaeogeography, Palaeoclimatology, Palaeoecology 265:159–169.

Briles, C. E., C. Whitlock, C. N. Skinner, and J. Mohr. 2011. Holocene forest development and maintenance on different substrates in the Klamath Mountains northern California, USA. Ecology 92:590–601.

Bright, W. 1978. Karok. In: Heizer RF (ed.) Handbook of North American Indians. Washington, DC: Smithsonian, pp. 180–189.

Broström, A., M.-J. Gaillard, M. Ihse, and B. vad Odgaard. 1998. Pollen–landscape relationships in modern analogues of ancient cultural landscapes in southern Sweden — a first step towards quantification of vegetation openness in the past. Vegetation History and Archaeobotany 7:189–201.

Broström, A., S. Sugita, and M.-J. Gaillard. 2004. Pollen productivity estimates for the reconstruction of past vegetation cover in the cultural landscape of southern Sweden. The Holocene 14:368–381.

Broström, A., S. Sugita, M.-J. Gaillard, and P. Pilesjö. 2005. Estimating the spatial scale of pollen dispersal in the cultural landscape of southern Sweden. The Holocene 15:252–262.

Bunting, M. J., M.-J. Gaillard, S. Sugita, R. Middleton, and A. Broström. 2004. Vegetation structure and pollen source area. The Holocene 14:651–660.

Bunting, M. J., R. Armitage, H. A. Binney, and M. Waller. 2005. Estimates of 'relative pollen productivity' and 'relevant source area of pollen' for major tree taxa in two Norfolk (UK) woodlands. The Holocene 15:459–465.

Bunting, M. J., and R. Middleton. 2005. Modelling pollen dispersal and deposition using HUMPOL software: simulating wind roses and irregular lakes. Review of Palaeobotany and Palynology 134:185–196.

Bunting, M. J., and R. Middleton. 2009. The Multiple Scenario Approach: a pragmatic method for past vegetation mosaic reconstruction. Holocene 19:799–803.

Bunting, M. J., and K. L. Hjelle. 2010. Effect of vegetation data collection strategies on estimates of relevant source area of pollen (RSAP) and relative pollen productivity

estimates (relative PPE) for non-arboreal taxa. Vegetation History and Archaeobotany 19:365–374.

Bunting, M. J., M. Farrell, A. Broström, K. L. Hjelle, F. Mazier, R. Middleton, A. B. Nielsen, E. Rushton, H. Shaw, and C. L. Twiddle. 2013. Palynological perspectives on vegetation survey: a critical step for model-based reconstruction of Quaternary land cover. Quaternary Science Reviews 82:41–55.

Bureau of Land Management (BLM). 2006. Geographic Coordinate Database (GCDB) Publication Point IDs. Accessed September 2019: http://nationalcad.org/download/BLM-PointID-standard-summary.pdf

Burnham, K. P., and D. R. Anderson. 2002. *Model selection and multimodel inference: a practical information-theoretic approach.* 2nd ed. New York, Springer-Verlag.

Busam, H. M. 2006. Characteristics and implications of traditional native American fire management on the Orleans Ranger District, Six Rivers National Forest. Master Thesis, California State University.

California Department of Forestry and Fire Protection. 2015. Vegetation (fveg) - CALFIRE FRAP [ds1327]. https://map.dfg.ca.gov/metadata/ds1327.html

Calcote, R. 1995. Pollen source area and pollen productivity: evidence from forest hollows. Journal of Ecology 83:591–602.

California Department of Fish and Game (2012) California Lakes. Accessed January 2020: https://gis.data.ca.gov/datasets/4d7024209b3d4b7796d4dd4119764d3e_5

California Department of Fish and Wildlife (CDFW). 2020. Wildlife Habitats - California Wildlife Habitat Relationships System. Accessed June 2, 2020:https://wildlife.ca.gov/Data/CWHR/Wildlife-Habitats

Carroll, A. L., and E. S. Jules. 2011. NOAA/WDS Paleoclimatology - Carroll - Page Mountain - CHLA - ITRDB OR081.crn. NOAA National Centers for Environmental Information. https://doi.org/10.25921/pecm-3d66

Chartfkoff, J.L., and K. K. Chartkoff. 1975. Late period settlement of the middle Klamath River of northwest California. American Antiquity 40(2):172–179.

Cheng, S. T. E. 2004. Forest Service Research Natural Areas in California. General Technical Report PSW-GTR-188. Pacific Southwest Research Station, Forest Service, U.S. Department of Agriculture, Albany, CA.

Christen, J. A., and C. Fox. 2010. A general purpose sampling algorithm for continuous distributions (the t-walk). Bayesian Analysis 5:263–281.

Christensen, G. A., A. N. Gray, O. Kuegler, N. A. Tase, and M. Rosenberg. 2017. AB 1504 California Forest Ecosystem and Harvested Wood Product Carbon Inventory: 2006 - 2015. Final Report. California Department of Forestry and Fire Protection agreement no. 7CA02025. Sacramento, CA: California Department of Forestry and Fire Protection and California Board of Forestry and Fire Protection.

Churchill, D. J., A. J. Larson, M. C. Dahlgreen, J. F. Franklin, P. F. Hessburg, and J. A. Lutz. 2013. Restoring forest resilience: from reference spatial patterns to silvicultural prescriptions and monitoring. Forest Ecology and Management 291:442–457.

Cocking, M. I., J. M. Varner, and R. L. Sherriff. 2012. California black oak responses to fire severity and native conifer encroachment in the Klamath Mountains. Forest Ecology and Management 270:25–34.

Cocking, M. I., J. M. Varner, and E. E. Knapp. 2014. Long-term effects of fire severity on oak–conifer dynamics in the southern Cascades. Ecological Applications 24:94–107.

Codding BF, Bird DW (2013) Forward: A global perspective on traditional burning in California. California Archaeology 5 (2):199–208.

Cogbill, C. V., A. L. Thurman, J. W. Williams, J. Zhu, D. J. Mladenoff, and S. J. Goring. 2018. A retrospective on the accuracy and precision of plotless forest density estimators in ecological studies. Ecosphere 9:e02187.

Collins, B. M., R. G. Everett, and S. L. Stephens. 2011. Impacts of fire exclusion and recent managed fire on forest structure in old growth Sierra Nevada mixed-conifer forests. Ecosphere 2:1–14.

Collins, B. M., J. M. Lydersen, R. G. Everett, D. L. Fry, and S. L. Stephens. 2015. Novel characterization of landscape-level variability in historical vegetation structure. Ecological Applications 25:1167–1174.

Collins, B. M., D. L. Fry, J. M. Lydersen, R. Everett, and S. L. Stephens. 2017. Impacts of different land management histories on forest change. Ecological Applications 27:2475–2486.

Colombaroli, D., and D. G. Gavin. 2010. Highly episodic fire and erosion regime over the past 2,000 years in the Siskiyou Mountains, Oregon. Proceedings of the National Academy of Sciences 107:18909–18914.

Commerford, J. L., K. K. McLauchlan, and S. Sugita. 2013. Calibrating vegetation cover and grassland pollen assemblages in the Flint Hills of Kansas, USA. American Journal of Plant Sciences 4:1–10.

Conners, P. A. 1998. A history of the Six Rivers National Forest: Commemorating the first 50 years. USDA Forest Service. Accessed November 2019: https://foresthistory.org/wp-content/uploads/2017/01/HISTORY-OF-THE-SIX-RIVERS-NATIONAL-FOREST.pdf

Cook, E. R., C. A. Woodhouse, C. M. Eakin, D. M. Meko, D. W. Stahle. 2008. North American Summer PDSI Reconstructions, Version 2a. IGBP PAGES/World Data Center for Paleoclimatology. Data Contribution Series #2008-046. NOAA/NGDC Paleoclimatology Program, Boulder, CO.

Cook, E. R., C. A. Woodhouse, C. M. Eakin et al. 2004. Long- term aridity changes in the western United States. Science 306(5698): 1015–1018.

Cooper, W. S. 1922. *The broad-sclerophyll vegetation of California: an ecological study of the chaparral and its related communities* (No. 319). Carnegie Institution of Washington.

Cottam, G., and J. T. Curtis. 1956. The use of distance measures in phytosociological sampling. Ecology 37:451–460.

Crawford, J. N. 2012. Evidence for native American land-use impacts on forest structure and fire regimes in the lower Klamath River region of California. PhD Dissertation, University of Nevada-Reno.

Crawford, J. N., S. A. Mensing, F. K. Lake, and S. R. H. Zimmerman. 2015. Late Holocene fire and vegetation reconstruction from the western Klamath Mountains, California, USA: A multidisciplinary approach for examining potential human land-use impacts. The Holocene 25:1341–1357.

Crowley, P. H. 1992. Resampling methods for computation-intensive data analysis in ecology and evolution. Annual Review of Ecological Systems 23:405–447.

Daniels, M. L., R. S. Anderson, and C. Whitlock. 2005. Vegetation and fire history since the Late Pleistocene from the Trinity Mountains, northwestern California, USA. The Holocene 15:1062–1071.

Dass, P., B. Z. Houlton, Y. Wang, and D. Warlind. 2018. Grasslands may be more reliable

carbon sinks than forests in California. Environmental Research Letters 13:074027.

Davies, A. L., and M. J. Bunting. 2010. Applications of palaeoecology in conservation. The Open Ecology Journal 3:54–67.

Davis, M. B. 1963. On the theory of pollen analysis. American Journal of Science 261:897–912.

Davis, M. B., and E. S. Deevey. 1964. Pollen accumulation rates: estimates from Late-Glacial sediment Rogers Lake. Science 145:1293–1295.

Davis, M. B. 1967b. Pollen deposition in lakes as measured by sediment traps. Geological Society of America Bulletin 78: 849–58.

Davis, M. B., R. E. Moeller, and J. Ford. 1984: Sediment focusing and pollen influx. In Haworth, E. Y. and J. W. G. Lund (eds), Lake sediments and environmental history. University of Minnesota Press, 261–93.

Davis, M. B. 2000. Palynology after Y2K: Understanding the source area of pollen in sediments. Annual Review of Earth Planetary Sciences 28:1–18.

Dawson, A., C. J. Paciorek, J. S. McLachlan, S. Goring, J. W. Williams, and S. T. Jackson. 2016. Quantifying pollen–vegetation relationships to reconstruct ancient forests using 19th century forest composition and pollen data. Quaternary Science Reviews 137:156–175.

Dawson, A., C. J. Paciorek, S. J. Goring, S. T. Jackson, J. S. McLachlan, and J. W. Williams. 2019. Quantifying trends and uncertainty in prehistoric forest composition in the upper Midwestern United States. Ecology 100:1–18.

Delcourt, P. A., P. Haccou, P. A. Delcourt, and H. R. Delcourt. 2004. Prehistoric Native Americans and Ecological Change: Human Ecosystems in Eastern North America Since the Pleistocene, Cambridge University Press.

Department of Natural Resources, Karuk Tribe. 1999. Karuk Forest Management Perspectives: Interviews with Tribal Members. Vol. 1: Report and Interview Transcripts.

Department of Natural Resources, Karuk Tribe. 1999. Karuk Forest Management Perspectives: Interviews with Tribal Members, Vol. 2: Appendices.

Detling, L. E. 1961. The chaparral formation of southwestern Oregon, with considerations of its postglacial history. Ecology 42:348–357.

Doher, L. I. 1980. Palynomorph preparation procedures currently used in the paleontology and stratigraphy laboratories, U.S. Geological Survey Circular 830:1–28.

Dolph, K. L., S. R. Mori, and W. W. Oliver. 1995. Long-term response of old-growth stands to varying levels of partial cutting in the eastside pine type. Western Journal of Applied Forestry 10:101–108.

Duren, O. C., P. S. Muir, and P. E. Hosten. 2012. Vegetation Change from the Euro-American Settlement Era to the present in relation to environment and disturbance in southwest Oregon. Northwest Science 86:310–28.

Egan, D., and E. A. Howell. 2005. The historical ecology handbook: a restorationist's guide to reference ecosystems. 2nd ed. Island Press, Washington, DC, USA.

Eisenhut, G. 1961. Untersuchungen über die Morphologie und Ökologie der Pol- lenkörner heimischer und fremdländischer Waldbäume. Paul Parey, Hamburg.

Ejarque, A., R. S. Anderson, A. R. Simms, B. J. Gentry. 2015. Prehistoric fires and the shaping of colonial transported landscapes in southern California: A paleoenvironmental study at Dune Pond, Santa Barbara County. Quaternary Science Reviews 112:181–196.

Eldridge, I. 1910. Salmon River in Sawyers Bar area. Photograph. Meriam Library Special Collections Department, California State University, Chico. Calisphere. Accessed 7 February 2020: https://calisphere.org/item/08c3f17e13a39eb554e2224c9ba2b41c/

Engber, E. A., J. M. Varner, L. A. Arguello, and N. G. Sugihara. 2011. The effects of conifer encroachment and overstory structure on fuels and fire in the oak woodland landscape. Fire Ecology 7:32–50.

Engeman, R. M., R. T. Sugihara, L. F. Pank, and W. E. Dusenberry. 1994. A comparison of plotless density estimators using Monte Carlo simulation. Ecology 75:1769–1779.

ESRI. 2011. ArcGIS Desktop: Release 10. Redlands, CA: Environmental Systems Research Institute.

Fægri, K., and J. Iversen. 1989. Textbook of Pollen Analysis. New York: Haffner Press.

Fagerlind, F. 1952. The real significance of pollen diagrams. Botaniska Notiser 105:185–224.

Falck, R. 1927. Über die Größen, Fallgeschwindigkeit und Schwebewarte dcr Pilzsporen und ihre Gruppierung mit Bezug auf die zu ihre Verbreitung nötigen temperatuströmungs-Geschindigkeit. Berichte der Deutschen Botanischen Geseselschaft 45:262–281.

Feldman, R., D. F. Tomback, and J. Koehler. 1999. Cost of mutualism: competition, tree morphology, and pollen production in limber pine clusters. Ecology 80:324–329.

Fire Resources Assessment Program. 2018. Priority Landscapes. Accessed January 2018: https://www.arcgis.com/apps/MapSeries/index.html?appid=f767d3f842fd47f4b35d8557f10387a7

Fites-Kaufman, J. 1997. Historic landscape pattern and process: fire, vegetation, and environment interactions in the northern Sierra Nevada. Ph.D. Dissertation. University of Washington, Seattle, WA.

Foreman, S. W. 1882a. Field notes for the subdivision lines of township 10 north range 4 east Humboldt Meridian, California. Digital archive from the Cadastral Survey Office, Bureau of Land Management Survey Records, Sacramento, California. Volume 323:233-299.

Foreman, S. W. 1882b. Field notes for the subdivision lines of township 13 north range 5 east Humboldt Meridian, California. Digital archive from the Cadastral Survey Office, Bureau of Land Management Survey Records, Sacramento, California. Volume 20:827–888.

Forest Climate Action Team. 2018. California Forest Carbon Plan: Managing Our Forest Landscapes in a Changing Climate. Sacramento, CA. 178p.

Forest Inventory and Analysis Database (FIADB). 2020. Forest Inventory and Analysis Database version 1.8.0.0.1. https://apps.fs.usda.gov/fia/datamart/datamart.html

Forest Inventory and Analysis (FIA). 2010. Regional biomass equations used by FIA to estimate bole, bark, and branches (updated 13-Jan-2010), USDA Forest Service, Pacific Northwest Research Station.

Friedman, S. K., and P. B. Reich. 2005. Regional legacies of logging: Departure from pre-settlement forest conditions in northern Minnesota. Ecological Applications 15:726–744.

Fry, D. L., and S. L. Stephens. 2006. Influence of humans and climate on the fire history of a ponderosa pine-mixed conifer forest in the southeastern Klamath Mountains, California.

Gaillard, M.-J., S. Sugita, M. J. Bunting et al. 2008. The use of modelling and simulation approach in reconstructing past landscapes from fossil pollen data: a review and results from the POLLANDCAL network. *Vegetation History and Archaeobotany* 17:419–443.

Gaillard, M.-J., S. Sugita, A. Broström, M. Eklöf, and P. Pilesjö. 2000. Long term land-cover changes on regional to global scales inferred from fossil pollen — how to meet the challenges of climate research? Pages Newsletter 8: 30–32.

Gaillard, M.-J., S. Sugita, F. Mazier, A. L. et al. 2010. Holocene land-cover reconstructions for studies on land cover-climate feedbacks. Climate of the Past 6:483–499.

Galatowitsch, S. M. 1990. Using the original land survey notes to reconstruct pre-settlement landscapes in the American West. Great Basin Naturalist 50:181–191.

Giesecke, T. 2005. Moving front or population expansion: how did *Picea abies* (L.) Karst. become frequent in central Sweden? Quaternary Science Reviews 24:2495–509.

Giesecke, T., and S. L. Fontana. 2008. Revisiting pollen accumulation rates from Swedish lake sediments. Holocene 18:293–305.

Gonzalez, P., J. J. Battles, B. M. Collins, T. Robards, and D. S. Shah. 2015. Aboveground live carbon stock changes of California wildland ecosystems, 2001-2010. Forest Ecology and Management 348:68–77.

Goring, S. J., D. J. Mladenoff, C. V. Cogbill, S. Record, C. J. Paciorek, S. T. Jackson, M. C. Dietze, A. Dawson, J. H. Matthes, J. S. McLachlan, and J. W. Williams. 2016. Novel and lost forests in the Upper Midwestern United States, from new estimates of settlement-era composition, stem density, and biomass. PLoS ONE 11: e0151935.

Graham, N. E., M. K. Hughes, C. M. Ammann et al. 2007. Tropical Pacific: Mid-latitude teleconnections in medieval times. Climate Change 83: 241–285.

Graumlich, L. J. 2005 NOAA/WDS Paleoclimatology - Graumlich - Grizzly Peak - PIPO - ITRDB CA524.crn. NOAA National Centers for Environmental Information. https://doi.org/10.25921/fbhr-3030. Accessed 2012.

Gregory, P. H. 1973. The Microbiology of the Atmosphere. London: L. Hill.

Grimm, E. C. 1984. Fire and other factors controlling the Big Woods vegetation of Minnesota in the mid-nineteenth century. Ecological Monographs 54:291–311.

Grimm, E. C. 1987. CONISS: A FORTRAN 77 program for stratigraphically constrained cluster analysis by the method of incremental sum of squares. Computational Geoscience 13:13–35.

Grissino-Mayer, H. D. 2001. Evaluating crossdating accuracy: a manual for the program COFECHA. Tree Ring Research 57:115-124.

Hagmann, R. K., J. F. Franklin, and K. N. Johnson. 2013. Historical structure and composition of ponderosa pine and mixed-conifer forests in south-central Oregon. Forest Ecology and Management 304:492–504.

Hagmann, R. K., J. F. Franklin, and K. N. Johnson. 2014. Historical conditions in mixed-conifer forests on the eastern slopes of the northern Oregon Cascade Range, USA. Forest Ecology and Management 330:158–170.

Hagmann, R. K., J. T. Stevens, J. M. Lydersen, B. M. Collins, J. J. Battles, P. F. Hessburg, C. R. Levine, A. G. Merschel, S. L. Stephens, A. H. Taylor, J. F. Franklin, D. L. Johnson, and K. N. Johnson. 2018. Improving the use of early timber inventories in reconstructing historical dry forests and fire in the western United States: Comment. Ecosphere 9:e02232.

Halbritter, H., S. Ulrich, F. Grímsson, M. Weber, R. Zetter, M. Hesse, R. Buchner, M. Svojtka, and A. Frosch-Radivo. 2018. Illustrated Pollen Terminology. Springer International Publishing.

Halpern, A. A. 2016. Prescribed fire and tanoak (*Notholithocarpus densiflorus*) associated cultural plant resources of the Karuk and Yurok Peoples of California. UC Berkeley, PhD dissertation. Retrieved from ProQuest Dissertations and Theses database.

Han, Y., H. Liu, Q. Hao, X. Liu, W. Guo, and H. Shangguan. 2017. More reliable pollen productivity estimates and relative source area of pollen in a forest-steppe ecotone with improved vegetation survey. The Holocene 27:1567–1577.

Hanberry, B. B., S. Fraver, H. S. He, J. Yang, D. C. Dey, and B. J. Palik. 2011. Spatial pattern corrections and sample sizes for forest density estimates of historical tree surveys. Landscape Ecology 26:59–68.

Hanberry, B. B., J. Yang, J. M. Kabrick, and H. S. He. 2012a. Adjusting forest density estimates for surveyor bias in historical tree surveys. The American Midland Naturalist 167:285–306.

Hanberry, B. B., B. J. Palik, and H. S. He. 2012b. Comparison of historical and current forest surveys for detection of homogenization and mesophication of Minnesota forests. Landscape Ecology 27:1495–1512.

Hanberry, B. B., R. F. Brzuszek, H. T. Foster II, and T. J. Schauwecker. 2019. Recalling open old growth forests in the Southeastern Mixed Forest province of the United States. Écoscience. https://doi.org/10.1080/11956860.2018.1499282

Hanberry, B. B., and D. C. Dey. 2019. Historical range of variability for restoration and management in Wisconsin. Biodiversity and Conservation 28:2931-2950.

Harley, G. L., C. H. Baisan, P. M. Brown et al. 2018. Advancing dendrochronological studies of fire in the United States. Fire, 1:1–6.

Heinselman, M. L. 1973. Fire in the virgin forests of the Boundary Waters Canoe Area, Minnesota. Quaternary Research 3:329–382.

Hessburg, P. F., J. K. Agee, and J. F. Franklin. 2005. Dry forests and wildland fires of the inland Northwest USA: contrasting the landscape ecology of the pre-settlement and modern eras. Forest Ecology and Management 211:117–139.

Hellman, S., Gaillard, M.J., Broström, A., and S. Sugita. 2008a. The REVEALS model, a new tool to estimate past regional plant abundance from data in large lakes: validation in southern Sweden. Journal of Quaternary Science 23:21–42.

Hellman, S., Broström, A., Gaillard, M.J., and S. Sugita. 2008b. Effects of the sampling design and selection of parameter values on pollen based quantitative reconstructions of regional vegetation: a case study in southern Sweden using the REVEALS model. Vegetation Historical Archaeobotany 17:445–460.

Hellman, S., Bunting, M. J., and M.-J. Gaillard. 2009. Relevant Source Area of Pollen in patchy cultural landscapes and signals of anthropogenic landscape disturbance in the pollen record: A simulation approach. Review of Palaeobotany and Palynology 153:245–258.

Greenhouse, J., Markos, S., Moe, R., Simono, S., Wetherwax, M., and L. Vorobik. 2012. The Digital Jepson Manual: Vascular Plants of California, Second Edition, Thoroughly Revised and Expanded (Baldwin B., Goldman D., Keil D., Patterson R., Rosatti T., & Wilken D., Eds.). University of California Press. Retrieved July 16, 2021, from http://www.jstor.org/stable/10.1525/j.ctt1pn9sv

Hicks, S. and Hyvarinen, H. 1999: Pollen influx values measured in different sedimentary environments and their palaeoecological implications. *Grana* 38:228–42.

Hicks, S. 2001. The use of annual arboreal pollen deposition values for delimiting tree-lines in the landscape and exploring models of pollen dispersal. Review of Palaeobotany and Palynology 117:1–29.

Hicks, S. 2006. When no pollen does not mean no trees. *Vegetation History and Archeobotany* 15:253–261.

Higgs, E., D. A. Falk., A. Guerrini, M. Hall, J. Harris, R. J. Hobbs, S. T. Jackson, J. M., Rhemtulla, and W. Throop. 2014. The changing role of history in restoration ecology. Frontiers in Ecology and Environment 12:499–506.

Higuera, P. E., Brubaker, L. B., Anderson, P. M. et al. 2009. Vegetation mediated the impacts of postglacial climatic change on fire regimes in the south-central Brooks Range, Alaska. Ecological Monographs 79: 201-219.

Hudiburg, T., Law, B., Turner, D. P., Campbell, J., Donato, D., and M. Duane. 2009. Carbon dynamics of Oregon and Northern California forests and potential land-based carbon storage. Ecological applications 19:163–180.

Hurteau, M. D., M. P. North, G. W. Koch, and B. A. Hungate. 2019. Opinion: Managing for disturbance stabilizes forest carbon. Proceedings of the National Academy of Sciences 21:10193–10195.

Hyde, H. R. 2002. Analysis of historical vegetation distributions in the Sierra Nevada using Government Land Office survey records. M.S. Thesis. University of California, Davis CA.

Hyvärinen, H. 1975. Absolute and relative pollen diagrams from northernmost Fennoscandia. Fennia 142:1–23.

IPBES 2018. The IPBES assessment report on land degradation and restoration. Montanarella, L., Scholes, R., and Brainich, A. (eds.). Secretariat of the Intergovernmental Science-Policy Platform on Biodiversity and Ecosystem Services, Bonn, Germany. 744 pages.

Irwin, W. P. 1981. Tectonic accretion of the Klamath Mountains. In: Ernst WG (ed.) The Geotectonic Development of California. Englewood Cliffs, NJ: Prentice Hall, pp. 29–49.

Jackson, S. T. 1990. Pollen Source Area and Representation in Small Lakes of the Northeastern United States. Review of Palaeobotany and Palynology 63:53–76.

Janssen, C. R. 1973. Local and regional pollen deposition. Quaternary Plant Ecology (eds H. J. B. Birks & R. G. West). pp. 31-42. Blackwell Scientific Publications, Oxford.

Juggins, S. 2015. Package 'rioja': Analysis of Quaternary science data. Version 0.9-26. CRAN Repository.

Jweda, J., and M. Baskaran. 2011. Interconnected riverine-lacustrine systems as sedimentary repositories: Case study in southeast Michigan using 210-Pb and 137-Cs sediment accumulation and mixing models. Journal of Great Lakes Research 37:432–446.

Karuk Forest Management Perspectives: Interviews with Tribal Members, Vol. 2: Appendices 1999. Karuk Interviews, 1996-97, Appendix 3, pp 6. Prepared for USDA Forest Service, Klamath National Forest, Yreka, CA. Prepared by Department of Natural Resources, Karuk Tribe, Orleans Ca. and Cultural Solutions, Ashland, OR.

Kimmerer, R. W., and F. K. Lake. 2001. The role of indigenous burning in land management. Journal of Forestry 99: 36-41.

King, J. H., W. R. Hildebrandt, S. A. Waechter. 2016. Cultural Resources Overview for Northwestern California. DOI-Bureau of Land Management, Arcata and Redding, CA.

Klimaszewski-Patterson, A., and S. A. Mensing. 2016. Multi-disciplinary approach to identifying Native American impacts on Late Holocene forest dynamics in the southern Sierra Nevada range, California, USA. Anthropocene 15:37–48.

Klimaszewski-Patterson, A., P. J. Weisberg, S. A. Mensing, and R. M. Scheller. 2018. Using paleolandscape modeling to investigate the impact of Native American–set fires on pre-Columbian forests in the southern Sierra Nevada, California, USA. Annuals of the American Association of Geography 4452:1–20.

Klimaszewski-Patterson, A. 2020. Package 'palyoplot': Visualization and multi-axis stratigraphic plotting of Quaternary science data. Version 0.0.13. CRAN Repository.

Klimaszewski-Patterson A., C. T. Morgan, and S. Mensing. 2021. Identifying a pre-Columbian Anthropocene in California. Annals of the American Association of Geographers. DOI: 10.1080/24694452.2020.1846488.

Knapp, R. O. 1969. How to know pollen and spores. W.C. Brown Company, University of Minnesota.

Knight, C. A., C. V. Cogbill, M. D. Potts, J. A. Wanket, and J. J. Battles. 2020. Settlement-era forest structure and composition in the Klamath Mountains: Reconstructing a historical baseline. Ecosphere 11:e03250.

Knight, C.A., M. Baskaran, M. J. Bunting, M. Champagne, M. D. Potts, D. Wahl, J. A. Wanket, and J. J. Battles. 2021 Linking modern pollen accumulation rates to biomass: Quantitative vegetation reconstruction in the western Klamath Mountains. The Holocene. https://doi.org/10.1177/0959683620988038.

Kroeber, T. 1959. The Inland Whale. University of California Press.

Kronenfeld, B. J., and Y.-C. Wang. 2007. Accounting for surveyor inconsistency and bias in estimation of tree density from pre-settlement land survey records. Canadian Journal of Forest Research 37:2365–2379.

Kronenfeld, B. J. 2015. Validating the historical record: a relative distance test and correction formula for selection bias in pre-settlement land surveys. Ecography 38:41–53.

Kujawa, E. R., S. Goring, A. Dawson, R. Calcote, E. C. Grimm, S. C. Hotchkiss, S. T. Jackson, E. A. Lynch, J. McLachlan, J-M. St-Jacques, C. Umbanhowar, and J. W. Williams. 2016. The effects of anthropogenic land cover change on pollen-vegetation relationships in the American Midwest. Anthropocene 15:60–71.

Kuparinen, A., T. Markkanen, H. Riikonen, and T. Vesala. 2007. Modeling air-mediated dispersal of spores, pollen and seeds in forested areas. Ecological Modelling 208: 177–188.

Lake, F. K. 2007. Traditional Ecological Knowledge to Develop and Maintain Fire Regimes in Northwestern California, Klamath-Siskiyou Bioregion: Management and Restoration of Culturally Significant Habitats. PhD Dissertation, Oregon State University.

Lake, F. K. 2013. Historical and cultural fires, tribal management and research issues in Northern California: Trails, fires and tribulations. Occasion: Interdisciplinary Studies in the Humanities 5:1–22.

Landres, P.B., Morgan, P., and F. J. Swanson. 1999. Overview of the use of natural variability concepts in managing ecological systems. Ecological Applications 9:1179–1188.

Larson, A. J., and D. Churchill. 2012. Tree spatial patterns in fire-frequent forests of western North America, including mechanisms of pattern formation and implications for designing fuel reduction and restoration treatments. Forest Ecology and Management 267:74–92.

Levin, D. A., and H. W. Kerster. 1974. Gene flow in seed plants. Evolutionary Biology 7:139–220.

Levine, C. R., C. V. Cogbill, B. M. Collins, A. J. Larson, J. A. Lutz, M. P. North, C. M. Restaino, H. D. Safford, S. L. Stephens, and J. J. Battles. 2017. Evaluating a new method for reconstructing forest conditions from General Land Office survey records. Ecological Applications 27:1498–1513.

Lewis, H. T. 1993. Patterns of Indian burning in California: ecology and ethnohistory. P. 55-116 in T.C. Blackburn and K. Anderson (eds). Before the wilderness: environmental management by native Californians. Ballena Press, Menlo Park, CA.

Liang, S., M. D. Hurteau, and A. L. Westerling. 2017. Potential decline in carbon carrying capacity under projected climate-wildfire interactions in the Sierra Nevada. Scientific Reports 7:2420.

Likens, G. E., and M. B. Davis. 1975. Post-glacial History of Mirror Lake and its Watershed in New Hampshire: an Initial Report. In: Mitteilungen Internationale Vereinigung für Theoretische und Angewandte Limnologie 19:982–993.

Lindbladh, M., M. Niklasson, M. Karlsson, L. Bjorkman, and M. Churski. 2008. Close anthropogenic control of *Fagus sylvatica* establishment and expansion in a Swedish protected landscape: implications for forest history and conservation. Journal of Biogeography, 35, 682–697.

Liu, F., D. J. Mladenoff, N. S. Keuler, and L. S. Moore. 2011. Broad scale variability in tree data of the historical Public Land Survey and its consequences for ecological studies. Ecological Monographs 81:259–275.

Long, C. J., C. Whitlock, P. J. Bartlein et al. 1998. A 9000-year fire history from the Oregon Coast Range, based on a high- resolution charcoal study. Canadian Journal of Forest Research 28:774–787.

Long, J. W., F. K. Lake, R. W. Goode, and B. M. Burnette. 2020. How traditional tribal perspectives influence ecosystem restoration. Ecopsychology 12:71-82.

Lutz, J. A., J. W. van Wagtendonk, and J. F. Franklin. 2009. Twentieth-century decline of large-diameter trees in Yosemite National Park, California, USA. Forest Ecology and Management 257:2296–2307.

MacDonald, G. M. 1993: Fossil pollen analysis and the reconstruction of plant invasions. Advances in Ecological Research 24:67–109.

Manies, K. L., D. J. Mladenoff, and E. V. Nordheim. 2001. Assessing large-scale surveyor variability in the historic forest data of the original US Public Land Survey. Canadian Journal of Forest Research 31:1719–1730.

Manley, P. N., J. A. Fites-Kaufman, M. G. Barbour, M. D. Schlesinger, and D. M. Rizzo. 2000. Biological integrity. pp. 401-598 In: D. D. Muphy and C. M. Knopp (eds.) Lake Tahoe watershed assessment: Volume 1. General technical Report PSW-GTR-175. USDA Forest Service, Pacific Southwest Research Station, Albany, CA.

Marquer L., M.-J. Gaillard, S. Sugita et al. 2014. Holocene changes in vegetation composition in northern Europe: why quantitative pollen-based vegetation reconstructions matter. Quaternary Science Reviews 90:199–216.

Matthias, I., and T. Giesecke. 2014. Insights into pollen source area, transport and deposition from modern pollen accumulation rates in lake sediments. Quaternary Science Reviews 87:12–23.

Maxwell, R. S, A. H. Taylor, C. N. Skinner, H. D. Safford, R. E. Isaacs, C. Airey, and A. B. Young. 2014. Landscape-scale modeling of reference period forest conditions and fire behavior on heavily logged lands. Ecosphere 5:1–23.

McCune, B., J. B. Grace, and D. L. Urban. 2002. Analysis of ecological communities (Vol. 28). Gleneden Beach, OR: MjM software design.

McIntyre, P. J., J. H. Thorne, C. R. Dolanc, A. L. Flint, L. E. Flint, M. Kelly, and D. D. Ackerly. 2015. Twentieth-century shifts in forest structure in California: Denser forests, smaller trees, and increased dominance of oaks. Proceedings of the National Academy of Sciences of the United States of America 112:1458–1463.

McLauchlan, K. K., P. E. Higuera, D. G. Gavin et al. 2014. Reconstructing disturbances and

their biogeochemical consequences over multiple timescales. BioScience 64:105–116.

Mensing, S. A. 2001. Late-glacial and early Holocene vegetation and climate change near Owens Lake, eastern California. Quaternary Research 55:57–65.

Meyer, K. E., and W. F. Laudenslayer. 1988. A guide to wildlife habitats of California. Sacramento: California Department of Fish and Game.

Miller, C., and D. L. Urban. 1999. Forest pattern, fire, and climatic change in the Sierra Nevada. Ecosystems, 2:76–87.

Miller, J. D., C. N. Skinner, H. Safford, E. E. Knapp, and C. M. Ramirez. 2012. Trends and causes of severity, size, and number of fires in northwestern California, USA. Ecological Applications 22:184–203.

Mohr, J. A., C. Whitlock, and C. N. Skinner. 2000. Postglacial vegetation and fire history, eastern Klamath Mountains, California. The Holocene 10:587–601.

Morecroft, M. D., C. E. Bealey, D. A. Beaumont et al. 2009. The UK Environmental Change Network: emerging trends in the composition of plant and animal communities and the physical environment. Biological Conservation, 142, 2814–2832.

Morisita, M. 1957. A new method for the estimation of density by spacing method applicable to nonrandomly distributed populations. Physiology and Ecology 7:134–144. English translation by USDA Division of Range Management 1960. http://math.hws.edu/~mitchell/Morisita1957.pdf

Morris, J. L., J. R. DeRose, and A. R. Brunelle. 2015. Long-term landscape changes in a subalpine spruce-fir forest in central Utah, USA. Forest Ecosystems 2:1–12.

Muggeo, V. M., 2008. Segmented: an R package to fit regression models with broken-line relationships. R news, 8:20–25.

Nielsen, A. B., and S. Sugita. 2005. Estimating Relevant Source Area of Pollen for Small Danish Lakes around AD 1800," The Holocene 15:1006–1020.

Niinemets, Ü., and F. Valladares. 2006. Tolerance to shade, drought, and waterlogging of temperate Northern Hemisphere trees and shrubs. Ecological Monographs 76:521–547.

Natural and Working Lands Climate Change Implementation Plan. 2019. California 2030 Natural and Working Lands Climate Change Implementation Plan. https://www.arb.ca.gov/cc/natandworkinglands/draft-nwl-ip-1.7.19.pdf

Odgaard, B. V. 1993. Wind-determined sediment distribution and Holocene sediment yield in a small, Danish kettle lake. *Journal of Paleolimnology* 8:3–13.

Odion, D. C., C. T. Hanson, A. Arsenault et al. 2014. Examining historical and current mixed-severity fire regimes in ponderosa pine and mixed-conifer forests of western North America. PLoS ONE 9:e87852.

Oswald, W. W., D. R. Foster, B. N. Shuman, E. S. Chilton, D. L. Doucette, D. L. Duranleau. 2020. Conservation implications of limited Native American impacts in pre-contact New England. Nature 3:241–246.

Overpeck, J. T., T. Webb, and I. C. Prentice. 1985. Quantitative interpretation of fossil pollen spectra: dissimilarity coefficients and the method of modern analogues. Quaternary Research 23, 87–108.

Paciorek, C. J., and J. S. McLachlan. 2009. Mapping ancient forests: Bayesian inference for spatio-temporal trends in forest composition using the fossil pollen proxy record. Journal of the American Statistical Association 104:608–622.

Parsons, R., and I. C. Prentice. 1981. Statistical approaches to R-values and the pollen vegetation relationship. Review of Palaeobotany and Palynology 32:127–152.

Pearsall, C. E., H. M. Pearsall, and H. L. Neall. 1928. History and genealogy of the Pearsall family in England and America. San Francisco: Printed by H.S. Crocker Co.

Peattie, D. C. 1950. A natural history of western trees. Boston, Massachusetts, Houghton Mifflin.

Picard, N., A. M. Kouyate, and H. Dessard. 2005. Tree density estimations using a distance method in Mali savanna. Forest Science 51:7–18.

Pollard, J. H. 1971. On distance estimators of density in randomly distributed forests. Biometrics 27:991–1002.

Poska, A., V. Meltsov, S. Sugita, and J. Vassiljev. 2011. Relative pollen productivity estimates of major anemophilous taxa and relevant source area of pollen in a cultural landscape of the semi-boreal forest zone (Estonia). Review of Palaeobotany and Palynology 167:30–39.

Pullen, R. 1996. Overview of the Environment of Native Inhabitants of Southwestern Oregon, Late Prehistoric Era. Report prepared for the USDA Forest Service, and DOI Bureau of Land Management. Medford District. Pullen Consulting, Bandon, OR.

Prentice, I. C. 1985. Pollen representation, source area, and basin size: towards a unified theory of pollen analysis. Quaternary Research 23:76–86.

Prentice, I. C., and T. Webb III. 1986. Pollen percentages, tree abundances and the Fagerlind effect. Journal of Quaternary Science 1:35–43.

Prentice, I. C. 1988: Records of vegetation in time and space: the principles of pollen analysis. In Huntley, B. and Webb, T., III, editors, Vegetation history. Kluwer Academic Publishers, 17–42.

Prentice, C., Guiot, J., Huntley, B., Jolly, D. and R. Cheddadi. 1996. Reconstructing biomes from palaeoecological data: a general method and its application to European pollen data at 0 and 6 ka. Climate Dynamics 12:185–194.

QGIS Development Team. 2020. QGIS Geographic Information System. Open-source geospatial foundation. Accessed in January 2020: http://qgis.org

R Core Team. 2018. Version 3.5.1.

R Core Team. 2020. Version 3.9.5. R: A language and environment for statistical computing. R Foundation for Statistical Computing, Vienna, Austria. URL https://www.R-project.org/.

Radeloff, V. C., D. J. Mladenoff, H. S. He, and M. S. Boyce. 1999. Forest landscape change in the northwestern Wisconsin Pine Barrens from pre-European settlement to the present. Canadian Journal of Forest Research 29:1649–1659.

Raiho, A., J. S. McLachlan, and C. J. Paciorek. 2016. Biomass stability during the Holocene in the Upper Midwest. American Geophysical Union Meeting. 2016AGUFM.B24A.08R.

Rhemtulla, J. M. and D. J. Mladenoff. 2007. Why history matters in landscape ecology. Landscape Ecology 22:1-3.

Rhemtulla, J. M., D. J. Mladenoff, and M. K. Clayton. 2009. Legacies of historical land use on regional forest composition and structure in Wisconsin, USA (mid-1800s–1930s–2000s). Ecological Applications 19:1061–1078.

Ritchie, J. C. 1969. Absolute pollen frequencies and carbon-14 age of Holocene lake sediment from the Riding Mountain area of Manitoba. Canadian Journal of Botany 47: 1345–1349.

Ritchie, M. W., B. M. Wing, and T. A. Hamilton. 2008. Stability of the large tree component in treated and untreated late-seral interior ponderosa pine stands. Canadian Journal of Forest Research 38:919–923.

Safford, H. D., and J. T. Stevens. 2017. Natural range of variation for yellow pine and mixed-conifer forests in the Sierra Nevada, southern Cascades, and Modoc and Inyo National

Forests, California, USA. Gen. Tech. Rep. PSW-GTR-256. Albany, CA: US Department of Agriculture, Forest Service, Pacific Southwest Research Station. p. 256.

Sapsis, D., J. Bede, J. Dingman, N. Enstice, T. Moody, K. Scott, J. Sherlock, L. Tarnay, and N. Tase. 2016. Forest fire, drought, restoration treatments, and carbon dynamics: A way forward. California Forestry Note 121, State of California, California Department of Forestry and Fire Protection. 23p.

Sawyer, J. O., and D. A. Thornburgh. 1977. Montane and subalpine vegetation of the Klamath Mountains. pp. 699–732 In M. G. Barbour and J. Major (eds.), Terrestrial Vegetation of California. John Wiley & Sons, New York.

Senate Bill Number 901 (SB-901). 2018. Wildfires, September 2018. Regular Session 2017-2018.

Schenk, S. M., and E. W. Gifford. 1952. Karok ethnobotany. Anthropological Record 13:377–92.

Schober, R., 1975. Ertragstafeln wichtiger Baumarten bei verschiedener Durchfor- stung. Sauerländer, Frankfurt a. M.

Scholl, A. E., and A. H. Taylor. 2010. Fire regimes, forest change, and self-organization in an old growth mixed-conifer forest, Yosemite National Park, USA. Ecological Applications 20:362–380.

Schulte, L. A., and D. J. Mladenoff. 2001. The original US public land survey records: their use and limitations in reconstructing pre-settlement vegetation. Journal of Forestry 99:5–10.

Schulte, L. A., D. J. Mladenoff, T. R. Crow, L. C. Merrick, and D. T. Cleland. 2007. Homogenization of northern US Great Lakes forests due to land use. Landscape Ecology 22:1089–1103.

Seppä, H. and S. Hicks. 2006. Integration of modern and past pollen accumulation rate (PAR) records across the arctic tree-line: a method for more precise vegetation reconstructions. Quaternary Science Review 25:1501–1516.

Seppä, H., T. Alenius, P. Muukkonen, T. Giesecke, P. A. Miller, and A. E. K. Ojala. 2009. Calibrated pollen accumulation rates as a basis for quantitative tree biomass reconstructions. Holocene 19:209–220.

Serra-Diaz, J. M., C. Maxwell, M. S. Lucash et al. 2018. Disequilibrium of fire-prone forests sets the stage for a rapid decline in conifer dominance during the 21st century. Scientific Reports 8:6749.

Show, S.B.; Kotok, E.I. 1924. The role of fire in the California pine forests. Bulletin No. 1294. Washington, D.C.: U.S. Department of Agriculture. 80 pp.

Sevillano, V., K. Holt, and J. L. Aznarte. 2020. Precise automatic classification of 46 different pollen types with convolutional neural networks. PLoS ONE 15:e0229751.

Shrader, G. 1965. Trinity Forest. pp 37–40 In: Yearbook of the Trinity County Historical Society. Weaverville, California, USA.

Sjögren P., W. O. van der Knaap, A. Huuskoc, and J. F. N. van Leeuwen. 2008. Pollen productivity, dispersal, and correction factors for major tree taxa in the Swiss Alps based on pollen-trap results. Review of Palaeobotany and Palynology 152:200–210.

Skinner, C. N. 2003a. Fire regimes of the upper montane and subalpine glacial basins in the Klamath Mountains of northern California. Tall timbers Research Station Miscellaneous Publication 13:145–151.

Skinner, C. N. 2003b. A tree-ring based fire history of riparian reserves in the Klamath Mountains. pp 116–119 In: P.M. Farber (ed.) California Riparian Systems: Processes and

Floodplains Management, Ecology, and Restoration. Riparian Habitat and Floodplains Conference Proceedings. Riparian Habitat Joint Venture.

Skinner, C. N., A. H. Taylor, and J. K. Agee. 2006. Klamath Mountains Bioregion. In: N.G. Sugihara, J.W. van Wagtendonk, J. Fites-Kaufmann, K.E. Shaffer, and A.E. Thode (eds.) 2006. Fire in California's ecosystems. University of California Press, Berkeley. pp. 170–194.

Skinner, C. N., A. H. Taylor, J. K. Agee, C. E. Briles, and C. Whitlock. 2018. Klamath Mountains bioregion. In: J. W. van Wagtendonk, N. S. Sugihara, S. L. Stephens, A. Thode, K. Shaffer, J. Fites-Kaufmann (eds.) Fire in California's ecosystems: 2nd Edition Revised. University of California Press, Berkeley. pp. 171–193.

Skinner, C. N. and A. H. Taylor. 2018. Southern Cascades Bioregion. In: J. W. van Wagtendonk, N. S. Sugihara, S. L. Stephens, A. Thode, K. Shaffer, J. Fites-Kaufmann (eds.). Fire in California's ecosystems: 2nd Edition Revised. University of California Press, Berkeley. pp. 195–218.

Soepboer, W., S. Sugita, A. F. Lotter, J. F. N. van Leeuwen, and W. O. van der Knaap. 2007. Pollen productivity estimates for quantitative reconstruction of vegetation cover on the Swiss Plateau. The Holocene 17:65–77.

Sowerwine, J., D. Sarna-Wojcicki, M. Mucioki, L. Hillman, F. K. Lake, E. Friedman. 2019. Enhancing Food Sovereignty. Journal of Agriculture, Food Systems, and Community Development, 9:167-190.

Spelter, H. 2002. Conversion of board foot scaled logs to cubic meters in Washington State, 1970–1998. Gen. Tech. Rep. FPL-GTR-131. Madison, WI: US Department of Agriculture, Forest Service, Forest Products Laboratory. p. 131.

Stahle, D. W., R. D. Griffin, D. M. Meko, et al. 2013. The Ancient Blue Oak Woodlands of California: Longevity and Hydroclimatic History. Earth Interactions 17:1–23.

Stephens, S. L., and N. G. Sugihara. 2006. Fire management and policy since European settlement. In: Sugihara NG, van Wagtendonk J, Shaffer KE, Fites-Kaufman J, Thode AE (Eds.), Fire in California's Ecosystems. University of California Press, Berkeley, California, pp. 431–443.

Stephens, S. L., R. E. Martin, and N. E. Clinton. 2007. Prehistoric fire area and emissions from California's forests, woodlands, shrublands, and grasslands. Forest Ecology and Management 251:205-216.

Stephens, S. L., J. M. Lydersen, B. M. Collins, D. L. Fry, and M. D. Meyer. 2015. Historical and current landscape-scale ponderosa pine and mixed conifer forest structure in the Southern Sierra Nevada. Ecosphere 6:1–63.

Stephens, L., D. Fuller, N. Boivin et al. 2019. Archeological assessment reveals Earth's early transformation through land use. Science 365:897-902.

Stewart, W. C., and B. Sharma. 2015. Carbon calculator tracks the climate benefits of managed private forests. California Agriculture. January-March: 21-26.

Stockmarr, J. 1971. Tablets with spores used in pollen analysis. Pollen and Spores 13:615–621.

Stokes, M.A., and Smiley, T.L. 1968. An introduction to tree-ring dating. University of Chicago Press, Illinois, USA.

Stuart, J. D., and L. A. Salazar. 2000. Fire history of white fir forests in the coastal mountains of northwestern California. Northwest Science 74:280–285.

Sugita, S. 1993. A model of pollen source area for an entire lake surface. Quaternary Research 39:239–244.

Sugita, S. 1994. Pollen representation of vegetation in Quaternary sediments: Theory and method in patchy vegetation. Journal of Ecology 82:881–897.

Sugita, S., M.-J. Gaillard, and A. Broström. 1999. Landscape openness and pollen records: a simulation approach. The Holocene 9:409–421.

Sugita, S. 2007a. Theory of quantitative reconstruction of vegetation. I. Pollen from large sites REVEALS regional vegetation composition. Holocene 17:229–241.

Sugita, S. 2007b. Theory of quantitative reconstruction of vegetation. II. All you need is LOVE. Holocene 17:243–257.

Sutton, O. G. 1947. The problem of diffusion in the lower atmosphere. Quarterly Journal of the Royal Meteorological Society 73: 257–276.

Sutton, O. G. 1953. Micrometeorology. McGraw-Hill, New York.

Swetnam, T. W., C. D. Allen, and J. L. Betancourt. 1999. Applied historical ecology: Using the past to manage for the future. Ecological Applications 9:1189–1206.

Taylor, A. H., and C. N. Skinner. 1998. Fire history and landscape dynamics in a late successional reserve, Klamath Mountains, California, USA. Forest Ecology and Management 111:285–301.

Taylor, A. H. 2000. Fire regimes and forest changes in mid and upper montane forests in the southern Cascades, Lassen Volcanic National Park, California, USA. Journal of Biogeography 27:87–104.

Taylor, A. H., and C. N. Skinner. 2003. Spatial patterns and controls on historical fire regimes and forest structure in the Klamath Mountains. Ecological Applications 13:704–719.

Taylor, A. H., A. M. Vandervlugt, R. S. Maxwell, R. M. Beaty, C. Airey, and C. N. Skinner. 2014. Changes in forest structure, fuels and potential fire behavior since 1873 in the Lake Tahoe Basin, USA. Applied Vegetation Science 17:17–31.

Taylor, A. H., V. Trouet, C. N. Skinner, and S. Stephens. 2016. Socioecological transitions trigger fire regime shifts and modulate fire–climate interactions in the Sierra Nevada, USA, 1600–2015 CE. Proceedings of the National Academy of Sciences 113:13684–13689.

Tepley, A. J., J. R. Thompson, H. E. Epstein, and K. J. Anderson-Teixeira. 2017. Vulnerability to forest loss through altered postfire recovery dynamics in a warming climate in the Klamath Mountains. Global Change Biology 23:4117–4132.

Theuerkauf, M., A. Kuparinen, and H. Joosten. 2012. Pollen productivity estimates strongly depend on assumed pollen dispersal. The Holocene 23: 14–24.

Thomas-Van Gundy, M. A., and G. N. Nowacki. 2013. The use of witness trees as pyro-indicators for mapping past fire conditions. Forest Ecology and Management 304:333–344.

Tonkova, S., S. Hicks, E. Bozilovaa, and J. Atanassova. 2001. Pollen monitoring in the central Rila Mountains, Southwestern Bulgaria: comparisons between pollen traps and surface samples for the period 1993±1999. Review of Palaeobotany and Palynology 117:167–182.

Tripp, B., A. Watts-Tobin, and J. Dyer. 2017. Cultural resources specialist report. CRSR-SBIFMP. pp 1–22.

Tulowiecki, S. J. 2014. Assessing native American influences upon pre-European tree species composition in western New York: an approach using original land survey records and species distribution models. PhD dissertation, University at Buffalo, SUNY.

Tushingham, S., and R. L. Bettinger. 2013. Why forager choose acorns before salmon: storage, mobility and risk in aboriginal California. Journal of Anthropological Archeology 32:527–537.

USDA Forest Service 1947 S - Plans - Timber Management - Six Rivers (Requa Working Circle). Memorandum to the files regarding his July 2 discussion with Duncan Dunning regarding logging methods and strategies in the NRPU. (Accession No. 95-62C524, Locn. 48485, Box 9).

USDA Forest Service. 2000. Timber Cruising Handbook and Amendments. Technical Report FSH 2409.12. Washington, DC, USA.

USDA Forest Service. 2001. Six Rivers National Forest: Vegetation Plant Associations, Sub-series and Seral Stages of the Six Rivers National Forest. In-house spatial dataset on file at Six Rivers National Forest, Eureka, CA.

USDA Forest Service. 2005. Sampling protocol, estimation, and analysis procedures for the down woody materials indicator of the FIA program. General Technical Report NC-256. North Central Research Station: St. Paul, MN, USA.

USDA Forest Service. 2010. Field Key to Calveg Alliances North Coast and Montane - Zone 1. Accessed 2019:https://www.fs.usda.gov/Internet/FSE_DOCUMENTS/fsbdev3_046099.pdf

USDA Forest Service. 2011. Region five ecological restoration: Leadership intent. March 2011. USDA Forest Service, Pacific Southwest Region, Albany, California, USA.

USDA Forest Service. 2013. Ecological restoration implementation plan. R5-MB-249. USDA Forest Service, Pacific Southwest Region, Albany, California, USA.

USDA Forest Service, Automated Lands Program. 2019. Administrative Forest. https://data.fs.usda.gov/geodata/edw/edw_resources/meta/S_USA.AdministrativeForest.xml

USDA Forest Service Forest Activity Tracking System. 2020. Timber harvest plans. Accessed January 2020: http://data.fs.usda.gov/geodata/edw/datasets.php

USDOI, Bureau of Land Management. 2019. BLM CA Cadastral PLSS Standardized Data – Cadastral Reference. Version 1.0 (CADNSDI), Edition: 1. https://navigator.blm.gov/api/download/239740

US Geological Survey National Elevation Dataset. 2013. Accessed November 2019: http://ned.usgs.gov/

1947 "Forest Situation in Humboldt and Del Norte Counties." Unpublished ms. prepared by Six Rivers National Forest. (On file: SRNF, SO, Heritage Resources Office.)

Vachula, R. S., J. M. Russell, and Y. Huang. 2019. Climate exceeded human management as the dominant control of fire at the regional scale in California's Sierra Nevada. Environ Res Lett 14:104011.

Vale, T. R. 2002. The Pre-European landscape of the United States. In: Vale TR (ed) Fire, native peoples, and the natural landscape. Island Press, Washington, DC, pp 1–39.

Van Wagtendonk, J., and D. R. Cayan. 2008. Temporal and spatial distribution of lightning strikes in California in relation to large-scale weather patterns. Fire Ecology 4:34-56.

Von Post, L. 1918. Skogsträdspollen i sydsvenska torfmosslagerföljder. In: Forhandlinger ved de 16. Skandinaviske Naturforskeresmøte 433–465.

Wahrhaftig, C. and J. H. Birman. 1965. The Quaternary of the Pacific mountain system in California. In H.E Wright and D. G. Frey (eds.) Quaternary of the United States. Princeton, Princeton University Press.

Wang, Y., and U. Herzschuh. 2011. Reassessment of Holocene vegetation change on the upper Tibetan Plateau using the pollen-based REVEALS model. Review of Palaeobotany and Palynology 168(1): 31–40.

Wanket, J. 2002. Late Quaternary vegetation and climate of the Klamath Mountains. PhD Dissertation, University of California.

Warburton, A. D., and J. F. Endert. 1966. Indian Lore of the North California Coast. Pacific Pueblo Press, Santa Clara, CA.

Waterman, T. T. 1920. Yurok geography. Berkeley: University of California Press.

Webb, T., S. Howe, R. Bradshaw, and K. Heide. 1981. Estimating plant abundances from pollen percentages: the use of regression analysis. Review of Palaeobotany and Palynology 34:269–300.

West, G. J. 1985. Holocene Vegetation and Climatic Changes in California's North Coast Ranges. In: Archaeological Investigations on Pilot Ridge: Results of the 1984 Field Season, J.F. Hayes and W.R. Hildebrandt (eds.) Pages: 8-29. Report on file at the Six Rivers National Forest, Eureka.

Westerling, A. L. 2018. Wildfire Simulations for California's Fourth Climate Change Assessment: Projecting Changes in Extreme Wildfire Events with a Warming Climate. California's Fourth Climate Change Assessment, California Energy Commission. Publication Number: CCCA4-CEC-2018-014.

Wheeler, F. E., and C. I. Doman. 1995. Field notes of the dependent resurvey of a portion of the subdivisional lines, and the subdivision of section 24 and 25, township 10 north range 4 east, Humboldt Meridian, California. Digital archive from the Cadastral Survey Office, Bureau of Land Management Survey Records, Sacramento, California. Volume 600:369-407.

Whitlock, C., C. N. Skinner, P. J. Bartlein, T. Minckley, and J. A. Mohr. 2004. Comparison of charcoal and tree-ring records of recent fires in the eastern Klamath Mountains, California, USA. Canadian Journal of Forest Research 3:2110–2121.

Whitney, G. G., and J. P. DeCant. 2001. Government land office surveys and other early land surveys. Pages 147–172 in D. Egan and E. A. Howell, editors. Historical ecology handbook. Island Press, Washington, D.C.

Whittaker, R. H. 1960. Vegetation of the Siskiyou Mountains, Oregon and California. Ecological Monographs 30:279–338.

Williams, M. A., and W. L. Baker. 2010. Bias and error in using survey records for ponderosa pine landscape restoration. Journal of Biogeography 37:707–721.

Wills, R. D., and J. D. Stuart. 1994. Fire history and stand development of a Douglas-fir hardwood forest in northern California. Northwest Science 68:205–212.

Wright, H. E., and M. L. Heinselman. 1973. The ecological role of fire in natural conifer forests of western and northern North America: introduction. Quaternary Research 3:319–328.

Zhou, X., and M. A. Hemstrom. 2009. Estimating aboveground tree biomass on forest land in the Pacific Northwest: a comparison of approaches. PNW-RP-584. US Department of Agriculture, Forest Service, Pacific Northwest Research Station.

Zybach, B. 2005. Indian burning of the Oregon Coast Range. Oregon State University, PhD Dissertation.

APPENDIX 1 – CHAPTER 1

Table S1. Taxa designations by deputy surveyor. The majority (>90%) of surveys were conducted by crews under Brunt, Foreman, Haughn, Holcomb, and McCoy. They each varied in their level of taxonomic discrimination, which we accounted for in the analysis (see methods).

	Brunt	Foreman	Haughn	Holcomb	McCoy	Other	Grand Total
Taxa	**11**	**20**	**22**	**29**	**9**	**8**	
Fir	121	562	554	1381	225	175	3018
Pine	35	726	613	501	81	115	2071
Oak		577	879	168	9	61	1694
Madrone	23	388	461	249	144	34	1299
Black oak	457				45	171	142	815
Yellow pine	144			620	25	12	801
NTWL	1	278	336	149	2	34	800
NA	77	35	47	44	106	282	591
White oak	382		1	20	20	111	534
Tanoak				122	261	1	384
Spruce	131	2		164	27	25	349
Live oak	77		14	134	39	15	279
PI		2	10	159	52	29	252
Alder	6	110	78	10	8		212
Cedar	14	9	15	70	52	22	182
Sugar pine	6	2	10	51	12	5	86
Maple	14	1	6	14	11	2	48
Red fir				30		7	37
Pitch pine				25		1	26
Tamarack				15	5	5	25
Chincapin				1	16	3	20
Bull pine			3	16			19
White fir				14		4	18
Dogwood		8	4		3		15
Laurel	13						13
Blue oak						11	11
Pinion						10	10
Cottonwood	8						8
Manzanita				1	1	6	8
Yew				2	4		6
Buckeye	2					2	4
Chestnut				4			4

Nut pine						4	4
Pepper			4				4
Willow	1		2	1			4
Ash	3						3
Myrtle	2		1				3
Scrub oak			2			1	3
Aspen				2			2
Granite rock	2						2
Pepperwood			2				2
Scrub pine			2				2
Chestnut oak	1						1
Mountain oak						1	1
Mountain pine						1	1
Redwood						1	1
Grand Total	1520	2700	3044	4012	1274	1122	13672

Table S2. Correction factors by corner types (exterior and interior, section and quarter). Methods followed Goring et al. (2016).

Corner type	Less than equal halves correction	Azimuthal correction	Near tree correction	Union correction	Small diameter correction
Exterior Section	1.10	1.27	1.10	1.41	0.58
Exterior Quarter	1.14	1.11	1.08	1.30	0.68
Interior Section	1.08	1.21	1.11	1.36	0.65
Interior Quarter	1.17	1.03	1.09	1.26	0.71
All	1.14	1.11	1.09	1.31	0.68

Table S3. Descriptions for FVEG found in the Six Rivers National Forest (USDA Forest Service 2010). Alliances are based on the Calveg system, which was crosswalked to the California Wildlife Habitat Relationship System (FVEG) and its subsequent versions (Meyer and Laudenslayer 1988).

FVEG	Description
Chaparral	A combination of two FVEG classes, mixed chaparral and montane chaparral. Both types have > 50% shrub cover. Species composition dominated by a mix of *Ceanothus* and *Arctostaphylos.*
Douglas Fir	Douglas-fir has > 75% canopy cover
Klamath Mixed Conifer	Any of these species in combination are present but do not dominate the canopy cover: noble fir, Alaska cedar, Engelmann spruce, Brewer spruce, Port Orford cedar, pacific yew, subalpine fir, Pacific silver fir
Montane Hardwood	A mixture of hardwoods on productive sites, including black oak, madrone, tanoak, bigleaf maple, and/or tree chinquapin in combination have > 50% hardwood canopy cover
Montane Hardwood-Conifer	Any of these species in combination are present but do not dominate the canopy cover: Oregon white oak, tanoak, Pacific madrone, red alder, Douglas-fir, western red cedar, western hemlock, ponderosa pine, sugar pine, and knobcone pine
True Fir	A combination of two FVEG classes, red fir and white fir. Red fir and white fir in combination have > 75% canopy cover

Table S4. Settlement forest structure summary for Six Rivers National Forest from General Land Office survey data (1880's). Bias corrected results for the six most common contemporary vegetation types (called alliances). Two types (Chaparral and True Fir) represent higher order aggregations of two alliances. Information about vegetation types at http://vegetation.cnps.org/. Results include only trees > 20 cm DBH. Means and standard errors (SE) reported for each vegetation alliance. Confidence interval (CI) defined as the range of values between the 2.5% and 97.5% percentiles; percentiles calculated from resampled estimates.

Contemporary Vegetation Alliance	N (points)	Density (stems/ha)			Basal area (m²/ha)		
		Mean	SE	CI	Mean	SE	CI
Chaparral	313	71	9.7	56-93	11.9	1.5	9.2-14.9
Douglas Fir	2,174	85	3.1	79-91	13.6	0.9	11.8-15.4
Klamath Mixed Conifer	459	72	5.5	63-84	7.1	0.8	5.6-8.9
Montane Hardwood	386	83	8.4	69-100	18.9	2.4	14.5-23.9
Montane Hardwood-Conifer	837	90	5.2	80-101	15.8	1.9	12.4-19.8
True Fir	262	73	6.6	61-87	7.8	1.1	5.9-10.2
Other	230	51	5.0	41-61	11.6	2.9	6.9-18.2
All	4,661	81	2.0	78-85	13.3	0.6	12.2-14.5

Table S5. Contemporary forest structure summary for Six Rivers National Forest from FIA Phase 2 inventory plots (2008-2017). Results for the six most common contemporary vegetation types (called alliances). Two types (Chaparral and True Fir) represent higher order aggregations of two alliances. Only trees > 20 cm DBH included. Means and standard errors (SE) reported for each vegetation alliance. Confidence interval (CI) defined as the range of values between the 2.5% and 97.5% percentiles; percentiles calculated using a student t distribution.

Contemporary Vegetation Alliance	N (plots)	Density (trees/ha)			Basal area (m²/ha)		
		Mean	SE	CI	Mean	SE	CI
Chaparral	7	69	14.8	41-97	11.6	2.9	6.1-17.1
Douglas Fir	98	272	14.5	248-296	41.3	2.4	37.3-45.3
Klamath Mixed Conifer	5	288	96.4	94-482	52.7	11.8	28.9-76.5
Montane Hardwood	19	126	18.4	94-158	17.0	4.6	9.0-25.0
Montane Hardwood-Conifer	13	392	71.7	265-519	48.5	5.5	38.8-58.2
True Fir	31	275	25.9	231-319	40.8	3.8	34.4-47.2
Other	11	208	52.8	113-303	19.3	3.9	12.3-26.3
All	184	255	11.9	235-275	37.1	1.7	34.3-39.9

Table S6. Settlement forest composition summary for Six Rivers National Forest from General Land Office survey data (1880s). Results for the six most common contemporary vegetation types. Two types (Chaparral and True Fir) represent higher order aggregations of two alliances. Compositional information based on generic taxa; results based on relative basal area.

Contemporary Vegetation Type	Basal Area	Douglas-fir	Pines	Oaks	True firs	Madrone	Cedars	Other conifers	Other hardwoods
	(m²/ha)	(%)	(%)	(%)	(%)	(%)	(%)	(%)	(%)
Chaparral	11.9	17.1	40.2	11.6	12.8	3.8	11.5	1.6	1.5
Douglas Fir	13.6	38.6	20.7	24.1	0.3	12.5	2.5	0.0	1.3
Klamath Mixed Conifer	7.1	33.6	39.8	15.3	1.6	6.1	1.2	0.6	1.8
Montane Hardwood	18.9	34.1	14.0	37.2	0.0	7.7	5.9	0.0	1.1
Montane Hardwood-Conifer	15.8	44.6	21.6	23.7	0.0	6.3	0.9	0.6	2.3
True Fir	7.8	25.5	22.3	13.8	28.8	4.9	2.0	1.5	1.2
Other	11.6	47.1	10.8	27.3	2.3	8.0	2.5	0.0	1.9
All	13.3	34.4	24.2	21.9	6.5	7.0	3.8	0.6	1.6

Table S7. Contemporary forest composition summary for Six Rivers National Forest from FIA Phase 2 inventory plots (2008-2017). Results for the six most common contemporary vegetation types. Two types (Chaparral and True Fir) represent higher order aggregations of two alliances. Compositional information based on generic taxa; results based on relative basal area.

Contemporary Vegetation Type	Basal Area	Douglas-fir	Pines	Oaks	True firs	Madrone	Cedars	Other conifers	Other hardwoods
	(m²/ha)	(%)	(%)	(%)	(%)	(%)	(%)	(%)	(%)
Chaparral	11.6	39.6	19.4	14.9	12.0	5.1	8.7	0.0	0.3
Douglas Fir	41.3	51.3	18.9	12.0	5.1	3.8	3.6	0.9	4.4
Klamath Mixed Conifer	52.7	36.7	54.1	0.1	1.0	0.3	6.8	0.4	0.6
Montane Hardwood	17.0	38.4	36.4	9.9	0.0	13.8	0.0	0.0	1.5
Montane Hardwood-Conifer	48.5	47.8	30.4	5.0	4.0	6.9	3.9	0.1	1.9
True Fir	40.8	14.1	12.2	1.2	62.3	3.7	5.1	0.0	1.4
Other	19.3	24.4	25.9	12.1	23.8	0.9	2.3	6.3	4.3
All	37.1	45.2	26.1	9.3	7.0	4.6	3.9	0.9	3.1

Table S8. Comparison of different seral stage harvest and
salvage types across Six Rivers National Forest (USDA Forest Service 2003).

Harvest types	Hectares
Early harvest with mid-mature stands	1,143
Early harvest	21,507
Early salvage	158
Late harvest	2,581
Late salvage	91
Mid-harvest with mid-mature stands	442
Mid-harvest	11,581
Mid-salvage	869
Old harvest	784
Old salvage	145
Pole harvest	31,309
Pole salvage	848
Shrub harvest	25,372
Shrub salvage	2,258
Total harvest	99,088
SRNF total ha	394,420

Results for uncorrected reconstructions

These tables contain the "uncorrected" reconstructions of density and basal area. More trees were included in the uncorrected reconstructions; therefore, the mean density of all alliances is greater.

Table S9. Settlement forest structure summary for Six Rivers National Forest from General Land Office survey data (1880's). Results for the six most common contemporary vegetation types without bias corrections. All trees included; more than 95% of trees ≥ 10.16 cm DBH. Means and standard errors (SE) reported for each vegetation alliance.

Contemporary Vegetation Alliance	N (points)	Density (stems/ha)		Basal area (m^2/ha)	
		Mean	SE	Mean	SE
Chaparral	313	80	11	9.2	1.2
Douglas Fir	2,174	96	3.5	10	0.69
Klamath Mixed Conifer	459	82	6.2	5.4	0.60
Montane Hardwood	386	95	9.6	14	1.8
Montane Hardwood-Conifer	837	102	5.9	12	1.5
True Fir	262	83	7.4	5.9	0.82
Other	230	58	5.6	8.8	2.1
All	4,661	92	2.3	10	0.44

Table S10. Contemporary forest structure summary for Six Rivers National Forest from FIA Phase 2 inventory plots (2008-2017). Results for the six most common contemporary vegetation types. Results calculated for trees $\geq$ 10.16 cm DBH. Means and standard errors (SE) reported for each vegetation alliance.

Contemporary Vegetation Alliance	N (plots)	Density (trees/ha)		Basal area (m²/ha)	
		Mean	SE	Mean	SE
Chaparral	7	103	30.2	10.6	3.0
Douglas Fir	98	566	37.1	47.1	2.4
Klamath Mixed Conifer	5	503	106.4	21.6	4.5
Montane Hardwood	19	650	139.9	49.5	6.9
Montane Hardwood-Conifer	13	535	55.8	45.5	4.0
True Fir	31	460	209.4	59.7	12.9
Other	11	585	135.2	26.3	4.3
All	184	539	28.2	41.9	1.8

a)

b)
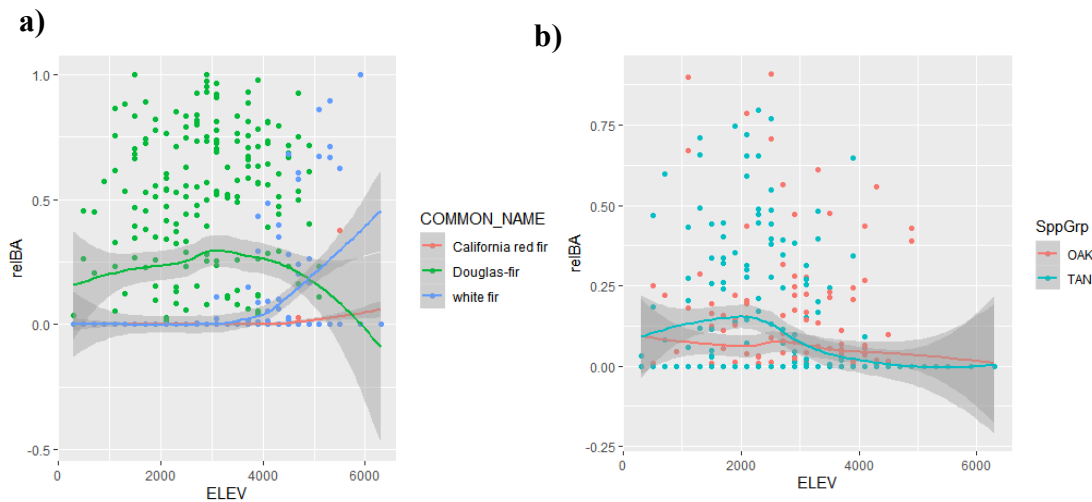
Figure S1. (a) The relative basal area (m²/ha) of red fir (red points), Douglas-fir (green points), and white fir (blue points) across the observed elevation of SRNF. Red and white fir show increased presence above 4,500 feet, while Douglas-fir predominantly occurred below 4,000 feet. **(b)** The relative basal area (m²/ha) of oak (red points) and tanoak (blue points) across the observed elevation of SRNF. The ranges of oak and tanoak overlapped substantially at all elevations.
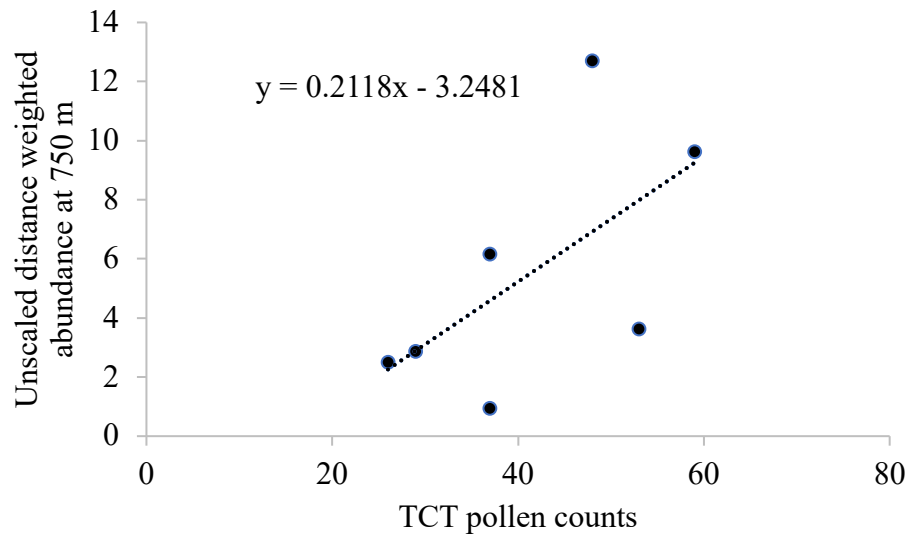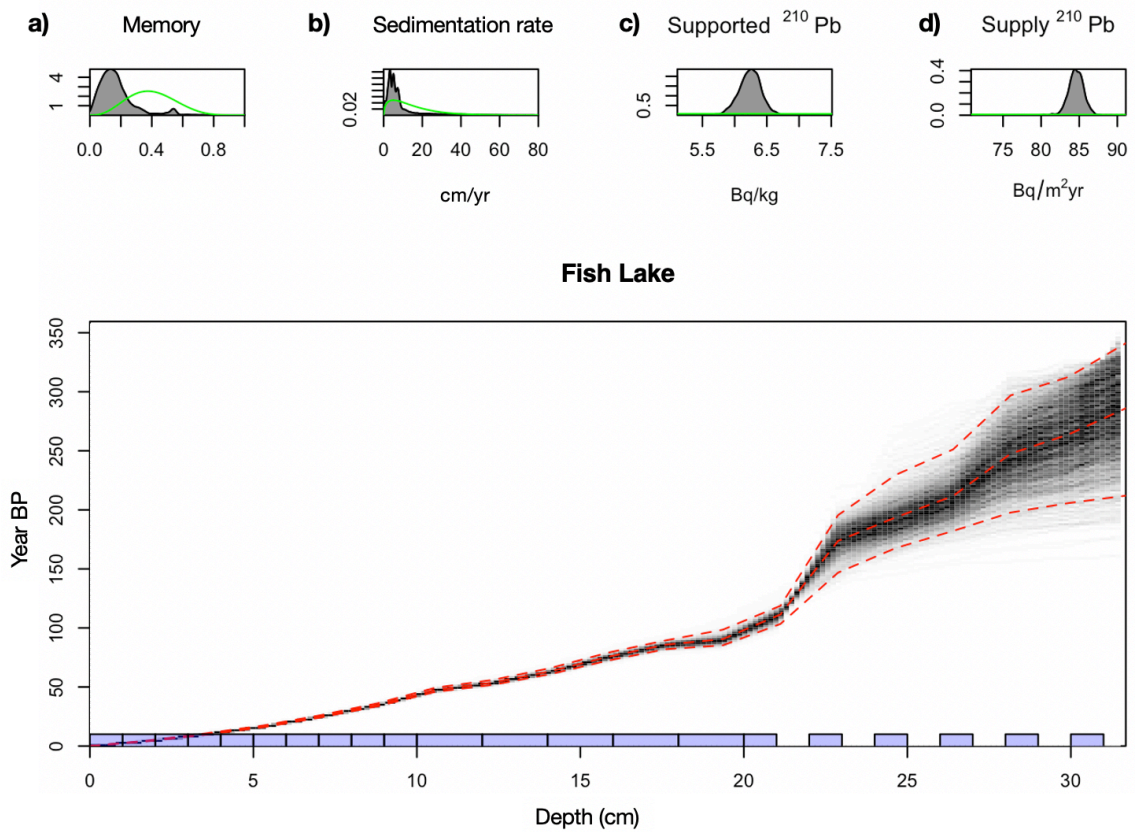
y = 0.2118x - 3.2481

Figure S1. TCT pollen counts corrected to the same base sum plotted against unscaled distance weighted plant abundance at 750m to determine the reference taxon for the PolERV model.
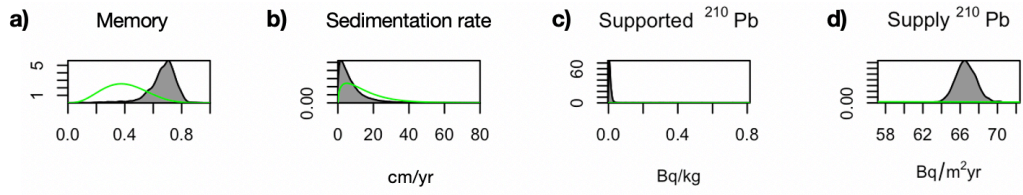
Sediment dating and age-depth model

We used lead-210 (^{210}Pb; 22.3 yr half-life) to assign ages to sediment deposited in the last 150 years. Surface bulk sediments from 0 cm to a maximum of 45 cm were taken from each core and dried to 105°C (see Tables S1-S7). ^{210}Pb activity was determined by alpha spectrometry, via ^{210}Po. An aliquot of 0.2 to 1.0 g of dried and pulverized sample was digested using concentrated HF, HNO$_3$, and HCl and a known amount of ^{209}Po spike in an oven at 90°C for ~ 24 hours. The digested solution was dried, and the residue was mixed with 1 M HCl until the pH was ~2. Auto-plating of Po was cold-plated onto an Ag disk for 24 hours at room temperature (Jweda and Baskaran 2011). The plated disk was assayed for Po using Octete PC ORTEC alpha spectrometer. The reagent blanks were run simultaneously with each batch of eight samples and were subtracted. Certified reference materials were periodically run. For the determination of parent-supported (i.e., background) ^{210}Pb, several samples were run for the activity of ^{226}Ra (using 352 and 609 keV) along with ^{137}Cs (661.6 keV) by Ge-well detector (Baskaran et al. 2015). Small sample sizes prevented reliable ^{137}Cs from being obtained.
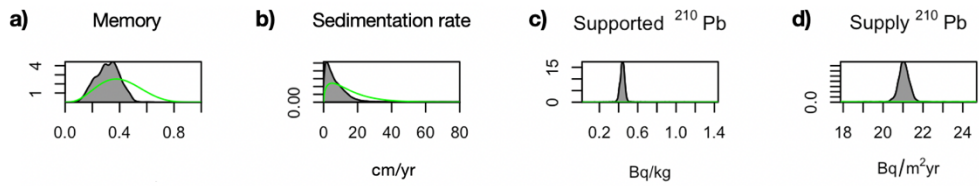
We used the Bayesian-based Plum software to develop age models from excess (unsupported) ^{210}Pb data (Aquino-López et al. 2018). The Plum model is related to the constant rate of supply (CRS) method (Appleby and Oldfield 1978) and retains two of the basic assumptions of CRS: the rate of supply of ^{210}Pb is constant and there is no vertical mixing of radionuclides. Testing these assumptions requires independent validation using another marker, which is outside of this paper's scope. The Plum model is formulated within a robust statistical framework to quantify uncertainty (Aquino-López et al. 2018). Plum uses a self-adjusting Markov Chain Monte Carlo (MCMC) algorithm called the t-walk (Christen and Fox 2010). Plum uses millions of MCMC iterations to model the accumulation of sediment, using a gamma autoregressive semiparametric age-depth function (Blaauw and Christen 2011). This algorithm results in a probability envelope around the mean age model. The envelope allows the precision at any depth to be estimated explicitly. Plum makes use of prior information to determine the datable horizon, which is affected by two factors: the precision of methodology (alpha versus gamma counting) and the initial amount of excess lead. In Plum, the chronology limit is determined by the rate of supply of ^{210}Pb to the site and the equipment error, usually ~3 Bq/kg for a sample size of 1 g by alpha spectrometry for research laboratories. Supported ^{210}Pb activities were determined from the direct measurements of ^{226}Ra by gamma-ray spectrometry.

Figure S2. The age-to-depth results of the Plum model for Fish, Ogaromtoc, Onion, North Twin, Red Mountain, and South Twin Lakes. The grey lines are simulation from Plum and the dashed red lines represent the mean age and the 95% interval. The small panels at the top show the prior (green) and posterior (grey) distributions for **(a)** the memory (ω), **(b)** the sedimentation rate (α), **(c)** the supported ^{210}Pb (P^S), which is the background level of ^{210}Pb already present in the sediment, and **(d)** and the supply of ^{210}Pb (Φ).

Ogaromtoc Lake

Onion Lake

a) Memory b) Sedimentation rate c) Supported ^{210}Pb d) Supply ^{210}Pb

cm/yr   Bq/kg   Bq/m^{2}yr

North Twin Lake

Year BP

Depth (cm)

a) Memory b) Sedimentation rate c) Supported ^{210}Pb d) Supply ^{210}Pb

cm/yr   Bq/kg   Bq/m^{2}yr

Red Mountain Lake

Year BP

Depth (cm)
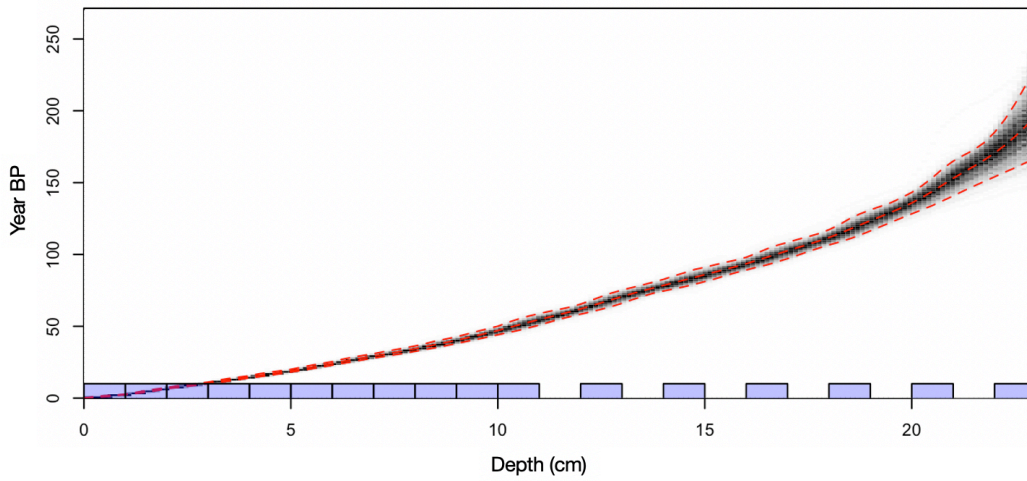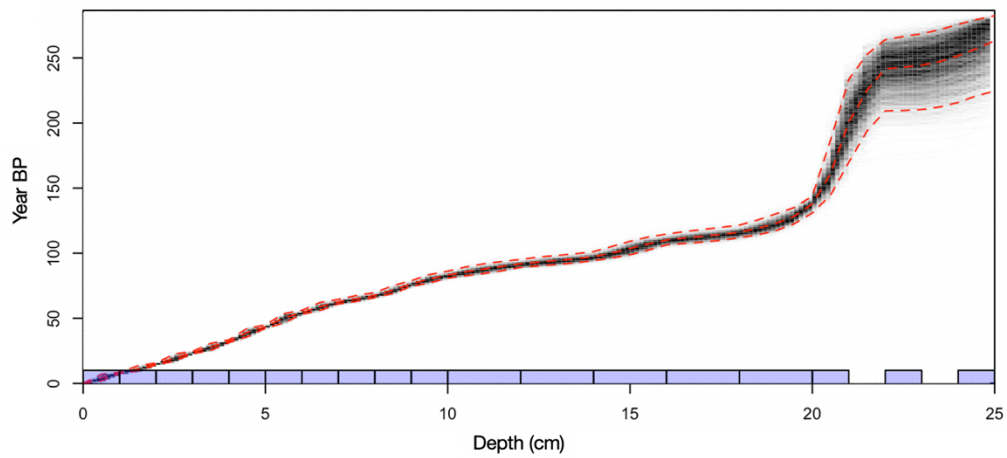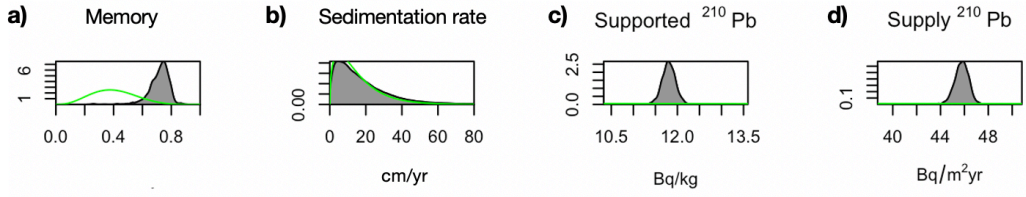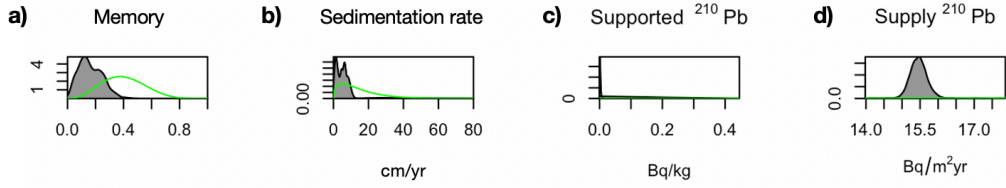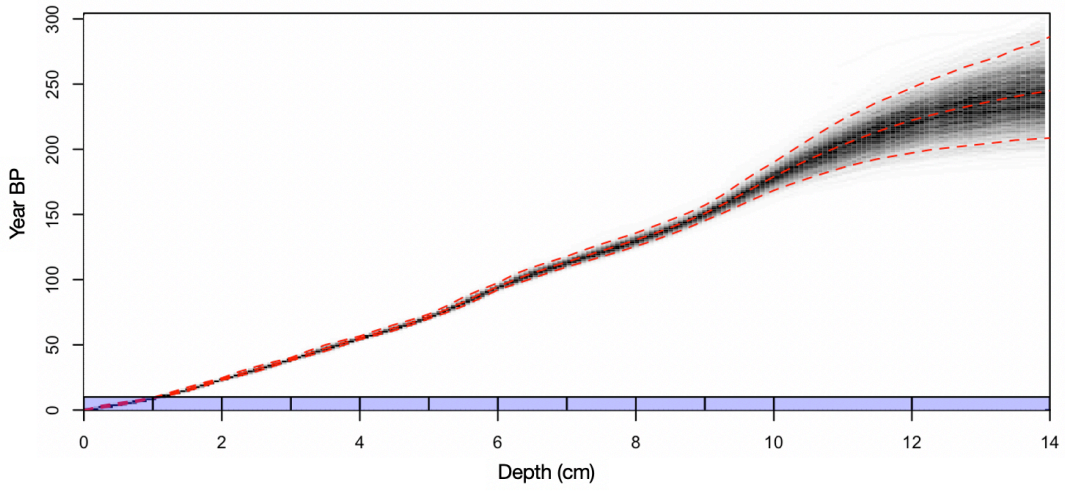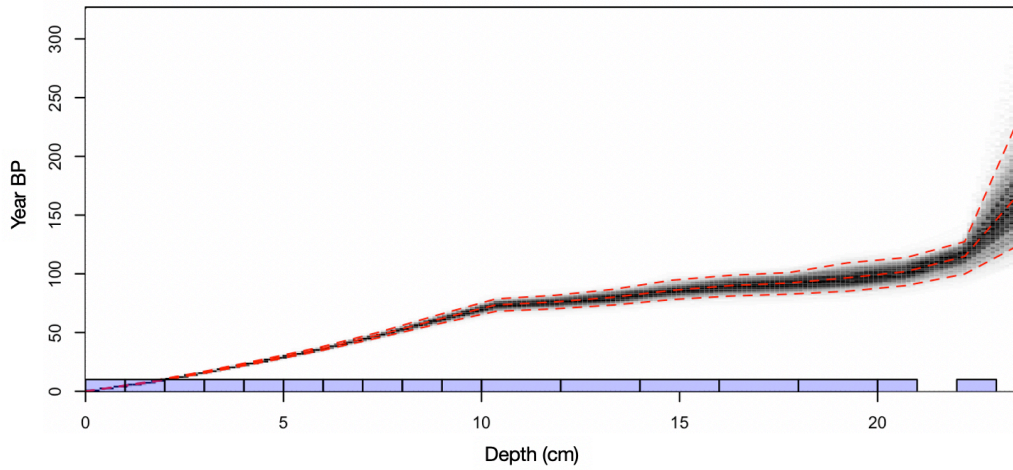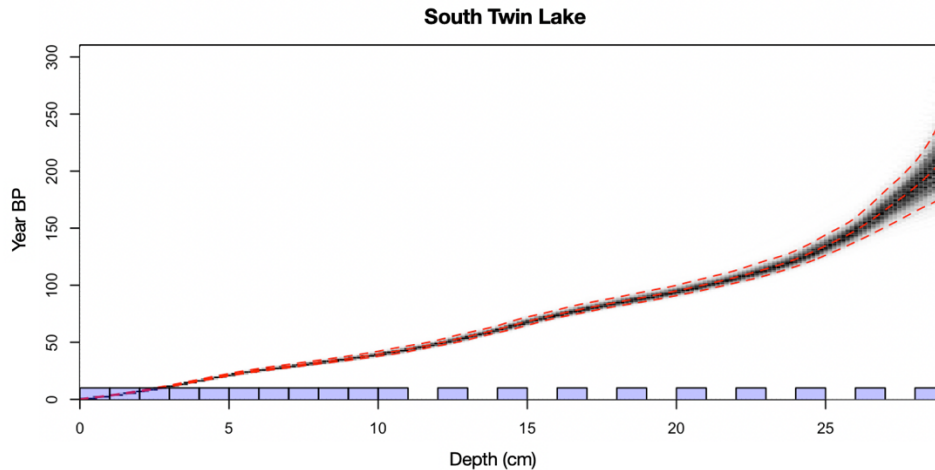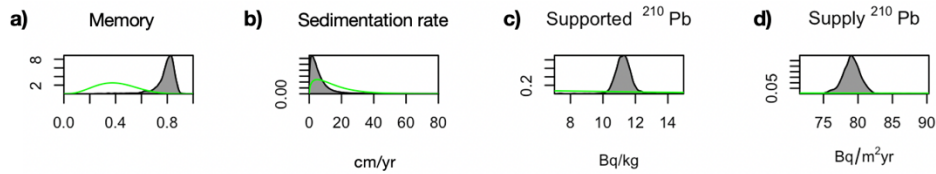
Lithology
Cores were split lengthwise and measured for magnetic susceptibility at every half centimeter using a calibrated MS2E surface scanning point sensor (MS Bartsoft). Changes in lithology were described and documented. The water content and dry bulk density were determined for each core in 1 or 2 cm intervals (Tables S14-S20), matching the sampling pattern for radioisotopic analysis (Table S1-S7).

Cores were composed of unlaminated gyttja. Occasional diatomaceous lenses (<1 cm thick) were present in Blue and Ogaromtoc lakes. For the Onion lake core, pine needles were visible in the top 3 cm, but needles were not seen in the other cores. Magnetic susceptibility was near zero for Blue, North Twin, Red Mountain, and South Twin lakes, and although magnetic susceptibility in Ogaromtoc lake was also generally low, Ogaromtoc had two distinct peaks (Fig. S3). Fish and Onion lakes showed higher overall magnetic susceptibility than the other lakes, as well as more variation across depths (Fig. S4). Peaks in magnetic susceptibility generally corresponded to increases in dry bulk density (g cm^{-3}) for Ogaromtoc, Fish, and Onion lakes (Tables S19, S17, S16, respectively). For example, two peaks at 14-15cm and 22-23cm in Ogaromtoc matched the depths where dry bulk density tripled and doubled, respectively. Ogaromtoc also had two light blue clay bands at 14-15cm and 22-23cm. Other cores did not contain clear stratigraphic markers.
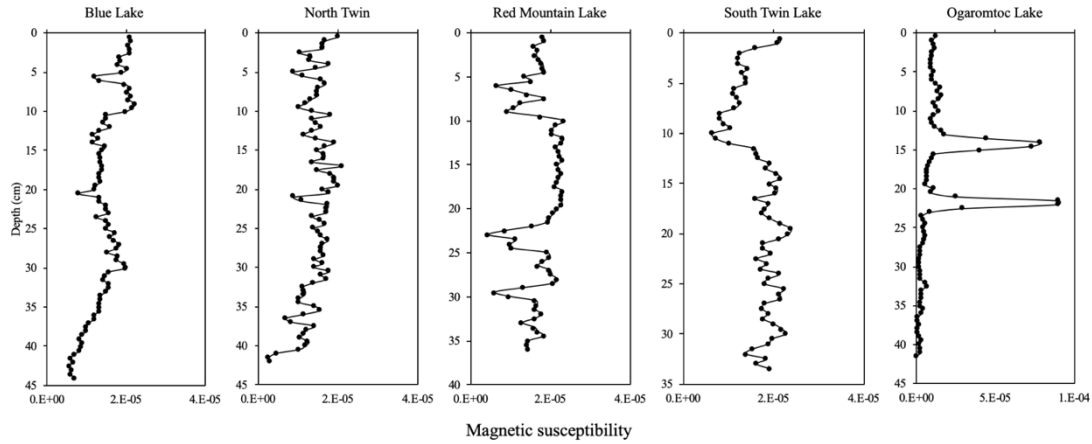
Figure S3. Magnetic susceptibility for the five study sites. The magnetic susceptibility was near zero with some variability for five lakes (note different x-axis for Ogaromtoc) – Blue, North Twin, Red Mountain, South Twin and Ogaromtoc Lakes.
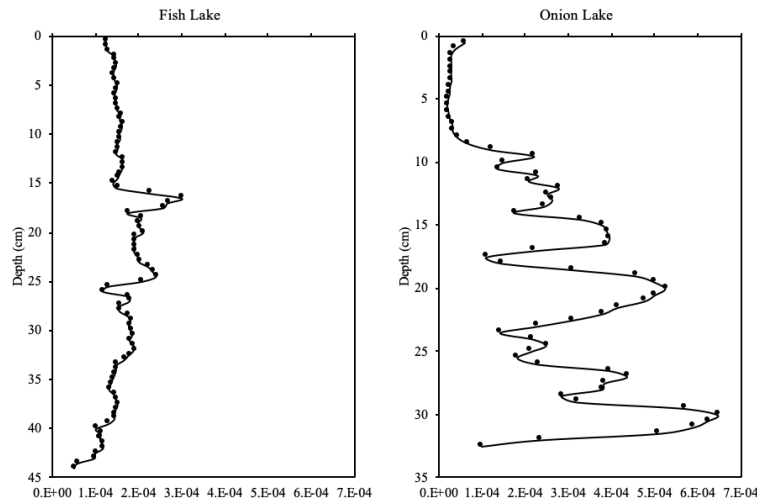
Figure S4. Magnetic susceptibility for the two study sites. Fish and Onion lakes (same x-axis) displayed higher overall magnetic susceptibility than the other five lake sites.

111

Table S1. [210]Pb dates used to create the Blue Lake age model.

Sample	Depth (cm)	Age (yr)	Uncertainty (yr)	Sample	Depth (cm)	Age (yr)	Uncertainty (yr)
210Pb_1	0.5	3	0.3	210Pb_12	13.0	38	2
210Pb_2	1.5	6	0.5	210Pb_13	15.0	45	3
210Pb_3	2.5	9	0.6	210Pb_14	17.0	50	3
210Pb_4	3.5	12	0.7	210Pb_15	19.0	57	4
210Pb_5	4.5	15	0.9	210Pb_16	20.5	69	5
210Pb_6	5.5	19	1	210Pb_17	22.5	87	9
210Pb_7	6.5	23	1	210Pb_18	24.5	103	13
210Pb_8	7.5	27	2	210Pb_19	26.5	125	21
210Pb_9	8.5	31	2	210Pb_20	28.5	146	27
210Pb_10	9.5	34	2	210Pb_21	30.5	175	57
210Pb_11	11.0	37	2				

Table S2. [210]Pb dates used to create the Fish Lake age model.

Sample	Depth (cm)	Age (yr)	Uncertainty (yr)	Sample	Depth (cm)	Age (yr)	Uncertainty (yr)
210Pb_1	0.5	2	0.2	210Pb_12	12.5	58	2
210Pb_2	1.5	5	0.4	210Pb_13	14.5	70	3
210Pb_3	2.5	8	0.5	210Pb_14	16.5	82	4
210Pb_4	3.5	12	0.6	210Pb_15	18.5	90	6
210Pb_5	4.5	15	0.7	210Pb_16	20.5	110	7
210Pb_6	5.5	20	0.8	210Pb_17	22.5	175	25
210Pb_7	6.5	25	1	210Pb_18	24.5	197	32
210Pb_8	7.5	30	1	210Pb_19	26.5	224	40
210Pb_9	8.5	36	1	210Pb_20	28.5	244	51
210Pb_10	9.5	44	2	210Pb_21	30.5	277	60
210Pb_11	10.5	49	2				

Table S3. [210]Pb dates used to create the Ogaromtoc Lake age model. An outlier point at 6.5cm was excluded from the model.

Sample	Depth (cm)	Age (yr)	Uncertainty (yr)	Sample	Depth (cm)	Age (yr)	Uncertainty (yr)
210Pb_1	0.5	3	0.2	210Pb_9	9.5	47	3
210Pb_2	1.5	7	0.4	210Pb_10	10.5	55	4
210Pb_3	2.5	11	0.6	210Pb_11	12.5	71	5
210Pb_4	3.5	15	0.8	210Pb_12	14.5	86	5
210Pb_5	4.5	19	1	210Pb_13	16.5	103	6
210Pb_6	5.5	24	1	210Pb_14	18.5	124	7
210Pb_7	7.5	34	2	210Pb_15	20.5	153	12
210Pb_8	8.5	40	2	210Pb_16	22.5	197	34

Table S4. ^{210}Pb dates used to create the Onion Lake age model.

Sample	Depth (cm)	Age (yr)	Uncertainty (yr)	Sample	Depth (cm)	Age (yr)	Uncertainty (yr)
210Pb_1	0.5	8	0.6	210Pb_10	9.5	83	3
210Pb_2	1.5	15	0.7	210Pb_11	11.0	88	4
210Pb_3	2.5	24	0.9	210Pb_12	13.0	94	4
210Pb_4	3.5	32	1	210Pb_13	15.0	104	5
210Pb_5	4.5	44	1	210Pb_14	17.0	113	5
210Pb_6	5.5	54	2	210Pb_15	19.0	123	7
210Pb_7	6.5	63	2	210Pb_16	20.5	201	32
210Pb_8	7.5	68	2	210Pb_17	22.5	244	29
210Pb_9	8.5	77	2	210Pb_18	24.5	263	29

Table S5. ^{210}Pb dates used to create the North Twin Lake age model.

Sample	Depth (cm)	Age (yr)	Uncertainty (yr)	Sample	Depth (cm)	Age (yr)	Uncertainty (yr)
210Pb_1	0.5	2	0.4	210Pb_7	6.5	112	4
210Pb_2	1.5	24	0.8	210Pb_8	7.5	128	5
210Pb_3	2.5	39	1	210Pb_9	8.5	147	6
210Pb_4	3.5	55	1	210Pb_10	9.5	173	10
210Pb_5	4.5	71	2	210Pb_11	11.0	197	18
210Pb_6	5.5	94	3	210Pb_12	13.0	229	30

Table S6. ^{210}Pb dates used to create the Red Mountain Lake age model.

Sample	Depth (cm)	Age (yr)	Uncertainty (yr)	Sample	Depth (cm)	Age (yr)	Uncertainty (yr)
210Pb_1	0.5	5	0.3	210Pb_10	9.5	71	5
210Pb_2	1.5	10	0.2	210Pb_11	11.0	75	6
210Pb_3	2.5	16	0.8	210Pb_12	13.0	79	7
210Pb_4	3.5	23	1	210Pb_13	15.0	87	8
210Pb_5	4.5	30	2	210Pb_14	17.0	91	9
210Pb_6	5.5	37	2	210Pb_15	19.0	96	12
210Pb_7	6.5	45	2	210Pb_16	20.5	104	12
210Pb_8	7.5	53	3	210Pb_17	22.5	146	37
210Pb_9	8.5	62	4				

Table S7. ^{210}Pb dates used to create the South Twin Lake age model.

Sample	Depth (cm)	Age (yr)	Uncertainty (yr)	Sample	Depth (cm)	Age (yr)	Uncertainty (yr)
210Pb_1	0.5	3	0.3	210Pb_11	10.5	44	3
210Pb_2	1.5	7	0.4	210Pb_12	12.5	55	3
210Pb_3	2.5	12	0.6	210Pb_13	14.5	68	4
210Pb_4	3.5	17	0.8	210Pb_14	16.5	80	4
210Pb_5	4.5	22	1	210Pb_15	18.5	90	4
210Pb_6	5.5	26	1	210Pb_16	20.5	95	5
210Pb_7	6.5	29	1	210Pb_17	22.5	114	7
210Pb_8	7.5	33	2	210Pb_18	24.5	135	9
210Pb_9	8.5	36	2	210Pb_19	26.5	166	16
210Pb_10	9.5	40	2	210Pb_20	28.5	186	38

Assumptions of the Prentice-Sugita-Sutton PVM

As noted in section 2.2, the Prentice-Sugita-Sutton model has certain assumptions (Sugita 1994, Gaillard et al. 2008), which we describe in full here:

1) that there is a comprehendible and spatially and temporally consistent relationship between pollen loading and distance-weighted plant abundance
2) the vegetation surface where the pollen is derived from is flat
3) the sampling basin is a circular opening in the canopy
4) pollen productivity (the amount of pollen produced per vegetation cover unit) is a constant for a given pollen taxon
5) pollen is dispersed as single grains
6) pollen dispersal is largely via wind above the canopy and gravity beneath the canopy, and pollen transport into a basin (canopy opening) can be modelled by considering the canopy component only
7) wind is uniform in every direction therefore pollen dispersal is evenly distributed around the source
8) most pollen deposition takes place via sedimentation due to gravity and deposition by interception is negligible
9) the deposition of pollen at a specified distance from a plant can be approximated using a diffusion model of the dispersal of small particles from a ground level source (Sutton 1953)
10) inter-taxon pollen grain differences (e.g., grain size, weight, and density) affect pollen dispersal and can be quantitatively estimated, and use of a single value to represent each taxon is sufficient to capture
11) atmospheric conditions during pollen deposition can be modelled as "stable" which affects parameters C_z and n (Eq.3,3a)
12) all lake sites experience the same conditions

PAR calculation

After grains were counted, pollen concentrations and PAR were determined. Using the *Lycopodium* marker grains, pollen concentrations (C_i, grains cm^{-3}) were calculated for each pollen type *i* using the following equation:

$$C_i = \frac{A_i \times L_a}{L_c \times V_i} \tag{1}$$

Where A_i is the number of pollen grains counted for the taxon *i*, L_a is the number of added marker grains, L_c is the number of counted marker grains in each slide, and V_i is the volume of the pollen sample (e.g., 0.63 cm^3) (Stockmarr 1971). Concentrations were used for PAR calculations by multiplying the concentration values by the sediment accumulate rate, which differed by lake site and was determined by the Plum age model in increments of 0.5cm. The equation used was:

$$PAR_i = C_i \times S \tag{2}$$

Where PAR$_i$ is the pollen accumulation rate for taxon *i*, C_i is the pollen concentration (grains cm^{-3}) for taxon *i*, and S is the sedimentation rate (cm yr^{-1}) (Davis and Deevey 1964).

Table S8. Coefficients for the predicted aboveground live biomass (Mg ha^{-1}) of trees as a function of basal area (m^2 ha^{-1}) using a linear log-log (natural) equation. Results for all species encountered in the forest inventory conducted for the seven lakes in the Klamath Mountains. The p-value of the regression was < 0.0001 in all cases except for white alder where p = 0.034. B$_0$ is the intercept; B$_1$ is the slope coefficient; SEE = standard error of the estimate.

Genus	Species	Common name	B$_o$	B$_1$	R$^2_{adj}$	SEE (Mg ha^{-1})
Abies	*concolor*	white fir	1.65	1.07	0.95	0.40
Abies	*magnifica*	California red fir	1.47	1.19	0.92	0.46
Acer	*macrophyllum*	bigleaf maple	1.30	1.11	0.94	0.24
Alnus	*rhombifolia*	white alder	1.26	1.30	1.00	0.07
Arbutus	*menziesii*	Pacific madrone	1.55	1.12	0.94	0.29
Calocedrus	*decurrens*	incense-cedar	1.08	1.18	0.90	0.52
Chamaecyparis	*lawsoniana*	Port-Orford-cedar	1.16	1.19	0.97	0.37
Chrysolepis	*chrysophylla*	golden chinquapin	1.19	1.18	0.96	0.34
Cornus	*nuttallii*	Pacific dogwood	1.07	0.92	0.85	0.37
Notholithocarpus	*densiflorus*	tanoak	1.08	1.17	0.96	0.35
Pinus	*attenuata*	knobcone pine	1.18	1.06	0.96	0.21
Pinus	*jeffreyi*	Jeffrey pine	1.09	1.11	0.88	0.58
Pinus	*lambertiana*	sugar pine	1.67	1.22	0.85	0.59
Pinus	*ponderosa*	ponderosa pine	1.36	1.23	0.89	0.50
Pseudotsuga	*menziesii*	Douglas-fir	1.15	1.23	0.96	0.30
Quercus	*chrysolepis*	canyon live oak	1.47	1.12	0.92	0.43
Quercus	*kelloggii*	California black oak	1.62	1.11	0.96	0.27
Taxus	*brevifolia*	Pacific yew	0.83	0.82	0.94	0.21
Umbellularia	*californica*	California-laurel	0.95	1.30	0.95	0.38

Table S9. Fall speed (m/sec) for major taxa used in the simulation runs of this study.

Taxa	Fall-speed (v_s) estimates (m s^{-1})
Abies	0.120 [a]
Alnus	0.021[b]
Pinus	0.031[a]
Pseudotsuga	0.126[a]
Quercus	0.035[a]
TCT	0.016[c]

[a] Eisenhut (1961); [b] Schober (1975);
[c] Calculated from empirical measurements using Stoke's Law with Falck's (1927) correction

Table S10. PAR values of main taxa from 2018 (a modeled age) at each lake site.

Lake Site	*Pinus*	*Pseudotsuga*	*Quercus*	*TCT*	*Notholithocarpus*	*Alnus*	*Abies*
Blue	1760	5461	758	4490	1031	1183	789
Red Mt.	3672	5068	672	3051	2844	1034	569
Onion	10797	2014	1063	1622	559	951	4811
North Twin	1749	6808	1686	2311	2935	812	1999
South Twin	2384	7152	1463	2005	2059	1300	325
Fish	1479	4606	840	1782	3741	2858	34
Ogaromtoc	3376	4609	1558	844	454	1753	260

Table S11. Results from the linear regressions predicting distance-weighted aboveground live biomass (AGL$_{dw}$) as a function of pollen accumulation rate (PAR) for the pollen taxa present at the seven lake sites in the Klamath Mountains. The assemblage-level relevant source area of pollen (aRSAP) was defined as a circle with a radius of 625 m from centroid of the lake. Parameters provided the linear regression: AGL$_{DW}$ = B$_0$ + B$_1$ * PAR where AGL$_{dw}$ is measured in Mg ha^{-1}; PAR in grains cm^{-2} yr^{-1}; SEE = standard error of the estimate; ΔAICc = the difference in the Akaike Information Criterion for small samples between the top ranked model and the second ranked model.

Pollen Taxa	ΔAICc	B$_0$	B$_1$	SEE (Mg ha^{-1})	R$^2_{adj}$	P
Pseudotsuga	6.6	0	0.0180	19.1	0.96	< 0.001
Pinus	5.4	0	0.00740	8.42	0.94	<0.001
Notholithocarpus	4.2	0	0.0211	16.5	0.89	<0.001
TCT	4.0	0	0.00954	9.43	0.87	<0.001
Quercus[1]	--	--	--	--	--	--
Alnus	3.0	3.8	0.00341	1.05	0.84	0.002
Abies	4.2	0	0.0138	13.8	0.80	0.0018

[1]There was no evidence of a significant linear relationship for Quercus. For predicting AGL$_{dw,}$ a null model was used with the intercept = 1.54 and the standard error = 1.46.

Table S12. Results from the linear regressions predicting distance-weighted aboveground live biomass (AGL$_{dw}$) as a function of pollen accumulation rate (PAR) for the pollen taxa present at the seven lake sites in the Klamath Mountains. The taxon-specific source area of pollen (tRSAP) was defined as a circle with a radius determined by the strength of correlation (R^2) between plant abundance and PAR. Parameters provided the linear regression: AGL$_{dw}$ = B$_0$ + B$_1$ * PAR where AGL$_{dw}$ is measured in Mg ha^{-1}; PAR in grains cm^{-2} yr^{-1}; SEE = standard error of the estimate.

Pollen Taxa	B$_0$	B$_1$	SEE (Mg ha^{-1})	R$^2_{adj}$	P
Pseudotsuga	0	0.0180	19.1	0.96	< 0.001
Pinus	0	0.00558	6.78	0.95	<0.001
Notholithocarpus	0	0.0205	16.2	0.91	<0.001
TCT	0	0.00849	8.97	0.87	<0.001
Quercus[1]	--	--	--	--	--
Alnus	-3.8	0.00341	1.05	0.84	0.002
Abies	0	0.0138	13.8	0.83	0.0018

[1]There was no evidence of a significant linear relationship for *Quercus*. For predicting AGL$_{dw,}$ a null model was used with the intercept = 1.54 and the standard error = 1.46.

Table S13. Results from the linear regressions predicting distance-weighted aboveground live biomass (AGL$_{dw}$) as a function of pollen accumulation rate (PAR) for the pollen taxa present at the seven lake sites in the Klamath Mountains. These equations all include an intercept and slope term even if they were not the best fit. The relevant source area of pollen (aRSAP) was defined as a circle with a radius of 625 m from centroid of the lake. Parameters provided the linear regression: AGLdw = B$_0$ + B$_1$ * PAR where AGL$_{dw}$ is measured in Mg ha^{-1}; PAR in grains cm^{-2} yr^{-1}; SEE = standard error of the estimate.

Pollen Taxa	B$_0$	B$_1$	SEE (Mg ha^{-1})	R^2$_{adj}$	P
Pseudotsuga	-14.7	0.0206	20.3	0.74	0.008
Pinus	-5.5	0.00829	8.23	0.92	<0.001
Notholithocarpus	16.8	0.0149	14.7	0.61	0.02
TCT	-12.1	0.0138	8.33	0.78	0.005
Quercus	-2.9	0.00386	3.84	0.0083	0.4
Alnus	-3.8	0.00341	1.05	0.84	0.002
Abies	-9.4	0.0168	12.35	0.84	0.002

Table S14. Dry bulk density (g cm^{-3}) for Blue Lake.

Lake	Depth (cm)	Dry Bulk Density (g cm^{-3})
Blue	0-1	0.102
Blue	1-2	0.093
Blue	2-3	0.085
Blue	3-4	0.095
Blue	4-5	0.088
Blue	5-6	0.087
Blue	6-7	0.089
Blue	7-8	0.085
Blue	8-9	0.084
Blue	9-10	0.078
Blue	10-12	0.087
Blue	12-14	0.096
Blue	14-16	0.102
Blue	16-18	0.093
Blue	18-20	0.095
Blue	20-21	0.095
Blue	22-23	0.104
Blue	24-25	0.089
Blue	26-27	0.090
Blue	28-29	0.090
Blue	30-31	0.093
Blue	40-42	0.124

Table S15. Dry bulk density (g cm^{-3}) for Red Mountain Lake.

Lake	Depth (cm)	Dry Bulk Density (g cm^{-3})
Red Mt.	0-1	0.080
Red Mt.	1-2	0.090
Red Mt.	2-3	0.074
Red Mt.	3-4	0.078
Red Mt.	4-5	0.068
Red Mt.	5-6	0.068
Red Mt.	6-7	0.071
Red Mt.	7-8	0.074
Red Mt.	8-9	0.079
Red Mt.	9-10	0.074
Red Mt.	10-12	0.081
Red Mt.	12-14	0.090
Red Mt.	14-16	0.112
Red Mt.	16-18	0.098
Red Mt.	18-20	0.110
Red Mt.	20-21	0.100
Red Mt.	22-23	0.121
Red Mt.	24-25	0.141
Red Mt.	26-27	0.146
Red Mt.	28-29	0.144
Red Mt.	30-31	0.150
Red Mt.	35-37	0.158

Table S16. Dry bulk density (g cm^{-3}) for Onion Lake.

Lake	Depth (cm)	Dry Bulk Density (g cm^{-3})
Onion	0-1	0.084
Onion	1-2	0.093
Onion	2-3	0.082
Onion	3-4	0.074
Onion	4-5	0.073
Onion	5-6	0.065
Onion	6-7	0.049
Onion	7-8	0.047
Onion	8-9	0.061
Onion	9-10	0.082
Onion	10-12	0.128
Onion	12-14	0.140
Onion	14-16	0.157
Onion	16-18	0.195
Onion	18-20	0.224
Onion	20-21	0.235
Onion	22-23	0.227
Onion	24-25	0.228
Onion	26-27	0.246
Onion	28-29	0.189
Onion	30-31	0.223

Table S17. Dry bulk density (g cm^{-3}) for Fish Lake.

Lake	Depth (cm)	Dry Bulk Density (g cm^{-3})
Fish	0-1	0.101
Fish	1-2	0.099
Fish	2-3	0.101
Fish	3-4	0.100
Fish	4-5	0.101
Fish	5-6	0.100
Fish	6-7	0.107
Fish	7-8	0.101
Fish	8-9	0.115
Fish	9-10	0.120
Fish	10-11	0.117
Fish	12-13	0.142
Fish	14-15	0.149
Fish	16-17	0.541
Fish	18-19	0.198
Fish	20-21	0.222
Fish	22-23	0.286
Fish	24-25	0.494
Fish	26-27	0.198
Fish	28-29	0.187
Fish	30-31	0.203

Table S18. Dry bulk density (g cm^{-3}) for South Twin Lake.

Lake	Depth (cm)	Dry Bulk Density (g cm^{-3})
South Twin	0-1	0.076
South Twin	1-2	0.073
South Twin	2-3	0.067
South Twin	3-4	0.059
South Twin	4-5	0.054
South Twin	5-6	0.050
South Twin	6-7	0.045
South Twin	7-8	0.047
South Twin	8-9	0.047
South Twin	9-10	0.050
South Twin	10-11	0.051
South Twin	12-13	0.060
South Twin	14-15	0.064
South Twin	16-17	0.073
South Twin	18-19	0.067
South Twin	20-21	0.075
South Twin	22-23	0.083
South Twin	24-25	0.110
South Twin	26-27	0.130
South Twin	28-29	0.130
South Twin	30-31	0.154

Table S19. Dry bulk density (g cm^{-3}) for Ogaromtoc Lake.

Lake	Depth (cm)	Dry Bulk Density (g cm^{-3})
Ogaromtoc	0-1	0.086
Ogaromtoc	1-2	0.083
Ogaromtoc	2-3	0.064
Ogaromtoc	3-4	0.064
Ogaromtoc	4-5	0.065
Ogaromtoc	5-6	0.068
Ogaromtoc	6-7	0.072
Ogaromtoc	7-8	0.074
Ogaromtoc	8-9	0.071
Ogaromtoc	9-10	0.066
Ogaromtoc	10-11	0.068
Ogaromtoc	12-13	0.081
Ogaromtoc	14-15	0.366
Ogaromtoc	16-17	0.116
Ogaromtoc	18-19	0.072
Ogaromtoc	20-21	0.096
Ogaromtoc	22-23	0.268
Ogaromtoc	24-25	0.147
Ogaromtoc	26-27	0.066
Ogaromtoc	28-29	0.061
Ogaromtoc	30-31	0.064

Table S20. Dry bulk density (g cm^{-3}) for North Twin Lake.

Lake	Depth (cm)	Dry Bulk Density (g/cm^3)
North Twin	0-1	0.099
North Twin	1-2	0.097
North Twin	2-3	0.101
North Twin	3-4	0.107
North Twin	4-5	0.108
North Twin	5-6	0.106
North Twin	6-7	0.092
North Twin	7-8	0.076
North Twin	8-9	0.076
North Twin	9-10	0.088
North Twin	10-12	0.132
North Twin	12-14	0.143
North Twin	14-16	0.145
North Twin	16-18	0.145
North Twin	18-20	0.141
North Twin	20-21	0.122
North Twin	22-23	0.133
North Twin	24-25	0.127
North Twin	26-27	0.137
North Twin	28-29	0.135
North Twin	30-31	0.137

In addition to results presented in section 2.1, here we present other relevant ethnographic and historical literature about the western Klamath Mountains (A), as well as other lines of evidence from Euro-American qualitative descriptions (B).

A. Documentation of tribal uses of Lake Ogaromtoc and Fish Lake

From Karuk Tribe Department of Natural Resources (1999, Vol 1):

1. Gathering Areas (pp. 57):
   "And there was an abundance of stuff. My family gathered at [nearby places]…and our gathering place for acorns at Frog pond [Lake Ogaromtoc]. Beautiful, beautiful acorn gathering place and mushroom gathering place." You got to stop them [USFS prescribed burn circa 1997] from burning Frog Pond. Like I said, they try to burn everything down and they don't realize there's a cloud coming in from the coast, coming in, let her hang up a little while there. Acorns, tan oak will hold back the moisture. Don't let that son of a whishhh past us like a freight train. Let it slow down, right there. Let it slow down, hold it back. But they don't do that. I see so much clear cuts on the Klamath River now and doing more. I was totally against them guys clear cutting Frog Pond. Beautiful, beautiful acorn gathering place and mushroom gathering place. A lot of basket materials. All of that stuff was there. Then to top it off, not only did they wreck a Medicine Trail, sacred Indian Trail, god damned bull dozers and loggers and the whole god damned…just ruined an Indian trail. The sacredness of that trail, very important to Mother Nature. Mother Nature itself. Cause you don't just walk down a sacred trail cause it's a trail. The sacredness of the trails going somewhere, leading you to somewhere, a special place in northern California mountains, on the Klamath National Forest. Destroyed. 'Where's that trail? It used to once be right there.' No, and they destroyed it." Charlie Thom, interview conducted 11/96.

From Karuk Tribe Department of Natural Resources (1999, Vol 2):

2. Basket Materials/Gathering Issues (pp. 2):
   "…then sometimes they'd [Indians] walk for miles to gather their materials. You'd try to find it close to your residence[village/homestead-allotment]. And they used to go over Rock Creek, over that way. And there used to be a fire burning area there for the bear grass. They traded things like spruce roots with the other side [coast Yurok/Tolowa]. They'd trade acorns and things that we had that were from here for them. Over there we'd get shells and whatever. So, it was a good way to go." Vera Arwood, interview conducted 08/07/1997.

3. Fire (pp. 42):
   "My dad lived five miles up Bluff Creek at the Garnet Ranch. In the fall of the year, it would get so smoky that you couldn't even see. It never burned nothing." Page 43: "This brush situation is getting damn tough around this place. There should be something done about it. They'd burned up here last year and then at Frog Pond. It got pretty hot in some places. They need to cut the stuff down so it will be on the ground and won't burn up into

the trees. They need to burn up some of these piss ants and other bugs." Ernie Spinks, interview conducted 11/1996.

Oral histories/informal interviews:

4. Norman Goodwin, Karuk Ceremonial Leader/elder. Informal discussion with Frank K. Lake at the Happy Camp-Ishkeesh Brush Dance, July 31, 2010. Norman said that there was an "old [Indian] trail that followed the serpentine ridge above Frog pond along the divide of Bark Shanty Gulch (tributary to Rock Creek) that head around/above Frog pond on the west/southwest to south/south east side towards the Klamath River. The trail connected from Eyese Village along the west side of the Klamath River.

5. Charlie Thom, Karuk Ceremonial Leader/elder. Informal discussion with Frank K. Lake at Katamin/Somes Bar "War Dance/gathering" May 29, 2010. Charlie said that Frog Pond was used as a camp for Indian Doctors. Coming from nearby villages on their way up to and back from the Elk/Flint Valley "High Country" [Southern Siskiyou Wilderness] area.

6. Kathy McCovey-Barger, Karuk Brush dance medicine woman/USFS Archaeologist. Informal discussion(s) with Frank K. Lake during a district archaeological/cultural resource tour on August 6, 2010. Kathy stated that she was told from Karuk elders that Frog Pond may have been a "village" at one time and asked if I found the "house pits" or other features.

7. Other related cultural or archaeological information. Frank Lake observations at Frog Pond (Lake Ogaromtoc):
   a. Siskiyou Wildfire 2008. South/south east side of pond, along flat. Found old Indian cooking fire-cracked rocks.
   b. Fire history sample collections Aug. 2010. Found granite stone hand grinder along serpentine ridge on west side of pond. Also, white quartz flake fragments (non-native soil at that place, later found natural white quartz rocks to the southeast, up the ridge about ½ from fragments.

Other relevant publications:

8. Yurok story of mother and son. Taking the "inland" trail back from Orleans (Karuk: Panamnick village") to her home. This trail went to and past Fish Lake over Kewet Mountain = Burrill Peak [Rivet Mt. circa 1920s maps] to down river Yurok village: Pages 24-25 visits to Fish lake: "…the two of them wandered on up through the hills as far as a small mountain lake called Fish Lake…made camp. They slept there the rest of the night by the lake; Son (*Toan*) going hunting/trapping Pages 28-29: "As *Toan* grew older and went hunting along or with other boys, he continued to bring his great-grandfather little birds, then bigger birds, and especially the red-headed woodpecker, and then the fur animals-whatever he could hunt or trap…*Toan* sometimes hunted inland on *Kewet* Mountain and as far as Fish Lake. Whenever he was at the lake, he wondered what had become of the log on which he had climbed that first time…"; Author's discussion

narrative Pages: 165-166 "The journey undertaken by the young mother of the story is accomplished as such a journey on foot would be today (see map accompanying the story): by trail from *Ko'otep*, skirting the river to the spot on Camp Creek (downriver side of Orleans, Karuk *Tishunik*, village and ceremonial grounds) where the Deerskin Dane was held. The return follows the same trail as far as Red Cap Creek; then inland away from the river, passing along Fish Lake and by *Kewet* {Burril Peak} Mountain, thus bypassing the populous village of *Weitspus*, coming out on the river again at *Murek*, and from there downstream to *Ko'otep* once more. (Krober 1959)

9. "A small circular lake. In myth times a number of 'people' gathered at this point to shoot a gigantic bird [condor] with wonderful feathers, which occupied the summit of the mountain *hegwono'L* (Shelton's butte), lying to the southeast, across the Klamath". (Waterman 1920) *See Rectangle G, Map 25. Notes on page 256: Site 1. "itprpr'".

10. "Our first sleep…would be spent by the boarders of a small lake to the north of Weitchpec, among the pine and fir timber. After we had followed a trail a mile or more up the river, we began to ascend the mountain…The lake, but few acres in extent, and almost covered with pond-lily pads, contained an abundance of trout, upon which we feasted" (Pearsall and Pearsall 1928).

B. Additional lines of evidence, including Euro-American qualitative descriptions:

11. Nineteenth century descriptive evidence from Euro-Americans provides additional corroborating insight into the landscape. The federal public land survey (PLS) conducted in 1882 at the townships covering Fish Lake and Lake Ogaromtoc documents that the area around Fish Lake contained a "number of settlements", "prairie and grassland", as well as "large bodies of fine sugar pine timber of good quality" (Foreman 1882a, 10N4E). At Lake Ogaromtoc, PLS surveyors witnessed a landscape "covered with pine and oak and considerable sugar pine of good quality" (Foreman 1882b, 13N5E). For the Karuk and Yurok, *Pinus lambertiana* (sugar pine) wood was a prized fire starter, and *P. lambertiana* stands were cultivated and managed by tribal groups (Schenk and Gifford 1952).

12. A traveler's 1908 account described considerable oak populations in the Bluff Creek area near Fish Lake: "the hills were covered with white oak and madrone… the rocky areas were covered with live oaks" and "a few sturdy firs scattered among the oaks" (Baldwin 1990).

13. Until the 1920s, one of the main passageways from Karuk habitation on Rock Creek southwards was along the ridgeline where Lake Ogaromtoc is situated. "It was common sight in the 1880's to see five or ten Indian men and women heading for their homes with heavy burdens of food, over almost obscure trails…having come ten to fifteen miles in one day over steep trails" (Warburton and Endert 1966). Many of these trails became USFS roads that facilitated timber extraction and fire suppression in the 1950s.

14. Although we expected tree biomass to increase and coincide with land use change starting in 1850, the magnitude of the shift was large. For instance, the predicted biomass at Lake Ogaromtoc in 1950 was 126 Mg/ha and rose to 320 Mg/ha by 2008. This increase in biomass in only a few decades is plausible: a 100 Mg/ha *P. menziesii* dominated forest grew to 360 Mg/ha in 40 years (Stewart and Sharma 2015). As a result of recent rapid increases in forest biomass, modern forest structure is unprecedented in the last 3000 years.

Additional results supporting the distinction of vegetation types

The two most abundant species are *Pseudotsuga menziesii* and *Notholithocarpus densiflorus,* with *Pseudotsuga menziesii* currently more abundant at Fish Lake and *Notholithocarpus densiflorus* more abundant at Lake Ogaromtoc. Mature overstory vegetation at both sites also includes: *Chamaecyparis lawsoniana, Pinus lambertiana, Arbutus menziesii, Alnus rhombifolia, Chrysolepis chrysophylla, Calocedrus decurrens, Quercus kelloggii,* and *Quercus garryana* (nomenclature follows Greenhouse et al. 2012).

We used ordination analysis to understand the vegetation groupings over time. Results support the vegetation response index (VRI) separation (*Quercus*/*Pinus* versus *Pseudotsuga*/*Notholithocarpus*) based on the shade tolerance scalar (Table S1). Although these groups occupy separate regions of ordination space and they divide along gradients in PDSI and CHAR, there are not strong gradients in the data. This is not surprising given that this study leverages two nearby lakes and analyses are limited to a time of vegetation stability.

Table S1 A classification of major pollen types by shade tolerance using a scale of Northern Hemisphere trees (Niinemets and Valladares 2006); the tolerance scale ranges from 0 (no tolerance) to 5 (maximal tolerance) with standard error estimates (SEE). Pollen types are organized from least tolerant (*Alnus*) to most tolerant (*Abies*).

Pollen type	Contributing species	Shade tolerance scale
Alnus	*Alnus rhombifolia*	1.5
Quercus	*Quercus kelloggii*	1.55
	Quercus garryana	2.4±0.3
Total *Pinus*	*Pinus ponderosa*	1.64±0.15
	Pinus jeffreyi	1.74±0.26
	Pinus lambertiana	2.66±0.14
Pseudotsuga	*Pseudotsuga menziesii*	2.78±0.18
Notholithocarpus	*Notholithocarpus densiflorus*	3.67±0.33
	Chrysolepis chrysophylla	3
TC	*Calocedrus decurrens*	3.21±0.53
	Chamaecyparis lawsoniana	3.67±0.38
Abies	*Abies magnifica*	3.5±0.22
	Abies concolor	4.33±0.28

Estimating forest biomass prior to European-American contact

To estimate the central tendency in the aboveground live tree biomass (AGL) at our sites, we fit a locally weighted smoothing regression (loess) to the AGL estimates at each lake (Fig. S1A,B). Given the changes in the pollen deposition rate and our systematic pollen sampling of the lake core (i.e., every 10 cm), the observations are not evenly distributed in time. In addition, at Lake Ogaromtoc, we intensified our sampling to refine the timing and magnitude of two peaks occurring ~2300 calBP and ~1100 calBP (the Fish Lake core was not suitable for additional sampling). The smoothing regression provides a means to normalize sample intensity and avoid over-representing any time period. We limited the regression to data prior to 100 calBP (1850). We generated predicted AGL by date at 50-year intervals (Table S2). The baseline AGL pre-contact was defined as the median of these predicted values. During the last three millennia, both sites maintained relatively low forest biomass values with median values between 128 Mg/ha at Fish Lake and 104 Mg/ha at Lake Ogaromtoc.
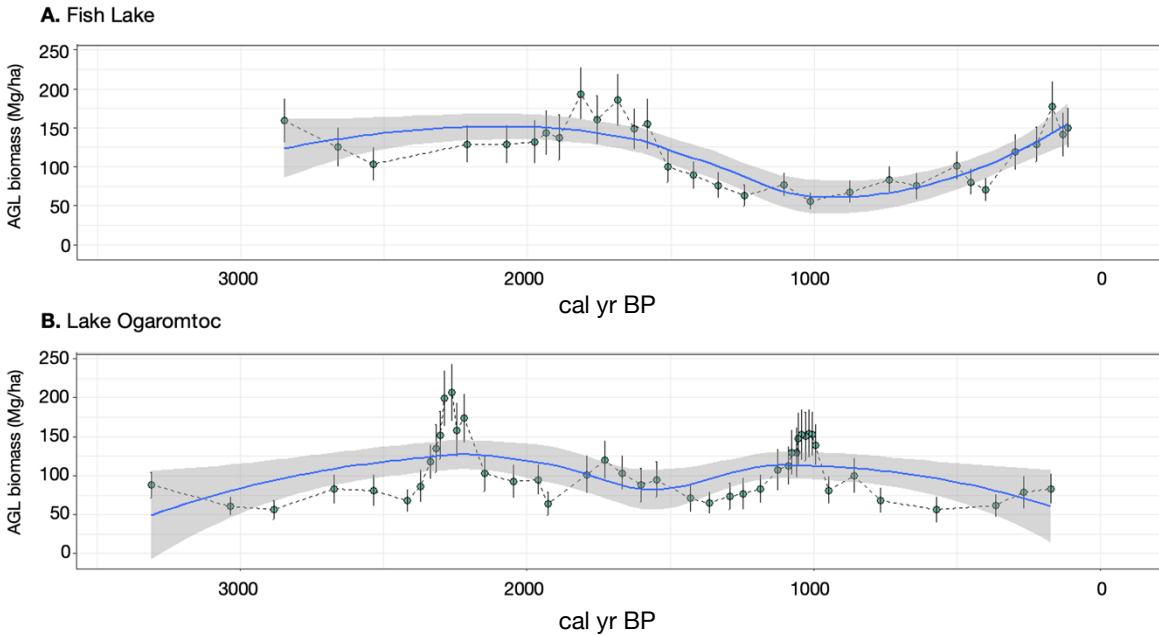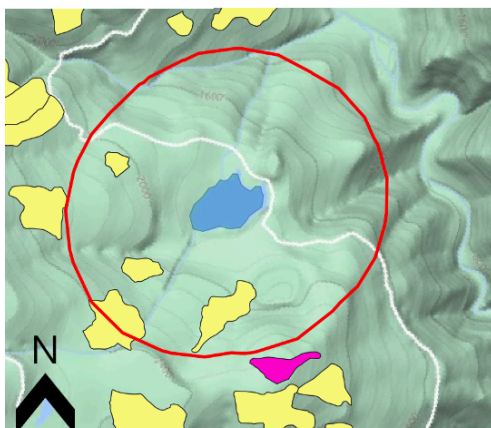
A. Fish Lake

B. Lake Ogaromtoc

Figure S1. Trends in estimated aboveground live tree biomass (AGL) at **(A)** Fish Lake and **(B)** Lake Ogaromtoc. The circles represent estimated AGL from pollen counts; the blue line represents the locally weighted regression line; and the grey band is the 95% confidence interval around the regression line.

Table S2. Summary of the locally weighted regression of aboveground live tree biomass (AGL) for the two lakes prior to European-American settlement. Standard error refers to the residual standard error of the regression; n is the number of predicted AGL values at 50-year intervals.

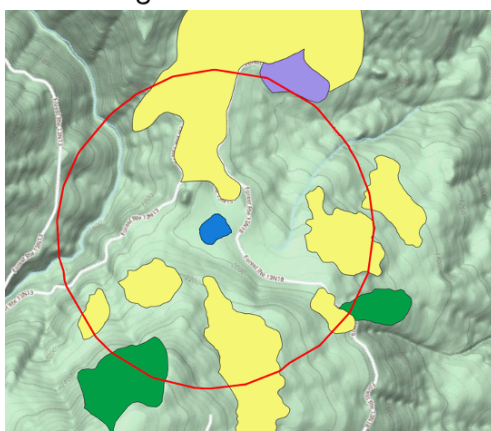| Lake	cal year BP	Standard Error	n	median	minimum	maximum
		Mg/ha		Mg/ha	Mg/ha	Mg/ha
Fish	2800-100	24.2	54	128	61	151
Ogaromtoc	3300-150	33.5	63	104	51	127

Fig. S2 Harvest perimeters from the federal Forest Activity Tracking System at **(A)** Fish Lake that took place in 1968, 1977, and 1985 and **(B)** Lake Ogaromtoc that took place in 1961, 1972 and 1984. The biomass record reflects local vegetation and potential disturbances within a ~650 m radius from the lake shore (133 ha) (Knight et al. 2021). Thin red circles demarcate the spatial extent recorded by the sediment-derived pollen record.
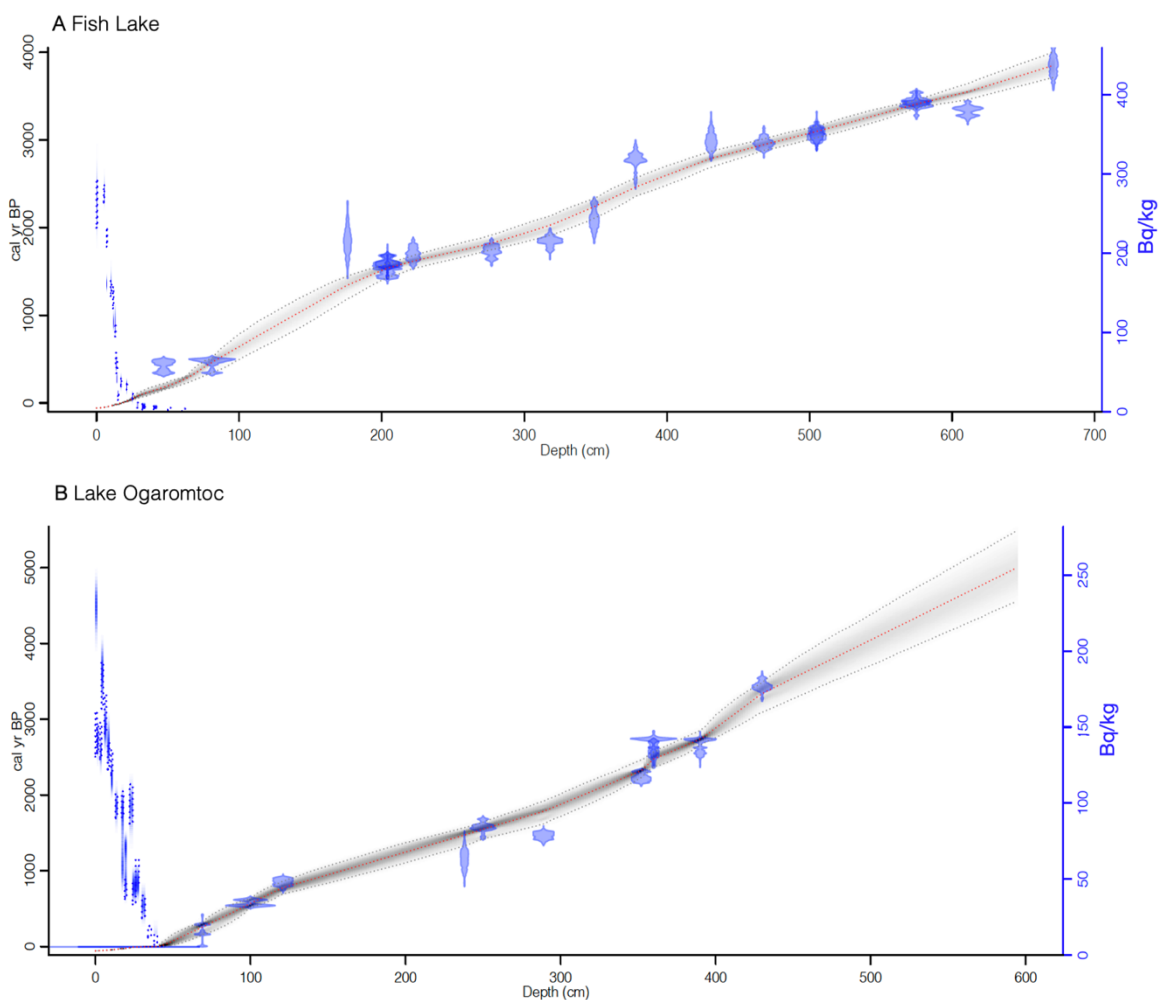
Fig. S3 Age-to-depth models for **(A)** Fish Lake and **(B)** Lake Ogaromtoc using Plum software (Aquino-López et al. 2018, Blaauw et al. 2020), which incorporates both ^{210}Pb dates and ^{14}C dates. Data from Crawford et al. (2015). The 2σ uncertainty band around the age model is enclosed by dotted grey lines; the highest probability age is the darkest grey shade and the red line represents the mean age. The second y-axis (blue, right) shows the ^{210}Pb activity in Bq/kg.

Vegetation Response Index (VRI)

For our study sites, we established a gradient in shade tolerance among the common tree species. We included *Pseudotsuga* and *Notholithocarpus* to represent shade-tolerant taxa and *Quercus* and *Pinus* as shade intolerant taxa (Niinemets and Valladares 2006, Table S1). The VRI was calculated from pollen counts: ((*Pseudotsuga* + *Notholithocarpus*) – (*Quercus* + *Pinus*))/(*Pseudotsuga* + *Notholithocarpus* + *Quercus* + *Pinus*). Positive VRI indicated a greater proportion of shade tolerant to shade intolerant pollen. Increases in VRI were interpreted as transitions toward more closed canopy forests. A negative VRI indicated a greater proportion of shade intolerant to shade tolerant pollen. Decreases in VRI were interpreted as transitions toward a more open canopy. Results from a non-metric multidimensional ordination (NMS) of tree abundance (as measured by AGL) at different sample dates supported the definition and interpretation of the VRI. In the 2-dimensional solution with the lowest stress (stress = 13.5), *Pseudotsuga* and *Notholithocarpus* clustered together in the upper left quadrant (Fig. S4). *Quercus* occurred on the edge of the diagonally opposite quadrant and *Pinus* was located closer to *Quercus* than either *Pseudotsuga* or *Notholithocarpus.* In addition, the ordination gradient from *Pseudotsuga* to *Quercus* was positively correlated with charcoal accumulation. However, the relatively high stress suggests that while the NMS provides a useful overview of the gradient space, the details of the analysis are less reliable (McCune et al. 2002).
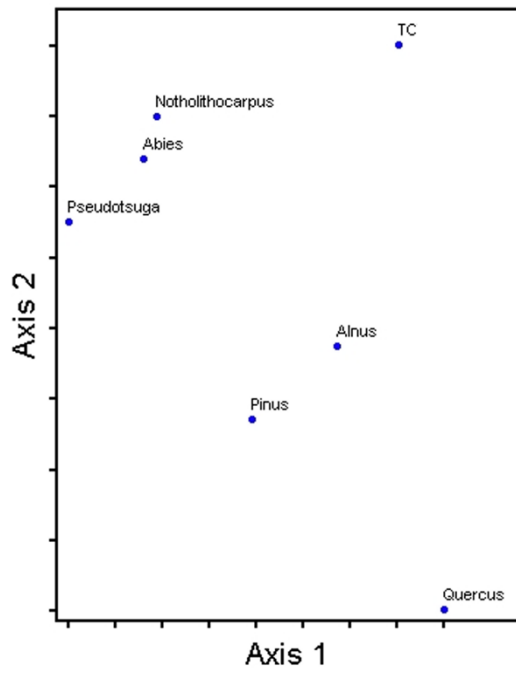
Figure S4. Two-dimensional solution of a non-metric multidimensional (NMS) ordination of forest composition at Fish Lake and Lake Ogaromtoc. Samples based on reconstructions of taxon-specific aboveground live biomass from pollen samples across a 3000-year gradient. NMS was calculated using PC-ORD v7 software (McCune et al. 2002) using a thorough search for the best solution (e.g., 400 iterations, 50 randomized runs). Stress of two-dimensional solution = 13.5.

Charcoal peaks using Char-Analysis

Significant charcoal peaks were determined using Char-Analysis software (Higuera et al. 2009). The minimum background smoothing was determined by dividing the record length (in years) by the number of charcoal samples and multiplying by 30 and "significant" peaks were those with a signal-to-noise index above 3.0 (Higuera et al. 2009). Significant charcoal peak records for Fish Lake (n=8) and Lake Ogaromtoc (n=5) (Fig. S5A,B) underestimated fire events when compared to the fire scar record, which is already known to be a conservative estimate of paleo fire. Nonetheless, we found time periods where charcoal peaks were consistent with biomass. At Fish Lake between 1500–650 calBP, biomass dropped and remained under 100 Mg/ha, coincident with significant charcoal peaks between 1500–900 calBP (Fig. S5A). At Lake Ogaromtoc, large charcoal peaks were associated with co-occurring reductions in biomass (Fig. S5B); for example, charcoal peaks at ~3,400 calBP and ~2300 calBP coincide with decreasing biomass. Biomass fluctuated at Lake Ogaromtoc but generally hovered around 100 Mg/ha between 2200 to 1200 calBP, during which time charcoal influx gradually increases. An absence of significant charcoal peaks between 1200 and 1000 calBP co-occurred with rising biomass which peaks at 1050 calBP to ~150 Mg/ha.
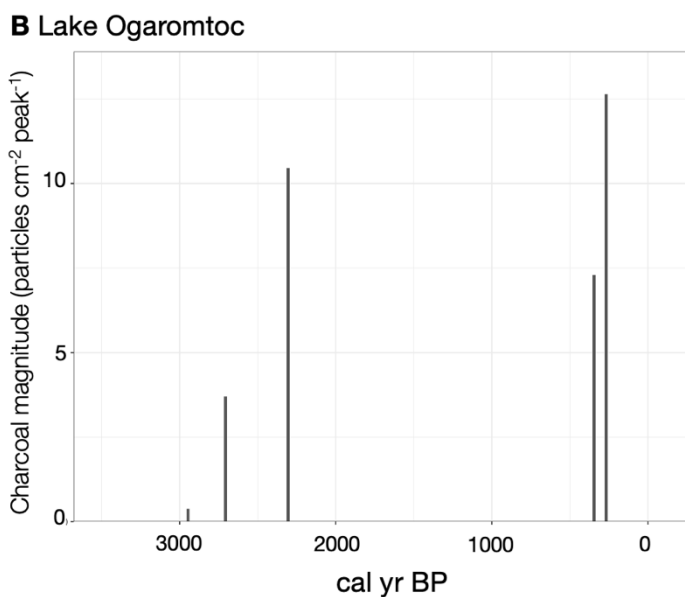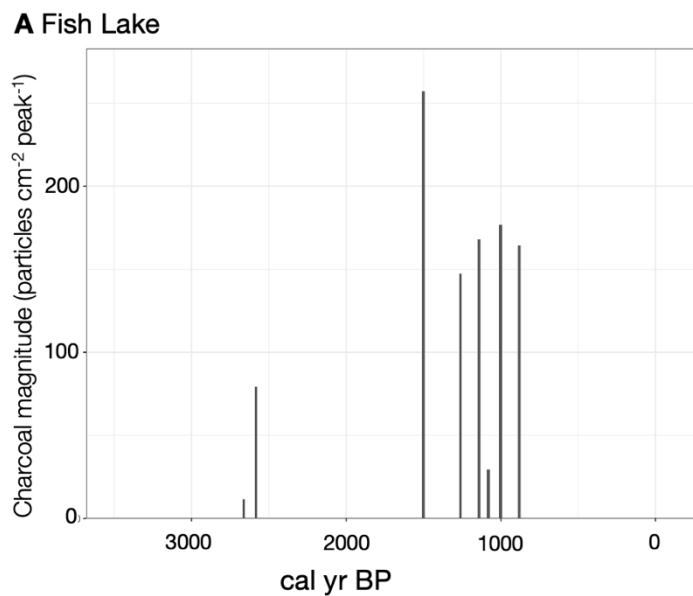
Fig. S5 Charcoal peaks were determined for **(A)** Fish Lake and **(B)** Lake Ogaromtoc using Char-Analysis software (Higuera et al. 2009). Charcoal peak (C_{peak}) was calculated as $C_{peak} = C_{interpolated} - $ local threshold value, where the peak significance threshold was set to the 95th percentile, signal-to-noise index >3, and background smoothing set to 200 years.